DIGITAL TWIN MACHINE TOOL FEED DRIVE TEST BENCH

DIGITAL TWIN MACHINE TOOL FEED DRIVE TEST BENCH FOR RESEARCH ON CONDITION MONITORING AND MODELING

By BRETT STEVEN DENIS SICARD,

A Thesis Submitted to the School of Graduate Studies in Partial Fulfillment of the Requirements for the Degree Master of Applied Science

McMaster University

MASTER OF APPLIED SCIENCE (2023)

Hamilton, Ontario, Canada (Mechanical Engineering)

TITLE:	Digital Twin Machine Tool Feed Drive Test Bench for Research on Condition Monitoring and Modeling
AUTHOR:	Brett Steven Denis Sicard BEng (Mechanical Engineering), McMaster University, Hamilton, Canada
SUPERVISOR:	Dr. Stephen Andrew Gadsden
NUMBER OF PAGES:	xiv, 190

Lay Abstract

Digital twins enable the real-time, accurate, and complex modeling and monitoring of mechanical systems. Machine tools are essential components of modern manufacturing. They are composed of various mechanical, hydraulic, and electrical systems such as the spindle, tool changer, cooling system, and linear and rotary feed drives. This work presents the design of a workbench of a machine tool linear feed drive, a fault detection strategy, and a digital twin modeling solution. The workbench enables the collection and analysis of large, varied, high-frequency data which can be used to construct a digital twin of the feed drive. A digital twin can enable many other useful functionalities. Some of these functionalities include condition monitoring, modeling, control, visualization, and simulation. These functionalities can enable maximum asset performance and are key in implementing effective predictive maintenance.

Abstract

Machine tools are essential components of modern manufacturing. They are composed of various mechanical, hydraulic, and electrical systems such as the spindle, tool changer, cooling system, and the linear and rotary feed drives. Due to their complexity, high cost, and importance to the manufacturing process it is recommended to implement some sort of condition monitoring and predictive maintenance to ensure that they remain reliable and high performing. One way of potentially implementing predictive maintenance and condition monitoring is digital twins. Digital twins enable the real-time, accurate, and complex modeling and monitoring of mechanical systems. They utilize data collected from the system to constantly update their models which can be used for monitoring of the systems state and future predictions. This work presents a digital twin workbench of a machine tool feed drive. The workbench enables the collection and analysis of large, varied, high-frequency data which can be used to construct a digital twin of the feed drive. A digital twin can enable many other useful functionalities. Some of these functionalities include condition monitoring, modeling, control, visualization, and simulation. These functionalities can enable maximum asset performance and are key in implementing effective predictive maintenance. The main contributions of this work are the following: The design and

construction of a machine tool feed drive which implements a novel external disturbance force method. A new method of fault detection in ball screws using interacting multiple models which was shown to provide accurate estimates of levels of preloads in a ball screw driven feed drive. A digital twin based modeling strategy and analysis of the data generated by the system including system modeling and observations on modeling difficulties.

Acknowledgements

A big thank you to all those who have helped me and supported me along the way. Thank you to all the ICE lab members. Thank you to Quade for assisting me and being my research partner on this project for the past two years. Thank you to Raveen, Eddy, Patrick, Andrew, and Alex for good friendship, fun, and for being great colleagues whom I look forward to seeing every day in the lab and have become close friends. Thank you also to Waleed, Naseem, and Alessandro for being good lab mates and good companions to SPIE each year. And thank you to any other ICE lab member whom I have not named here.

Thank you to Ford and the amazing individuals I have worked with there including Youssef, Michael, Ethan, and Dave. I enjoyed my visit to the Ford manufacturing facilities and the mentorship that I have received other the course of this project.

Thank you to my wonderful supporting family. My mother Diane, my father Gilles, my brother Reed, my grandmother Rosa, my deceased grandfather Henry, and all my other relatives and family. You have all been fully supporting of my schooling and education since kindergarten and have pushed me to always strive to be my best and to always take the next step.

And finally, thank you to my advisor Dr.Gadsden for providing knowledge, wisdom, guidance, and encouragement every step of my journey so far.

Table of Contents

List of Figures

List of Tables

Notation, Definitions, and Abbreviations

Abbreviations

4IR	Fourth Industrial Revolution
AI	Artificial intelligence
CAD	Computer aided design
CM	Condition monitoring
CNC	Computer numerical control
CNCMT	Computer numerical control machine tool
CPS	Cyber-physical system
DAQ	Data acquisition device
DT	Digital twin
FE	Finite element

FEA	Finite element analysis
FEM	Finite element modeling
EKF	Extended Kalman filter
HMI	Human Machine Interface
IMM	Interacting multiple models
I/O	Input / Output
IoT	Internet of Things
KF	Kalman filter
LFD	Linear feed drive
MCD	Mechatronic concept designer
ML	Machine learning
MT	Machine tool
NCU	Numerical control unit
NN	Neural network
ANN	Artificial Neural network
PM	Predictive maintenance
RUL	Remaining useful life
TIA	Total integrated automation

Chapter 1

Introduction

The manufacturing world has entered the Fourth Industrial Revolution (4IR) also known as Industry 4.0. The 4IR is characterized by increased digital integration in manufacturing, construction, healthcare, and other industries. Some of the key features are the following: implementation of the Internet of Things (IoT), collection and analysis of large heterogeneous data sets from various sources, implementation of artificial intelligence (AI), and developing cyber-physical systems (CPS). A type of CPS seeing increased popularity in the past 5-10 years is the digital twin (DT). DTs are virtual representations of objects, systems, and processes. They are made up of various models, whether that is a physics-based models or data-driven models. Various data steams are utilized to regularly update the model(s) of the DT to keep it up to date and representative of its real life counterpart. DTs can offer many useful functionalities such as condition monitoring, modeling, control, visualization, and simulation. DTs have been utilized in many different sectors such as building management, construction, autonomous vehicles, smart cities, chemical process management, and most commonly in manufacturing.

Manufacturing is one of the most important sectors in the 4IR. Modern manufacturing is reliant on a large quantity of automated assets working collaboratively. These assets include robotic arms, gantry cranes, autonomous vehicles, conveyor belts, and machine tools (MT). Computer numerical control (CNC) MTs are the backbone of modern manufacturing. They are responsible for various operations such as milling, turning, and grinding to name a few. Manufacturing facilities in sectors such as the automotive or aerospace industry will contain dozens or hundreds of MTs which can manufacture thousands to millions of parts per year. CNC MTs are often very expensive machines, costing between hundreds of thousands to millions of dollars on average. They represent a large capital investment, however this investment is offset by the large throughput, vast array of capabilities, and high precision offered by them. CNC MTs often contain various mechanical, electrical, and hydraulic subsystems. Some of these systems include the spindle, the tool changer, the cooling system, the control system, and the various rotary and linear feed drives (LFDs). LFDs position components in the MTs. LFDs are most often driven by either linear motors or a servo motor which turns a lead screw or ball screw . It is important that feed drives can quickly and accurately position parts while maintaining rigidity by resisting any process forces that occur while operating. Maintaining rigidity and accuracy are important to manufacture accurate parts with good surface finishes. If accuracy cannot be maintained parts may need to be scraped as they do not meet the manufacturing specifications that have been defined.

Due to the importance of feed drives functioning properly it is important that they are maintained in good condition. All equipment will degrade with regular use,

and with it will come reduced performance. It is impossible to completely stop degradation, but there are ways to track it and to act before critical levels of performance decline have been reached. Predictive maintenance (PM) is a maintenance paradigm that implements condition monitoring (CM) by utilizing signals from the equipment to track degradation to service and replace equipment at effective intervals. Implementing PM can help detect early signs of wear, reduced unexpected downtime due to critical equipment failure, and minimize replacement costs by replacing equipment near the very end of its useful lifetime.

One possible avenue of implementing PM is the use of DTs. DTs can be leveraged to collect and analyze large heterogeneous data streams which can be used for modeling and predicting wear, misalignment, and other faults. If PM can be implemented on MTs it could potentially substantially improve reliability, positioning accuracy, and overall profitability. Additionally a great deal of knowledge can be gained about the system which can be utilized for other research endeavours.

1.1 Research Objective

The original motivation and funding for this research came from Ford Motor Company. They wished to implement improved CM and fault detection in their MTs which are used in their transmission manufacturing facilities. To do this they wanted to better understand the data generated from their MTs and how it could be used to predict faulty components. Unfortunately it is not feasible to take a MT out of production to analyze it. To do in-depth analysis, an experimental setup was needed where many data sets could be generated under controlled conditions to better understand these machine signals and their underlying causes. Another research motivation

would be an additional system to collect data which would be used for other students and researcher's work.

The primary objective of this work was to design, construct, and test a workbench of a MT LFD. A MT LFD, in combination with various modeling methods can yield a great deal of functionality including the collection of a large heterogeneous dataset and mechanical simulation capabilities. Several modeling methods such as kinematic, finite element (FE), data-driven, and physics-based models can be used to implement a DT. This functionality can be utilized for a variety of purposes. These include: development of condition monitoring methods for the LFD, the generation of large labeled datasets which can be used to develop and test various data driven modeling techniques like machine learning (ML), and the development of various estimation methods for parameter estimation which can be validated using the workbench. Other objectives included analysis of the collected data and modeling of the system via several different methods. Using several different modeling techniques that are updated and refined using data generated by the system a DT will have been implemented on the system

This workbench will provide value for our industry sponsor, who can use the CM methods developed and tested on the test bench and implement them in their production system. It will also provide continued benefit to future research where it can be used to generate large, varied data sets for various forms of analysis and testing.

1.2 Organization of Thesis

The remainder of the thesis is organized as follows: Chapter 2 will cover the background information and relevant literature in the topics of MT LFDs, DTs and their application to MTs , and the various methods to implement CM. Chapter 3 will cover the design of the MT LFD test bench. Chapter 4 covers an IMM strategy for fault detection in ball screws. Chapter 5 covers analysis of the data generated by the workbench, modeling , and an overview of a DT modeling strategy. Chapter 6 concludes the work and discusses potential future work.

Chapter 2

Background Information and Literature Review

This section covers background information, as well as related literature to key topics related to this thesis. There are three main topics of interest relating to this work. These are: MT LFDs (2.1), CM, fault detection, and PM (2.2), and DTs (2.3).

2.1 Machine Tool Feed Drives

Modern manufacturing is reliant on capital investments in machinery which can improve manufacturing throughput, produced part quality, and reduce overall operating expenses in the long term. There are a variety of manufacturing assets seen in many factories across the world, some of these include: conveyor belts, gantry cranes, robotic arms, autonomous vehicles, and MTs. Industries such as the automotive, aerospace, and heavy machinery industries rely on MTs to manufacture components

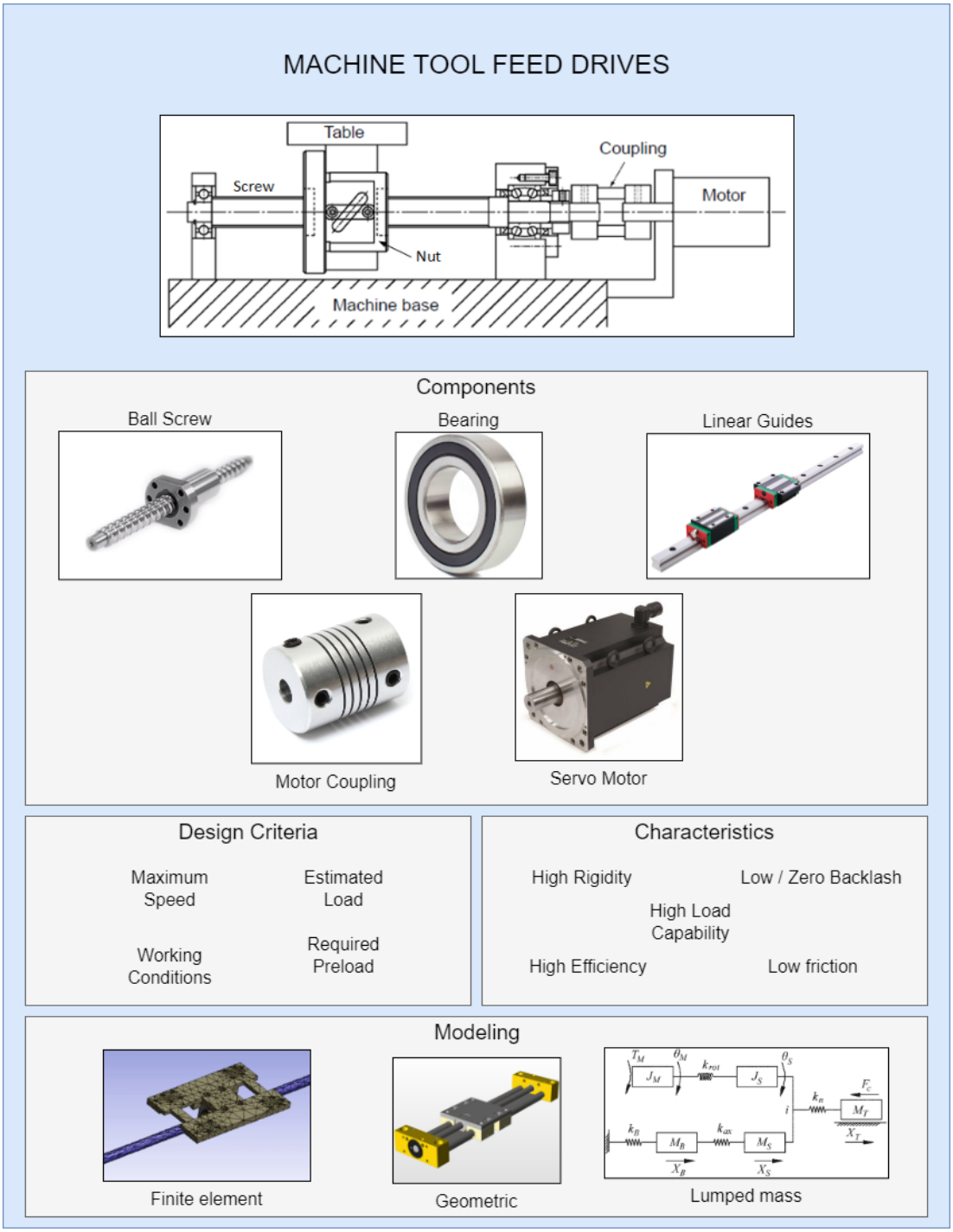

Figure 2.1: Overview of MT LFDs [13]

at a high throughput with high accuracy. MTs are complex systems containing mechanical, electrical, hydraulic, and pneumatic subsystems [119]. Some of these systems include the spindle, cooling system, tool changer, control system, and the linear and rotary feed drives. Many MTs contain either 3 or 5 axes of motion. Typically, 3-axis machines move linearly in the X, Y, and Z directions, with 5-axis machines employing an additional 2 rotational axis often labeled A and B [20]. Fast, accurate, and rigid motion of the various feed drives is essential to the performance of any MT.

When designing a LFD, it is important to know and understand the design requirements of the system. Additionally it is important to understand the key components and their features. These requirements and an understanding of the working principle of the key components will help with selection and sizing of the key components of the system. It is also necessary to understand how a LFD system can be modeled. An overview of section 2.1 can be seen in Figure 2.1.

2.1.1 Characteristics of a Ball Screw Feed Drive

LFDs can be driven a variety of ways, they are usually driven one of three ways: linear motors, servo motor which drives a lead screw or a ball screw, or a rack and pinion. For a screw driven system, they can either be direct drive, or there can some sort of transmission component between the motor and screw such as pulleys or gearing. Most modern MTs utilize either a direct drive ball screw or linear motor driven LFD. There are a few characteristics that make direct drive ball screw LFD the most commonly used feed drives [9] as listed below:

1. Low wear

2. High service life

3. High efficiency
4. Low heating
5. Zero / low backlash
6. High rigidity
7. High load capability

The reasons listed above make these systems ideal for use in industrial production MTs. MTs in these conditions operate near constantly, they only very occasionally are brought out of service for routine maintenance. They often require high torques to move heavy objects at high accelerations, as well as experiencing high external disturbances due to machining process forces. The low wear characteristics of ball screws enable a longer useful life, minimizing the cost of replacement parts, and maximizing replacement intervals. High efficiency ensures minimal power loss through friction. This results in decreased heat generated which can cause thermal distortion and increased wear. Zero or minimal backlash and high rigidity ensures repeatability, resistance to the effects of external disturbances, and increased movement precision. High load capability ensures that they can quickly position heavy work pieces while handling the large external forces generated from machining process forces. This is especially important in high speed manufacturing where process are run at maximum speeds to minimize cycle times.

2.1.2 Linear Feed Drive Components

Not every LFD is identical but most contain a few important components. For ball screw driven LFDs each end of the screw will normally be supported at each end by

a rotational bearing, usually a ball bearing. Additionally, the motor will need to be coupled to the screw via a motor coupling. Normally these LFDs will move some of work table or platform along the axis. This table or platform is most often supported on linear guides which provide a rigid path to follow while also reducing the sliding friction of the movement.

Ball Screws

Ball screws are the most common mechanism for linear motion in MT LDS. They convert the rotational motion of a servo motor into linear motion. Ball screws function similarly to lead screws, moving a nut, which is connected to the worktable, up and down a screw. However, ball screws possess certain characteristics that make them more desirable than lead screws for MT LFDs. These include their extremely high efficiency (>90%), the ability to run at continuous duty with large loads, high load capacities, and low wear properties [9].

Ball screws come in a variety of configurations. There are different options for diameters and leads, where the lead is the lateral distance traveled for one full rotation of the screw. With increasing diameters comes increasing rigidity and load rating, however, it also results in an increase to inertia / mass and therefore requires more torque and energy to rotate. Increasing the lead of the screw can yield faster travel of the axis, at the expense of increase torque required to rotate [24]. In addition to the variations in the screws there are different types of nuts available. To improve the rigidity and repeatability of ball screw feed drives, they are often preloaded .

Preloading a ball screw is the process of eliminating internal clearance between the ball nut and ball screw. Preload is applied primarily in two ways: by using oversized

Figure 2.2: A typical ball screw and nut [30]

balls, or by using a double nut to create a tension or compression force between the two nuts. Preload is normally designated as a percentage of the dynamic load capacity of the ball screw. Preloads typically range from 2% to 10% of the dynamic load capacity. A higher preload of 10% is most often used for MTs to maintain high rigidity and repeatability with high cutting loads and vibrations. Maintaining high preload is important not only to manufacture parts to tight tolerances, but also because preload loss is often a symptom of degradation of the raceway of a ball screw [123].

Bearings

Bearings are used to minimize friction in rotating machinery. In ball screw driven feed drives they are placed at each end of the ball screw. They typically come in two variants: fixed (or thrust) and free supports. Fixed supports constrain the movement in the axial direction while free bearings allow free movement along this axis.

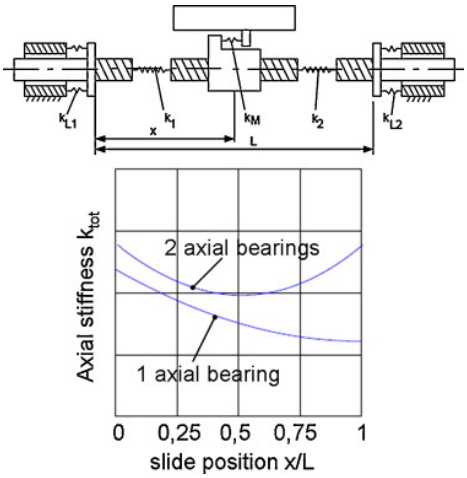

(a) Stiffness comparison of single or double thrust bearings [9]

(b) Typical bearing arrangement for a ball screw [101]

Figure 2.3: Bearings for LFDs

Typically there will be either one of each type or two fixed bearings being utilized. the primary affect this will have will be to alter the stiffness profile of the ball screw. Dual fixed bearing lead to a sort of inverted "U" shape where the system is least rigid in the middle of the screw. Single fixed bearing setups have a gradually decreasing stiffness from the fixed bearing end to the free bearing end [9].

Servo Motors

Most often LFDs are driven via a direct drive electric motor. The most common type of motor used in these applications are AC servo motors [6]. AC servo motors offer a few advantages over other types of driving mechanisms such as the following: high power-to-weight ratios, low noise generation, reliable, and they often have incorporated encoder for accurate positioning. These are the types of motor that will be used in most CNC MT applications. When selecting motors it is important to consider the characteristics and specifications of the motor to ensure it fits the

Figure 2.4: Siemens servo motor [95]

desired application. Some common specifications of motors are: maximum rotational speed, maximum continuous and instantaneous torque, motor rotor inertia, output shaft diameter. Before selecting a motor it is important that system parameters such as max travel speed, maximum force required, and weight of the moving platform are considered.

Linear Guides

Linear guides are a key components in most LFDs. There are a few different variations in LFDs, but they all work on the principle of reducing the friction of the movement of the system while providing rigidity [142]. Most often LFDs will have a circular cross section or an hourglass like profile seen in Figure 2.5. One type of linear rail uses sliding bushings. These bushings utilize grease and a low friction material such as a composite or brass bushing to reduce sliding friction. For further reduced friction a circulating ball bearing system can be used. This system functions similarly to a ball

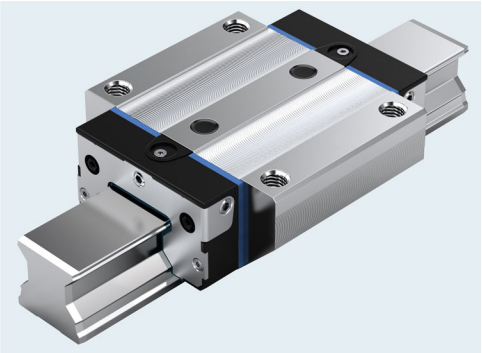

Figure 2.5: Typical profile linear guide [129]

Figure 2.6: Bellow motor coupling [94]

screw with ball bearings circulating through a raceway to minimize contact friction. Like ball screws linear guides can be preloaded to increase rigidity.

Motor couplings

In order to transfer the force from the servo motor to the ball screw there needs to be a coupling device between the two. There are many different types of motor couplings. Broadly they can be split into rigid and flexible [4]. Rigid are typically the simplest

design, but require the two shafts to be in near perfect alignment. An alternative is using a flexible coupling which can maintain high rigidity and zero backlash while allowing for some level of misalignment [17]. There are a few variations of flexible couplings including bellows, oldham, and diaphragm which can be seen in Figure 2.6. With couplings there are several methods to secure the coupling to the two shafts. If the shafts are keyed or splined the coupling will typically just have a female connection for the corresponding keyway or splines. If a straight shaft is used there are two typical ways to secure the shaft, either set screw(s) or clamping. Set screw couplers use one or more set screws to screw into the shaft to secure the coupling to the shafts. For clamping couplings there is a screw which when tightened decreases the diameter of the coupling which creates a clamping force around the motor and ball screw shaft. When selecting motor couplings it is important to consider the maximum speed, maximum instantaneous and continuous torque as well as the nature of the movement the coupling would be expected to experience.

2.1.3 Linear Feed Drive Modeling

There are various ways to model ball screws. Most common in the literature are white or grey box models where there is either some or a great deal of the underlying mechanisms and physics of the system. Three common methods are lumped element, geometric, and finite element models (FEM) [152, 61, 81]. Geometric models are most often created in computer aided design (CAD) software such as Solidworks or Inventor. They often serve as the base for other types of modeling such as kinematic or FEM. Kinematic analysis can be useful for simulating the movement of the system and its interaction with other components. Lumped mass modeling is usually created

using mathematical relationships such as differential equations, state space models or transfer functions. Lumped mass modeling is often combined with FEM to create a hybrid model. A few examples of models seen in the literature can be seen in Figure 2.7.

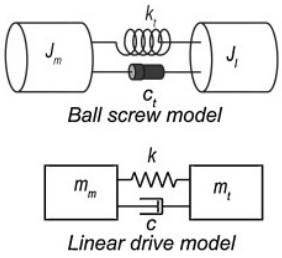

(a) Example of a lumped mass model common in control application [9]

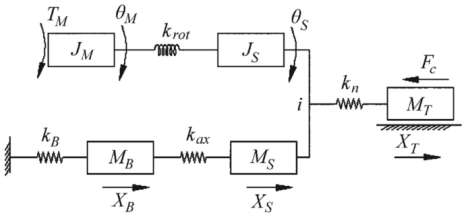

(b) Another example of a more complex lumped mass model [61]

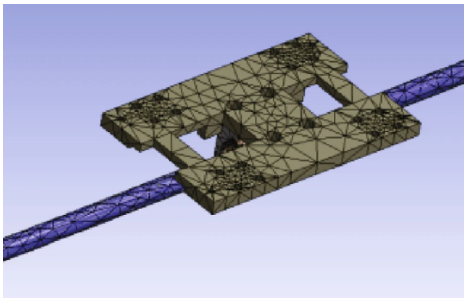

(c) FEM common to analyze stiffness, vibration, and temperature effects [61]

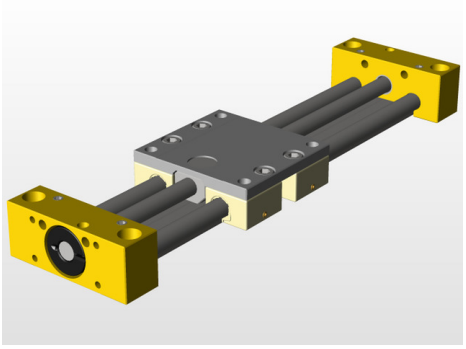

(d) Geometric model used as the basis for many other types of models [93]

Figure 2.7: Examples of models of ball screw LFDs

Lagrangian Mechanical Modeling

Mechanical models are used to predict and control the movement of ball screw systems. One of the most common mechanical models used for many different mechanical

systems are Lagrangian mechanical models. They consider the separate masses or inertias of the various components listed above along with the stiffness and friction between them. There are several different ways these systems can be modeled using this method. Some models consider the individual components and the interaction between them [104], while others may consider them as a lumped mass to simplify the analysis [103, 9]. This is often the method used for developing and testing control systems. One popular way of achieving this modeling method is using MATLAB, specifically Simulink. Simulink allows for the graphical representation of these models and allows for simulation of these models to allow for vibration and control performance analysis.

There are many examples of lumped mass models being used in the literature. Frey at al. [43] modeled a ball screw system using a lumped mass model and compared to a hybrid FEM-lumped mass model. They found that the simpler lumped mass model was suitable for analyzing the vibration characteristics of the system and determining the dominant eigen-modes. They found their model matched up well to experimental data. Ebrahimi and Whalley [38] analyzed a LFD of a system which was driven by a belt and pulley. They modeled their system using a block diagram and included nonlinearities such as coulomb friction and backlash. They analyzed the effect of stiffness, friction, backlash, and mass on feed drive performance. They believe this model can be used to optimize machine tool parameters and predict tool life. Huang et al. [58] utilized a lumped mass model to analyze the stiffness and friction characteristics of a feed drive. Using this model they were able to analyze the deformation of the feed drive and develop compensatory control methods to reduce tracking error . Altinas et al. [7] used a lumped mass model of a ball screw to develop a sliding-mode controller

for LFDs .

Finite Element Modeling

LFDs are often modeled in CAD software to create a geometric model of the system. Geometric models of LFDs can be used for other types of modeling such as FEM or used for dynamic mechanical system simulation. FEM are often used to study the stiffness, thermal, and vibration characteristics of the ball screw LFD.

Mechanical vibration is an important consideration when designing any mechanical system. It is important to understand the various natural frequencies, mode shapes, and forcing frequencies to design a system. There are many examples in the literature of utilizing FEM for vibration analysis in MT LFDs. One early example in the literature was work by Zaeh et al. [159] who created a FEM, simulated it and compared it to experimental results. Their work was intended to improve the control performance of MT feed drives. Since this early work there has been a steep increase in computing power and as a result the capabilities of FEM software. In further work, Zaeh and Oertli modeled the stiffness of a ball screw feed drive. Again, this model can be used to improve the control performance of the LFD [158]. In other work they applied their FEM combined with multi body simulation to predict and simulate machining performance [157]. In their thesis Okwudire [102] modeled a ball screw system using FEM, they utilized hybrid modeling with more rigid components modeled as lumped-parameter rigid bodies and more flexible members modeled using distributed-parameter structural members. They used this modeling scheme in several control schemes and were able to show that their modeling technique was superior to traditional techniques . Zhu et al. [169] used FE model and rigid body dynamics

model hybrid to create a vibration model of the system. They were able to model the frequency response of the system which was validated with experimental results. This analysis can be used to optimize the performance of feed drive systems. They identified the stiffness and damping ratio of the system. Vincente et al. [138] modeled a continuous LFD as a FEM using Ritz series approximation. Doing this they analyzed the effect of different transmission ratios on the vibration dynamics. They found that the transmission ratio of the system had a large effect on the frequency response .

Another common application for FEM of LFDs and their components is thermal analysis. Components will expand and contract as their temperature increases and decreases. As a result, thermal error is introduced which can decrease the machining accuracy of MTs. Wu et al. [148] Utilized FEM for analyzing thermal deformation of a ball screw. They compared the results of their modeling to experimental data collected from thermocouples, laser interferometer and a capacitance probe to measure thermal error. Using their hybrid model they could determine the strength of various heat sources and the resulting thermal error. Yun and Kung [156] used FEA to estimate the thermal errors of the ball screw and guide way. They found that thermal deformation of the linear guide way causes issues with straightness and angular errors, whereas the ball screw only caused linear errors. They validated their models through experimentation suing a laser interferometer to measure error . Min and Jiang [96] used FEM to analyze the thermal contact resistance between the end bearing and their housing to predict temperature increase and the resulting power loss. They validated their model using experimental data .

Other Types of Models

In addition to the most popular types of models of lumped mass modeling and FEM, there are other types of modeling that may be useful. One type of modeling that has seen some use in the literature is MATLAB Simscape. Simscape is an add-on for Simulink that allows for the physical modeling of systems on a component level such as mass', springs, hydraulic cylinders, lead screws, gears, etc as opposed to block diagrams of transfer functions used in Simulink as seen in Figure 2.8. There are a few examples in the literature of using Simscape for modeling LFDs. The primary objective of using this modeling method was simulation and controller design [54, 25, 105].

One other popular type of modeling is dynamic mechanical system simulation. This type of modeling is usually built on geometric modeling and uses model qualities such as mass and geometry to simulate mechanical movements. This type of modeling can be useful for estimating and measuring the forces, velocities, and accelerations that occur under certain conditions [49].

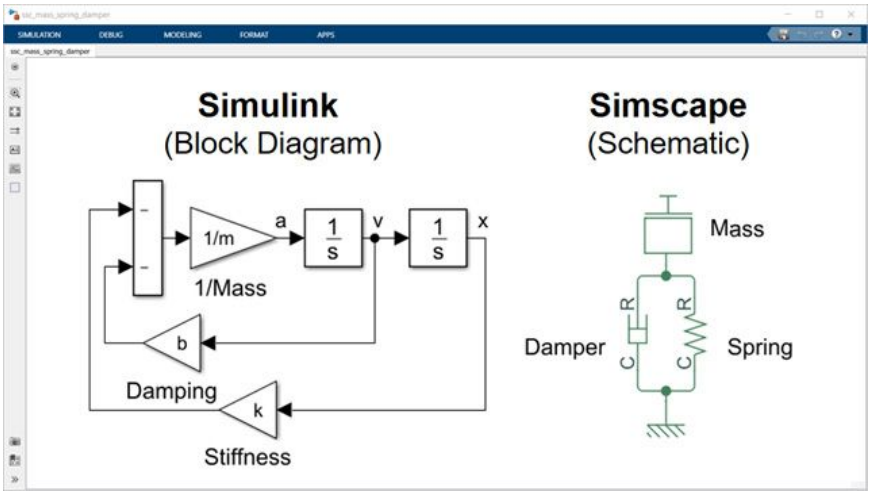

Figure 2.8: Simscape model versus Simulink model

2.2 Condition Monitoring, Fault Detection, Predictive Maintenance

Given the importance of capital investments such as MTs to modern manufacturing, it is important that they are kept in good working condition. Machines in good working condition can perform at high speeds and accuracy with high levels of reliability. To ensure that they are kept in good condition it is worthwhile to implement CM. CM is the process of collecting data from a system to create estimates of its condition and predictions of remaining useful life (RUL). CM is part of an effective maintenance management program.

Maintenance and machine condition has several associated costs which can be minimized if an effective maintenance program is implemented: expected downtime, unexpected downtime, quality, and replacement parts. Expected downtime is the lost production due to the machine being down for scheduled maintenance. When machines are down for maintenance they incur costs by reducing production throughput and requiring labour to service the machines. Unexpected downtime occurs due to sudden failures and crashes. These crashes cause damage to equipment in addition to incurring the costs of reduced throughput and required labour to repair the machine. Expected downtime is always preferred to unexpected downtime as it can be anticipated and its costs more easily predicted. Poor quality has associated costs. There is a cost with testing components periodically throughout production, the cost to scrap or rework components that do not meet specifications, or the cost if a non-conforming part makes it through production to a customer. Generally the further a component travels along production the greater the associated costs. In addition

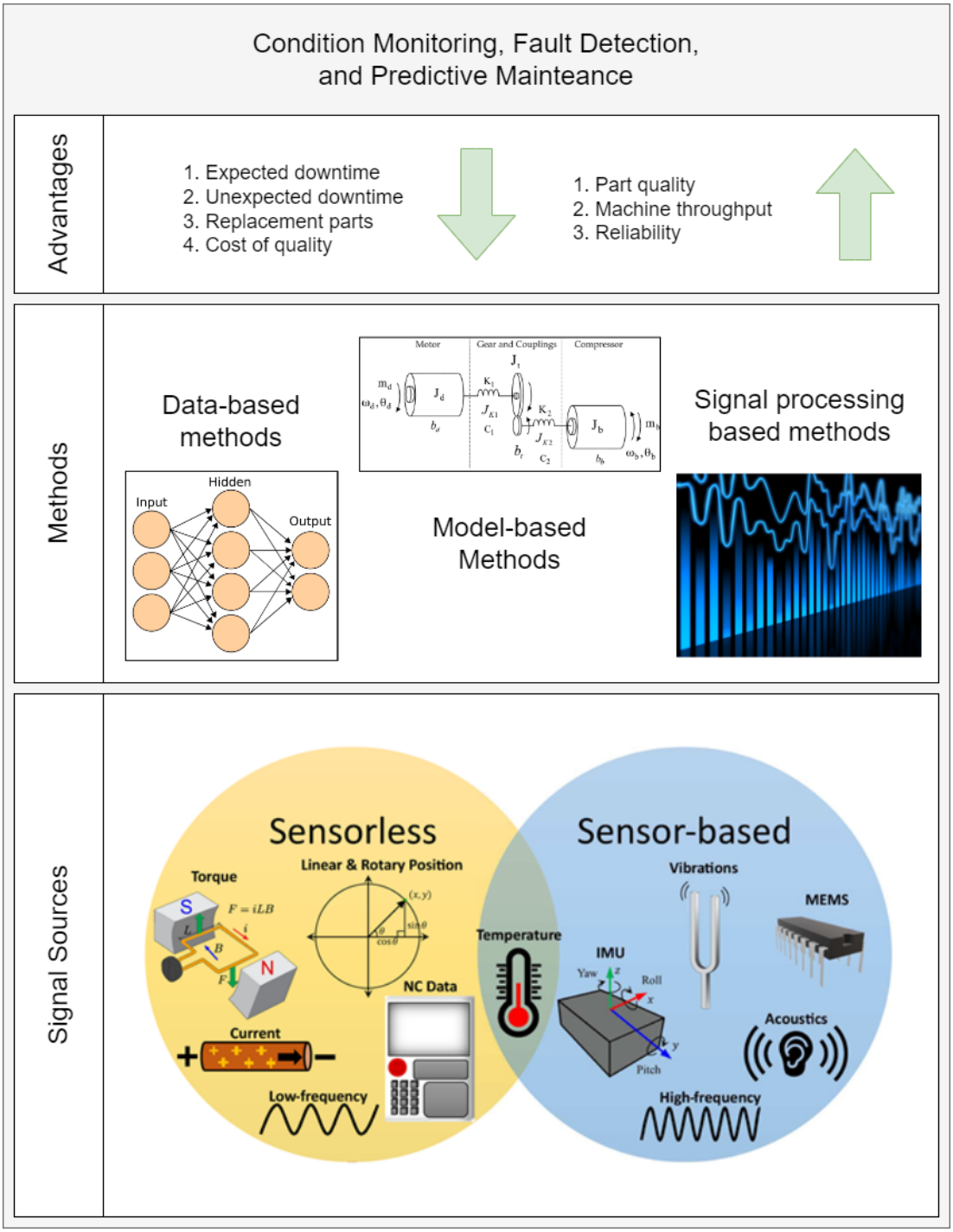

Figure 2.9: Overview of CM [20, 126, 97, 76]

to direct monetary cost, there is also often a cost to the damage to reputation that occurs if poor quality parts make it out of production. The replacement parts needed to service the equipment are a cost associated with maintenance. Not only the cost of the parts themselves but the value lost if components prematurely wear or are replaced before the end of their useful life. Additionally, if replacements parts are past their production life or there is a high demand additional costs may be incurred due to low stock or priority shipping.

Predictive and prognostic maintenance is the latest evolution of maintenance paradigms. The first level of maintenance paradigms is reactive maintenance. Reactive maintenance is simply fixing machines as they break. This is the least effective form of maintenance. Reactive maintenance increases unexpected downtime as unexpected failures arising from neglect force the machines down. The next level of maintenance is planned maintenance, where maintenance occurs at set intervals. This is a better method compared to reactive maintenance but is still not ideal. Doing maintenance at set intervals increases the cost of expected down times and can mean replacing parts that are still far away from the end of their life. PM involves analyzing data from the machine and predicting when it requires maintenance. This paradigm can reduce expected, and unexpected downtime costs as machines are serviced only when necessary and before critical failures occur. Cost of quality and replacement part costs can be reduced as well as parts are used for the majority of their useful life and not past the point where the cost of quality begins to rise. A summary of the relative costs of each paradigm is seen in Table 2.1. PM requires a great deal of data to analyze. Traditional CM is labour intensive and prone to human error. It often requires a worker to inspect and test machines over time individually. This approach

Table 2.1: Costs of maintenance

Paradigm	Associated cost			
	Expected downtime	Unexpected downtime	Quality	Replacement parts.
Reactive	Low	High	High	Moderate
Scheduled	High	Low	Low	High
Predictive	Moderate	Low	Low	Low

is too expensive to inspect at a high enough frequency, and inspection is done too infrequently, therein faults and wear are detected too late. Sensors can be installed on machines to collect a large stream of data in real-time. Data collected from the machines can be analyzed to determine the machine's condition. This information can be used to take corrective action if required. Autonomous CM will maximize machine performance and up-time, which will, in turn, maximize manufacturing efficiency.

There are many different condition monitoring strategies and methods in the literature [20, 121], a few of which will be discussed in the following subsections.

2.2.1 Sensor-Based and Sensor-Less Analysis

For MT CM analysis can be split into sensor based or sensor-less. Sensor-less based CM does in fact use sensors, however, it uses sensors which are already installed on most, if not all CNC MTs. An overview can be seen in figure 2.10. Common in sensor-less analysis is the use of machine encoders, and torque or current sensors. These sensors can be used to estimate preload [63, 27], backlash [117] and wear [92].

Sensor based analysis uses additional sensors installed on the system. The most common external sensors are accelerometers and thermometers [20, 121]. These are

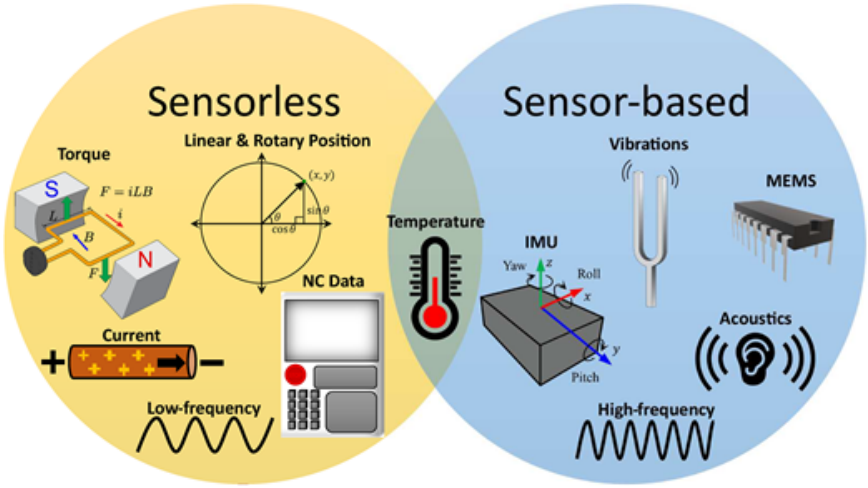

Figure 2.10: Sensor-based versus sensor-less analysis [20]

common because increased temperature and vibration are usually symptoms of wear or faults. Vibration analysis can be useful in estimating wear [109] in a system, or determining the natural frequency [82] for example. Temperature sensors are often used to monitor friction and lubrication [128, 67], or to estimate levels of preload [39]. Further discussion of sensor based and sensor-less analysis and other data streams can be found in section 3.2.3.

Sensor-based and sensor-less solutions are both valid approaches to condition monitoring and fault detection. The primary advantages of sensor-based solution is the opportunity for many additional data streams, however, introducing these additional data streams introduces additional complexity and cost for integrating these additional sensors. Sensor-less solutions are advantageous because they don't require any additional investment or complexity, however, they also limit the amount of data streams available.

2.2.2 Analysis Domain

When analyzing sensor or sensor-less based methods there are multiple domains to analyze the data. Data is most frequently collected as a time series. It is common to analyze the data in this domain as it can be used to observe changes to parameters over time. For example it may be useful to observe the changes in temperature over time [96]. Another common type of analysis occurs in the frequency domain. Frequency domain analysis is often achieved by using the Fast Fourier transform (FFT) which can decompose a signal into the sub-signals of various frequencies. Doing this it is possible to observe which are the dominant frequencies of vibration for example which can be seen in Figure 2.11. This is a common approach for methods which are examining vibration. They often will seek to determine the frequencies of the highest amplitude of vibration [84]. This frequency domain information can be helpful for controller design [138]. Another possibility is the combination of both domains. Short-time Fourier transform or Wavelet transform can be used to analyze in the time-frequency domain. Hilbert Huang transform is a method used often in the literature for time frequency domain analysis as it can yield instantaneous frequencies as a function of time [59].

2.2.3 Signal Processing Condition Monitoring

One typical approach to condition monitoring is to extract features from the various available signals. These features can be captured from any one of the sensors or analysis domains mentioned in the sections 2.2.1 and 2.2.2 above. These methods often extract time domain features such as mean squared error, maximum and minimum,

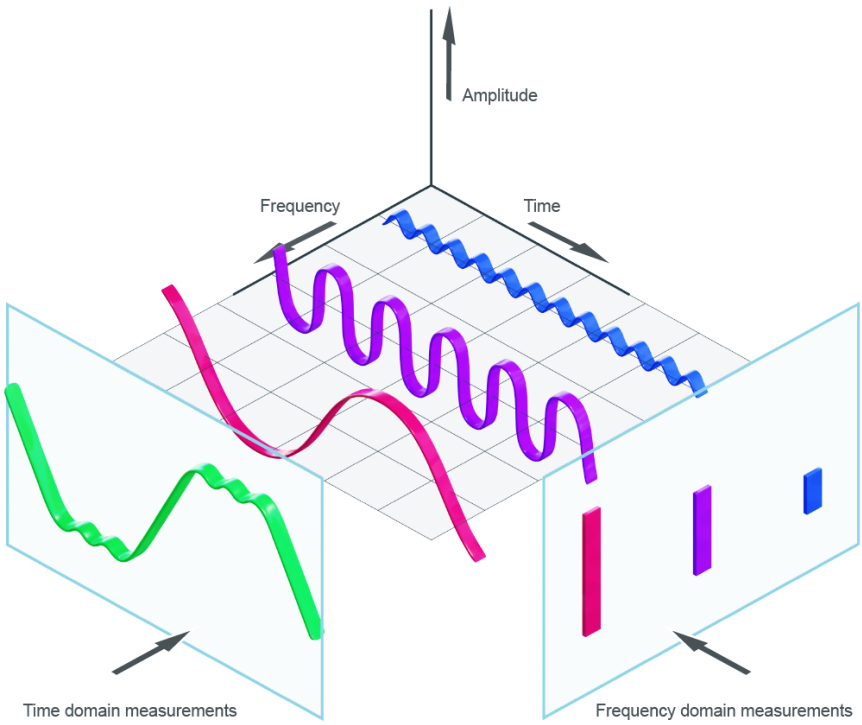

Figure 2.11: Time and frequency domain representations of a signal using Fourier transform [66]

and variance. There are also a variety of features that can be extracted from the frequency domain such as the the power spectral density at various frequencies. Often times these features will be measured at both healthy and degraded or fault states so that they can be identified from the machines signals.

2.2.4 Model-Based Condition Monitoring

Model-based CM relies on an understanding of the underlying mechanisms of the monitored system, it is a type of white box modeling. Model-based methods utilize

physical modeling of the systems which can be used to predict and describe the system. There are several types of models which can be used to describe the system, some of which are listed above in section 2.1.3. Often this type of analysis models various faults and seeks to match system measurements with the fault states. For example one paper by Jeong et al.[65] used mathematical motor current models to estimate inclination angle of a feed drive table . In a paper by Verl et al.[136] they created a model correlating feed velocity, preloading, and drag torque.

One additional approach to model based CM is using filtering methods such as the Kalman filter (KF) or particle filter. KF is typically used for state estimation [21] but it can be modified for CM purposes. Several studies used KFs to improve machine tool CM and control. Son et al. [127] used a KF for signal processing to improve RUL prediction. They applied their method to battery failure prognosis. Cai et al. [23] used particle filtering to improve surface finish estimations in milling processes. Sadhukhan et al. [110] and Niaki et al. [3] used the unscented Kalman filter (UKF) and extended Kalman filter (EKF) respectively to estimate cutting tool flank wear in inconel 718 turning operations. This model was used for online tool wear monitoring. They found their method improved estimation accuracy of tool wear compared to deterministic methods. One study by Huang et al. [60] used a KF based method for detecting faults in a ball screw system and were able to detect both measurement and mechanical failures. They used residual signals from the KF for fault detection and identification and also implemented FTC in their system. IMM is a estimation strategy which involves the use of multiple system models. It can be utilized for identifying if a system is in a fault state. Further discussion on the IMM method is discussed in section 4.2.2.

2.2.5 Data-Based Condition Monitoring

Unlike model-based methods, data-based CM does not rely on an understanding of the underlying system, they are a type of black box modeling. Data-based methods seek to understand the correlation of inputs and outputs for the purpose of predictive capabilities. The most popular types of data driven condition monitoring methods is ML [131]. ML methods can use both labeled and unlabeled data sets for prediction. ML is most successful when some sort of feature engineering is employed. Feature engineering is the process of eliminating data, fusing data, or creating new useful data from existing data. This is usually done to reduce the dimensionality, improve computing speed, reduce redundancy, and improve predictive capabilities. AI based methods are popular in the literature for CM of MTs. Muthuswamy et al. [99] found that most studies uses one of the following four AI techniques: artificial neural network (ANN), Fuzzy logic, Hidden Markov Model, and Support Vector Machine .

The most popular use case in the literature was applying neural networks (NN) to predicting levels of tool wear. Several studies examined tool wear in turning operations [15, 56, 36, 75, 112] using inputs such as the cutting parameters (depth of cut, feed rate, etc.), force signals, acoustic emission signals, motor current, and vibration data. One paper [75] also used a thermal image as an input. Salinas et al. [112] found that an ANN had much improved classification of wear compared to conventional empirical-analytical methods. Many studies also examined tool wear and RUL in milling operations [28, 2, 111, 22, 160]. They used most of the same input parameters used in the papers looking at turning operations. Baig et al. [108] created an ANN based on thrust force, cutting speed, spindle speed and feed to predict the number of holes that have been drilled. With this, the estimated amount of wear

could be deduced. Reinforcement learning wasn't as common as NN for machine tools. Ding et al. [35] used Q-learning for fault detection in bearings and a pump system. They were able to detect faults with a very high degree of accuracy.

2.3 Digital Twins

DTs are an emerging technology which seeks to connect physical systems to a virtual representation. The primary advantage of a DT is the ability to collect, analyze, and model large quantities of data. This connection can enable many useful services such as CM, advanced control, simulation, and future prediction analysis to name a few. The DT was first conceptualized and presented by Micheal Grieves [50]. He further expanded the concept via the introduction of concepts such as the DT instance, DT aggregate, and DT environment in the concept of the product life-cycle [51]. Although there is a general idea as to what a DT is and what constitutes one, there is currently a variety of definitions currently employed [68] as well as disagreement on their primary purpose or value [132]. The idea of the DT has had increasing interest over the years. One of the early adaptors of the concept was NASA [48]. DTs have seen applications in manufacturing [29], vehicles [57], buildings [71], power plants [80], and other critical assets. DT can also be an enabling technology for other types of advanced smart systems such as cognitive dynamic systems [55, 122, 47].

Although there has been applications of DTs to MTs, it is not as popular of a topic as those mentioned above. A concept similar to the DT is the virtual MT. The virtual MT is a concept of real time control and simulation of MTs [8, 69, 86]. One of the earlier works on conceptualizing the MT DT was in 2016 by Armendia et al. [10]. Their twin-control project sought to use many different signals that affect machining

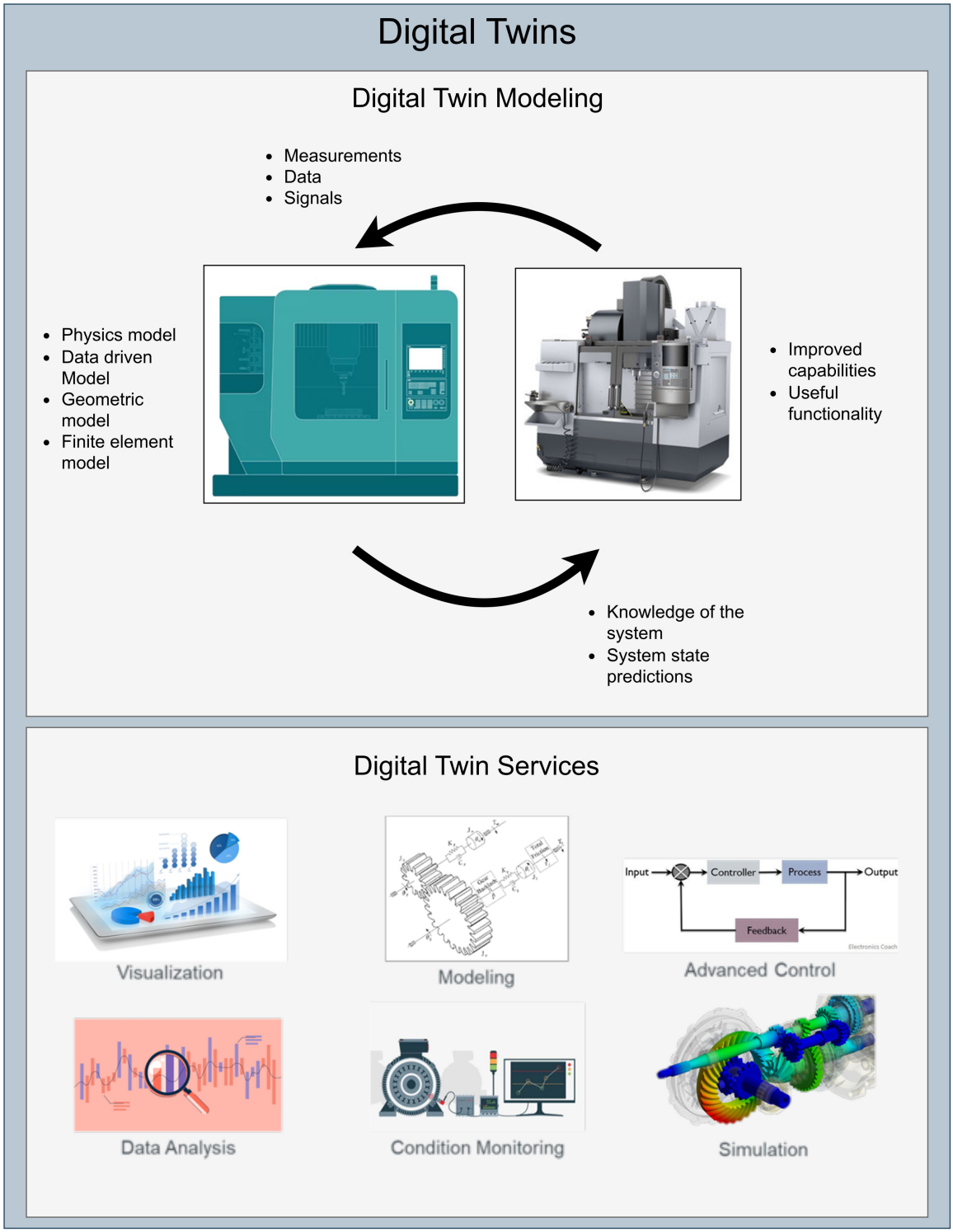

Figure 2.12: Overview of a MTDT

processes to better estimate and simulate machining performance [10]. One of the earlier and most popular conceptualization of the MT DT was by Luo et al. [89] who presented a modeling method for a DT of a CNC MT. Luo et al. identified a few key abilities of a MTDT: Precise simulation, self-sensing, self-adjustment, self-prediction, self-assessment. The nature of data collection, modeling, and simulation for a MTDT may differ based on the desired outcome, but there are a few characteristics that are generally desired. These traits include: scalability, extensibility, and modularity. After examining the literature, a few key services of DTs have been primarily applied to MTDTs to improve performance or reliability. These include improved system modeling, improved control and process optimization, and CM and fault detection. Previous work has been conducted examining the application of DT to MTs, which has been published as a conference proceeding [122].

2.3.1 Improved Modeling

DTs utilize virtual models to make predictions, observe trends, predict future behaviour, and for complex simulation. Modeling is a key aspect for MTDTS and most other services that rely on accurate modeling. DT modeling is especially useful in MTs, as MT components will degrade and their performance will change over time. This change over time necessitates a constantly evolving and updating model. An accurate model is necessary to maintain high performance to create highly accurate parts with high throughput. Model parameters can be identified and updated using DT [19]. Several studies used DT to improve modeling. Zhang et al. [163] were able to improve dynamic modeling of a ball screw and other rolling joints using a NN augmented DT. Their method was able to identify dynamic parameters with less than

3% error. Wang et al.[140] proposed a non-intrusive method using in-process CNC data for model estimation. They applied this to estimate system dynamic parameters during a drilling operation. Wei at al. [146] developed a method for consistency retention using vibration data. They would compare experimental data to FEA simulation results to update their wear model. This method ensures the digital model's parameters closely match the physical system.

Modeling is a key feature of many functions of a MT. Key to DTs are the model(s) that make up the virtual twin component. Most other DT services rely on modeling so it is key to have accurate up to date modeling. Several types of models are seen in MTDTs which are discussed in section 2.1.3. These models can be used independently, but to achieve maximum value they can can be used together in model fusion. For example in a paper by Liang et al. they used a fusion of multiple time scale and FEM for online process characterization [84].

2.3.2 Improved Control and Process Optimization

Precise control of the various moving components and stages is critical for MTs. Geometric tolerances can only be met if rigid and precise control of the various feed drives can be achieved. In addition the surface finish and tool life will depend of factors such as feed rate and spindle rpm. To ensure all of these parameters are maintained at optimal values and that positioning accuracy is maximal it is necessary to implement some sort of advanced control that can compensate in real time for actual machining conditions. Liu et al. [88] proposed a method for predicting and compensating for time varying error which could improve machining tolerances. They were able to

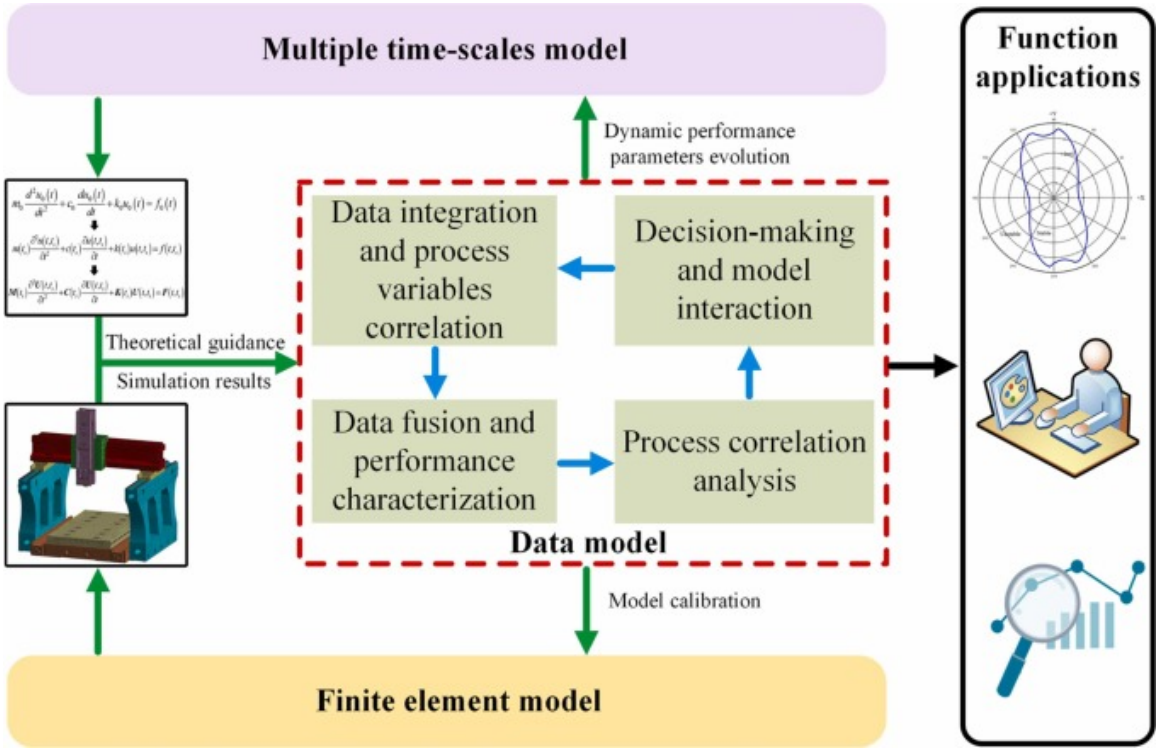

Figure 2.13: Model fusion of MT using DT [84]

reduce the hole pitch error by 69% by implementing real-time compensation. Armendia et al. [11] examined DT control in an aerospace and automotive machining application. They found that it was possible to improve process control using real time comparison of measured data to simulated data. There was several examples which utilized DT technology to improve surface finish in machining processes. In one example, Ma et al. [91] used a short term long term NN to compensate for thermal error and improve machining tolerances. By doing this, they were able to substantially decease the machining error in a drilling operation. Tong et al. [134] applied a DT framework to improve the tool path in a 5-axis milling machine by compensating for measured disturbance. As a result, the surface finish was improved and tracking error was decreased. Cai et al. [23] used a hybrid method for accurate on-line and

off-line prediction of surface finish in a vertical missing operation. DTs can also be used to optimize a machining process. Guo et al. [52] created a DT based method for collision detection to avoid work piece collision with work holding for turning operations. Using simulation tools Stan et al. [130] were able to reduce power consumption for a robotic de-burring process. In a paper by Shen et al. [116] they were able to determine parameters of a grinding procedure and optimize grinding wheel selection to reduce process time.

The improvements to control and process optimization allow MTDTs to maximize produced part quality through real time compensation and simulation capabilities. They could also maximize machine throughput, while reducing costs associated with machining, including electricity usage and tool replacement costs.

2.3.3 Condition Monitoring and Fault Detection

Ensuring machine reliability is of key importance. As mentioned earlier in section 2.2 one of the best ways top do this is to implement PM via CM and fault detection. CM ensures that MTs are working as intended. In addition to just monitoring the condition it is often useful to visualize this data. Several papers created dashboards containing real-time data for process monitoring. In a paper by Guo et al. [52] they created a real time virtual twin dashboard containing information such as spindle speed, operating temperature, and currently running CNC code. Xie et al. [150] created a framework for cutting tool degradation and a dashboard to display information about the condition of the tool which can be seen in Figure 2.14. Wang et al. [141] created a real time condition monitoring dashboard for a die cutting machine. Parameters such as machine availability and productivity are constantly being updated

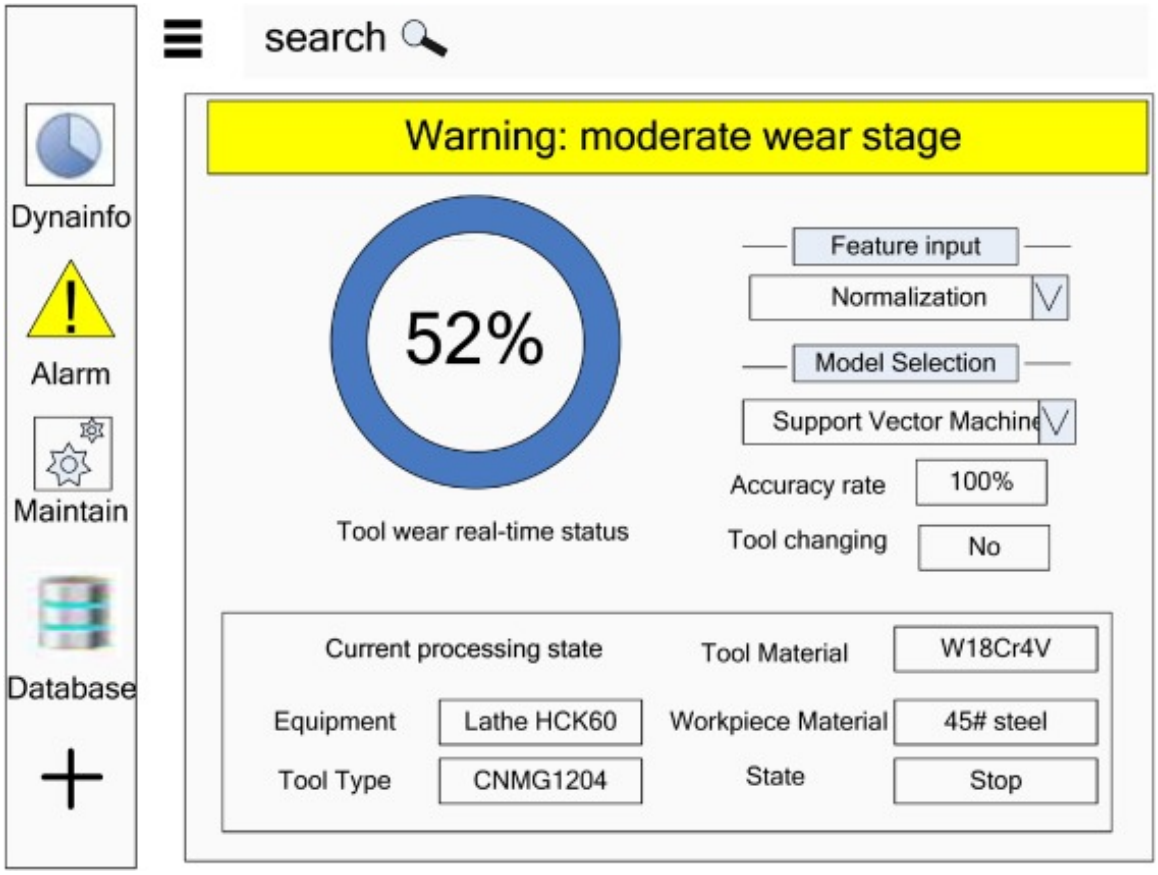

Figure 2.14: Tool monitoring dashboard [150]

and displayed for the user. Stan et al. [130] built a web based platform to monitor the process of robotic de-burring. Botkina et al. [18] proposed a framework for a DT of a cutting tool. They proposed a method of "tweeting" which periodically update the model of the cutting tool to reflect the updated condition.

An important function of condition monitoring is the ability to predict the RUL. This allows the optimal replacement of components, maximizing their life while minimizing the impact of poor performance or possibility of unexpected downtime. Hybrid data-based and model-based solutions for prediction of performance degradation and RUL were proposed by Yang et al. [153], and Luo et al. [90]. They both found that

the hybrid method performed better at predicting the replacement time than just a model-based or data-based method. Baig et al. [15] implemented an artificial neural network (ANN) to predict tool life in turning operations using vibration data and cutting parameters. Weckc et al. [144] monitored clamping force to estimate tool wear and to ensure proper clamping of the work piece was maintained during operation. In addition to estimating RUL it is useful to be able to identify and diagnose fault states. Xue et al. [151] built a model library of various fault states to diagnose faults in a MT spindle using ML.

Effective CM, fault detection are essential in maximizing machine reliability and performance. This is especially true for MTs where they often exist in an interdependant manufacturing system and are expected to maintain sub 0.001"(0.025 mm) tolerances, and are expensive capital investments. Because of these conditions and expectations there is a need for high throughput and to maintain high reliability. MTDTs have demonstrated that they can help achieve that goal.

Chapter 3

Experimental Setup

The experimental setup will be used to test various CM, fault detection, and control methods. These methods include estimation based methods such as utilizing the IMM based fault detection method mentioned in section 4, ML methods, and applying advanced control methods such as model predictive control or cognitive control.

There were two primary stakeholders in the design of the workbench: The industry sponsor Ford motor company who wished to utilize this experimental setup to design and test movements to quickly determine the state of health of their machine tools, and for academic purposes for collecting data and validating methods created for the various purposes mentioned above. In order to meet the needs and desires of both stakeholders several criteria, constraints and considerations need to be made.

The constraints and criteria of the design are discussed in section 3.1. After design criteria have been determined an examination of all the design considerations is made in section 3.2. The design process is discussed in section 3.3 and final design in section 3.4. The assembly of the system as well as the integration of all components are discussed in section 3.5.

3.1 Constraints and Criteria

Each of the two primary stakeholders in this research had their own set of constraints and criteria. Both sets of constraints and criteria needed to be met.

3.1.1 Industry Sponsor Constraints

The Industry sponsor of our project is Ford automotive. Their specific division is the manufacturing division. Their goal with funding this project is to get a greater understanding on how to translate signals collected from their CNC MTs into identifying and diagnosing faulty components in the LFDs of these machines. Their intermediate goal would be to run a quick set of movements which could be used to diagnose issues in their feed drive, such as a faulty ball screw or linear guide. Long term they would wish to do this diagnosis using data collected from regular production. By doing this they could Identify faulty machines without interrupting production. Their primary interest is identifying faults and issues with ball screws, as this seems to be the component that wears most rapidly in each of the linear feed drives of their machines.

Ball screws used in machine tools tend to have high levels of preload, often 6% to 10%. As a result they desired to use a ball screw that was preloaded at least 6%. Additionally, they wanted a screw that was preloaded via a double nut as that is what is used in each of their machines. Ideally they desired a stroke similar to that of the axes on their machine tools. Each of the stroke lengths of these axes was approximately 1000mm (1267mm, 952mm, 1022mm). Screw leads should be similar to that of the production machines (20mm, 30mm).

They have also indicated that they do not wish to implement additional external

sensors, preferring to use their internal sensors mentioned in section 3.2.3. For maximum compatibility and ease they preferred that the same CNC controller was used that is used on the production machines. This ensures that data collection procedures, CNC programs, and analysis methods are readily transferable to a production environment.

3.1.2 Academic Interest and Lab Constraints

In addition to the industry sponsors constraints this experimental setup will be used for academic research. The primary interest of research for this experimental setup is ML, estimation theory, and control algorithms. To study these topics additional sensors will be needed beyond simply the integral sensors. Sensors and data collection such as force feedback, vibration monitoring, and temperature monitoring is desired for evaluating the application of NNs for various applications. An external force application method was desired. External forces can be useful for examining how the system reacts under load. It is especially useful for developing control and estimation algorithms as they will need to take into account external disturbances.

There also needed to be constraints on the physical size of the entire system. There is limited lab space available so the footprint of the system needed to fit approximately a footprint of 4 feet by 15 feet so it could occupy an entire wall of our lab. Additionally, since the workbench will be a scaled down compared to an actual machine tool, smaller components such as ball screw, motor, bearings, linear rails, and platform will be used compared to an actual machine tool. The additional advantage of this is that any results obtained can be tested on a system of a different size to compare results and to ensure the system does not over-fit. There are also budgetary conditions,

there is a certain budget to design, manufacture, and assemble the system. Most of the components outside of the CNC control components, and common off the shelf components such as bearings, and fasteners would need to be manufactured in house to minimize costs.

3.2 Experimental Design Considerations

(a) Setup using magnetic brake as an external load [147]

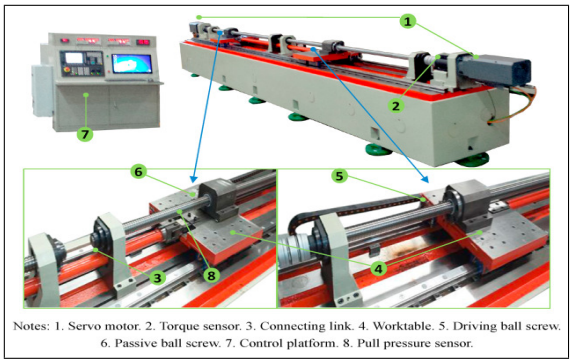

(b) Setup using second motor as an external load [165]

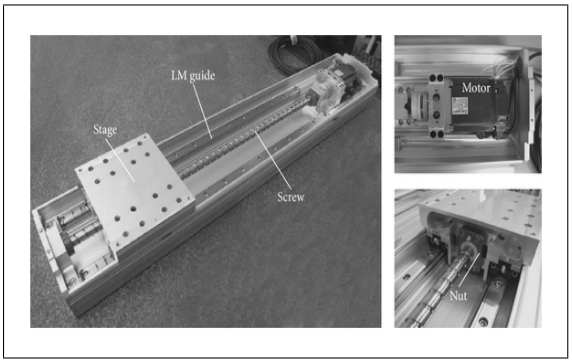

(c) Experimental setup from [79] which is similar to many others in the covered literature

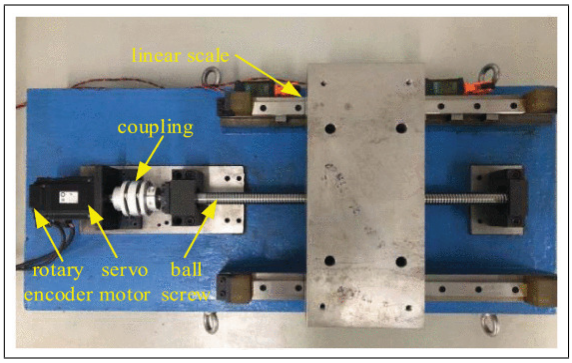

(d) Experimental setup from [62] which is similar to many others in the covered literature

Figure 3.1: A few examples of experimental setups from the examined literature

There are several key considerations that were made when designing this system. broadly they can be categorized as the following:

1. Applying external load
2. Simulating faults and wear
3. Which sensors and data streams to utilize
4. Which software platform(s) will be used to implement the DT, collect data, and control the system

The literature was examined to determine what experimental setups have been used in the past for condition monitoring of linear feed drives and their components, a few of these setups can be seen in Figure 3.1. Results from this investigation were published in two conference proceedings. The first work primarily examined experimental design of linear feed drive test benches and covers sub-sections 3.2.1 - 3.2.3 [121]. The second work covers design considerations for an IoT connected DT feed drive, this work covers sub-sections 3.2.3 - 3.2.4 [119].

3.2.1 Applying External Load

MT LFD experience external loads of various kinds through machining operations such as milling, drilling, and grinding to name a few. External loads can cause forces in both axial and lateral directions. It is often not practical to directly implement these machining loads so it may be necessary to implement some sort of external loading which can simulate these forces. In addition to machining loads, adding a work piece to the worktable will increase the systems mass. Increasing the systems

mass will often accelerate the wear on the system due to increased force demands. Through examining the literature there were several methods to implement external loading. The issue of changing mass is fairly simply solved by implementing a system of adding and subtracting weight plates of a known mass [136, 32]. This allows testing the system with a variety of different masses to examine the effect changing mass has on the system. Applying external loading to simulate machining processes is a more complicated process. Two predominant methods emerged in the literature. One involved using a magnetic brake which was connected to the table via a rack and pinion. Resistance from the magnetic brake would create an external load on the system [147, 162]. One other observed method was utilizing a second motor. One study used a second motor in torque control mode to apply a specific torque to the system [165]. Another couple studies used their second motor as a source of additional inertia [107, 106]. One advantage of using a second motor is that they can be controlled and data can be collected from a single CNC system quite easily. A few examples of applying external loads can be seen in Figure 3.2.

(a) Setup using magnetic brake as an external load [147]

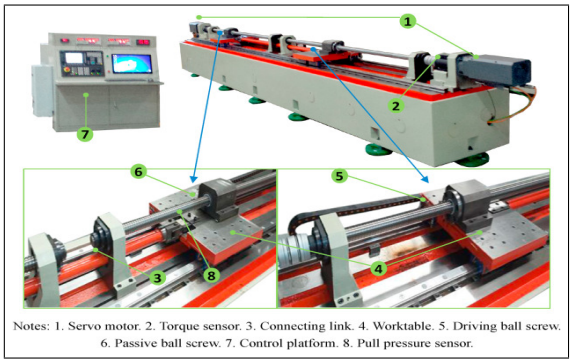

(b) Setup using second motor in torque control to drive a second platform coupled to main platform [165]

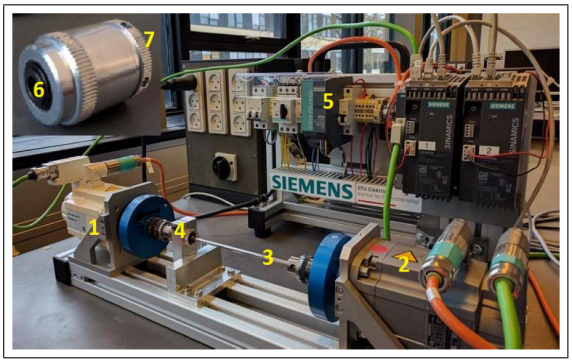

(c) Experimental setup which uses a second motor as additional inertia [107, 106]

Figure 3.2: Examples of external loading in the literature

3.2.2 Simulating Faults and Wear

When developing CM and fault detection applications it is necessary to have a set of data representing a faulty condition. A "Healthy" and "Faulty" set of data are needed to develop, test, and validate any fault detection or condition monitoring methods. For this reason it is necessary to be able to implement or simulate various faults. In a feed drive system there are several typical types of wear and faults. Common types of

faults include the following: lost preload in key components, misalignment, backlash. In addition to these faults general wear will occur on the various components which will cause degradation in performance. There existed examples in the literature of simulating wear and faults on various important components such as ball screws, linear guides, couplers, and bearings.

Simulated and Accelerated Wear

One possible method of obtaining worn components is by utilizing worn components from production, this approach can generate a great deal of data, and wear will follow what is seen in production use [67]. However, one issue with this approach is that you have little to no control or understanding of the contributing factors that caused this wear.

A different approach would be to directly apply the wear in a lab setting. There are several ways in which this can be accomplished. One method is running the system under heavy load as with heavier applied load comes faster wear. It is also possible to simply run the system over a small section of the stroke continuously to accelerate wear in a small section [83]. One other approach would be to contaminate or starve the lubrication system [137]. Adequate and clean lubrication are required to keep proper operation of a linear feed drive. Introduction contamination or removing it entirely will have the effect of prematurely wearing the system. One final method that was examined was directly machining wear into the component. Examples of this may include grinding a notch into a linear guide [139], bending a ball screw [85], or drilling a pit into a ball screw raceway [114].

Preload

Preload is an important factor in maintaining rigidity in ball screws and linear guides. Preload generally degrades over time with the degradation of the ball bearings and raceway. There are a few approaches to simulate decreased preload. One relatively simple method is by swapping in components of different levels of preload [27]. For example if the "healthy" condition is considered to be at 6% preload, a 2% preload screw could be swapped in to simulate the degradation of preload to a lower level. One other approach would be to replace the ball bearings with ones with a different diameter [41]. For example if a ball bearing of a diameter that is 1μm smaller would to be used preload would decrease. A final method which is more complicated but offers more control and adjustability would be to use a double nut with and adjustable preload spacer [100, 40, 39]. This would allow easy and exact adjustment of preload levels.

Misalignment

Misalignment is a common fault in machinery. There are several different types of misalignment such as angular, parallel and combined misalignment. These misalignment can occur between the various components such as the ball screw and linear guides, or the motor and ball screw for example. Misalignment can cause increase friction and wear, or cause incorrect travel trajectories in various axes. There are a few ways to implement misalignment. One of these ways is to use feeler gauges to force the components into a state of misalignment [41]. One other common method would be to adjust the position of components into a misaligned position and re-secure them there [33].

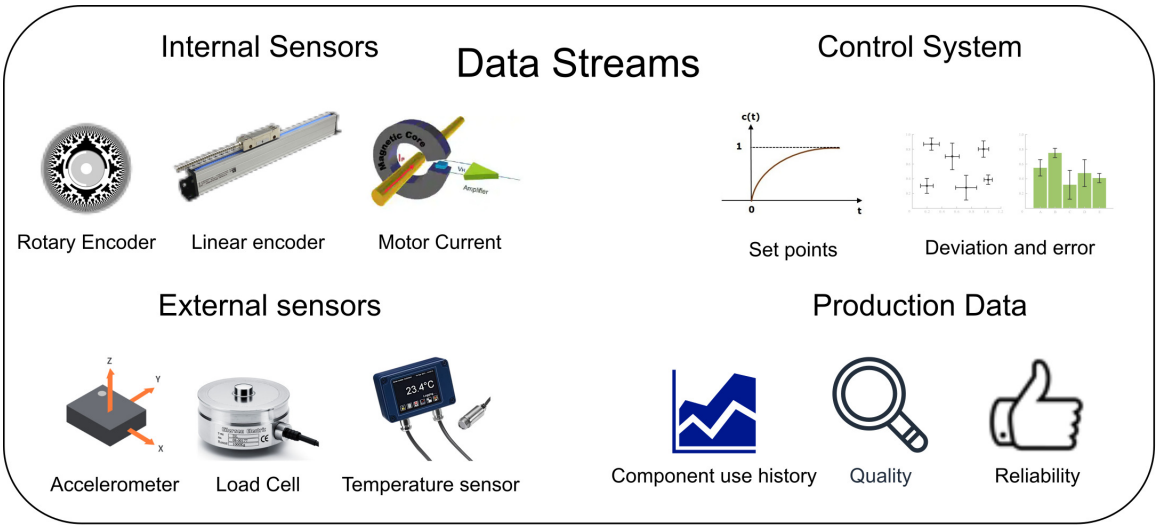

Figure 3.3: Data streams in an CNCMT [119]

3.2.3 Sensors and Data Streams

Selecting data streams is an important process in any data driven analysis. In a CNCMT system there are several possible data streams which can provide useful data, an overview can can be seen in Figure 3.3. These include the following:

1. Internal sensors
2. External sensors
3. Control system
4. Production data

Internal Sensors

As previously discussed in section 2.2.1 Internal sensors are defined as the sensors integral to the regular working capabilities of a regular CNC system. These would

include encoders and current measurements. CNCs use encoders, both linear and rotary, to determine the position of the various axes. They also typically measure the motor current to estimate the amount of power going into moving the various feed drives or rotating the spindle. These sensors can provide valuable information such estimated backlash, tracking error, and power consumption which can each be used for analyzing and detecting wear, misalignment or other faults. A few examples include the following: Xi et al. used stalling motor current to observe the effect of preload of friction in their experiment [149]. Chandrasekar et al used the difference in linear and rotary encoder to quantify backlash [26].

External Sensors

In addition to the sensors integral to the working of the CNC system, external sensors, those being non-essential to the function of the system, can be used. Popular sensors used for condition monitoring and fault detection include accelerometers, load cells or torque sensors [165], and thermometers to measure vibration, force, and temperature respectively. These data streams are common as increased vibration, force, or temperature are usually the result of wear, misalignment, or other faults. In addition to these sensors there are other sensors which are used. Inertial measurement units combine gyroscopes and accelerometers to complete measurements of position and orientation [139]. There have also been instances of using microscopes [147], or cameras [168] to take pictures or videos of components to track their condition over time. Strain gauges could also be used to directly measure deflection and strain in a system [136].

Production Data and Control System

While not as applicable in the LFD test bench, production data can provide valuable insight. This could include information such as component use history, quality, and machine reliability. Component use history means how many cycles or hours a component has been used, as well as what types of movements or actions were being performed. For instance it may be the case that a machine does certain movements only in a certain stroke of one of the axes which results in excessive wear in that part. Examining the quality of the produced parts can give insight into whether the machine is in good condition or not. If there are several machines producing the same part and one is producing parts of inferior quality it may be the case that that machine is in poor condition. Finally examining the reliability of the machine could uncover component health issues if it is constantly going out of service.

In any CNC system there will be a constant stream of data created from the various set points, whether these are the position, velocity, acceleration of the various axes, or the set points for the torque of the various motors of the system. This data is especially useful for comparing to actual positional or torque set-point to analyze the difference.

3.2.4 Computer Numerical Control Platforms

When designing the LFD test bench it is important to consider the software and hardware platforms that will be used. There are a few considerations as to what software will be needed. The primary considerations are going to be for the following:

1. CNC controller

   (a) Motor drives

   (b) Data input/output

   (c) Programmable logic controller (PLC)

2. Data analysis and storage

   (a) Data acquisition (DAQ)

   (b) Cloud

   (c) Local

3. Modeling and simulation

   (a) Computer aided design (CAD)

   (b) Computer aided engineering (CAE)

   (c) Computer aided manufacturing (CAM)

   (d) Other modeling software

4. Digital twin platforms

Machine tools function using a CNC controller, which controls the various components such as the feed drives and spindles, The PLC controller collects various data streams and sends various control signals to the numerous components using data collected from a data I/O system. For analysis, data will need to be collected via a DAQ and analyzed locally or on the cloud. For the digital part of the DT there needs to be software capable of fulfilling the various modeling and simulation needs of the system. In a production environment you would also want to collect production data, often this would be stored in an ERP system or a database. For the purpose of this test

bench the ERP system is not considered as production data will not be considered in the analysis. Many companies now offer DT platforms which can make designing and building a DT platform much easier.

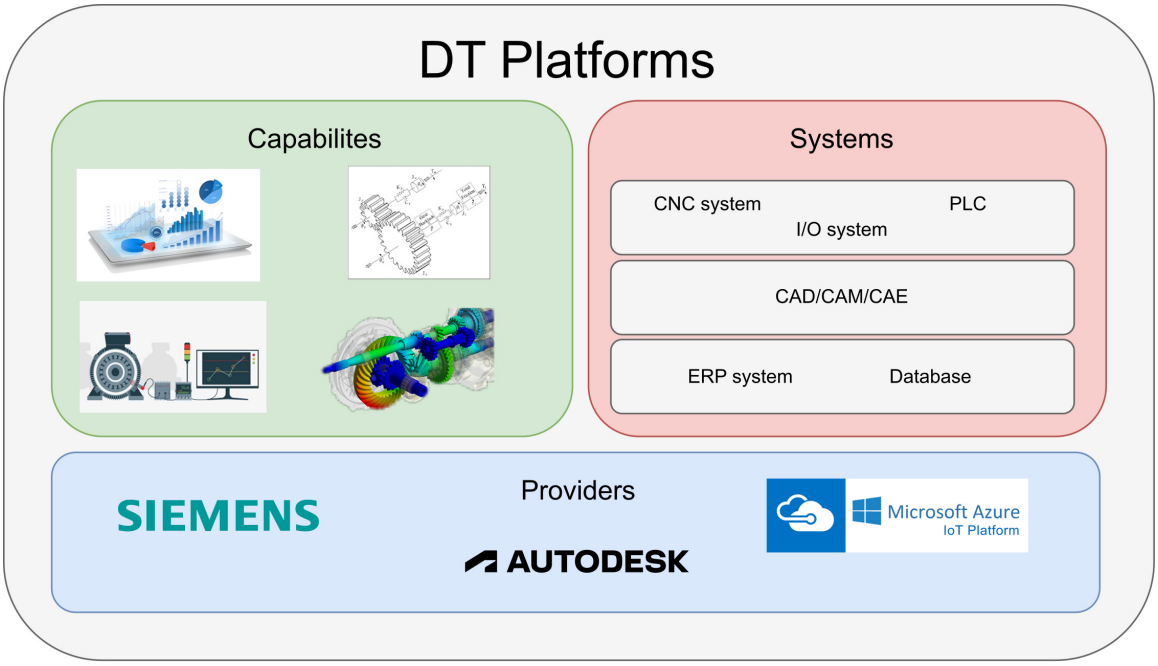

Figure 3.4: Requirements for DT platforms for a MT DT [120]

Controller and Data Acquisition

First, the CNC system will need to be selected. There are a few popular options that are popular in industry such as Fanuc, Haas, Heidenhain, and Siemens. Additionally there are popular hobby grade CNC controllers such as Mach 3 and Linux CNC[143]. CNC systems have several important roles in a machine tool. They deliver the signals to the various drive components, and collect and deliver control signals via the I/O system and PLC. The CNC system converts NC programs into sets of controls which execute in real time. When considering which CNC system it is important to consider

the application of the MT test bench and the various stakeholders. If for example, the DT is designed to be implemented in a production environment where all FANUC controllers are used, it would make sense to develop the test bench using the same FANUC platforms. Cost needs to also be considered, CNC systems, especially ones from large industry companies such as Siemens or Haas will be much more expensive than hobby grade ones such as Mach 3. However, industrial CNC controllers and software will also have greater capabilities.

Data Analysis and Storage

Data will need to be collected and analyzed from the system. The first consideration is data collection, some CNC systems may have built in data collection for external sensors, but some may not, and therefor require a DAQ. Data collected from the various sources outlined in section 3.2.3 will likely be heterogeneous, with different sampling frequencies, data types, and quality or reliability. A system is necessary to collect, process, and organize all this data.

After the data has been collected it needs to be analyzed. Analysis can happen primarily in two difference locations: locally, or on a centralized database or the cloud. There are advantages and disadvantages to each. Local analysis via edge computing has the advantage of lower latency data transmission and analysis. Data streams such as accelerometers will generate very high frequency data which can be several GBs after only a few minutes of data collection. It would not be feasible to stream this amount of data to the cloud. Often critical features such as amplitude of vibration at key frequencies can be extracted from this data and the raw data can be discarded, this would most feasible done on local edge computing. Some analysis or

services would also require low latency analysis. For example, if real time in process temperature or vibration monitoring were desired, edge computing would be required due to latency constraints.

Cloud computing or a central database has some advantages as well. They are valuable when collecting data from multiple machines and analyzing and comparing them to each other. It can be useful for services such as a dashboard comparing multiple machines to each other, or trend analysis of various machines. Cloud computing is best used if a great deal of computing power is required. A central computing entity can be used for efficient use of computing power rather than a less efficient distributed system.

Modeling and Simulation

There are various modeling and simulation needs for DTs and their services. There are several types of models that can be used. One of the most commonly used will be a geometric model, these are usually created using CAD platforms such as SolidWorks, Autodesk Inventor, or Siemens NX. Other models such as block diagrams or other coding methods for mathematical modeling of multi-domain dynamic systems such as using MatLab Simulink or other conventional programming languages such as Python and its various packages. Data driven models such as neural networks can also be used, these models are often created using Python, MatLab, or many other programming languages.

Simulation is another important part of DT modeling. There are several different types of simulation that may be useful. One common type of simulation is manufacturing process simulations which are often accomplished using CAM software.

Software such as MasterCam, NX, Fusion 360 allow the visualisation and simulation of various manufacturing processes. Simulations such as thermal, bending, and vibration modeling can be performed using finite element analysis, a type of CAE software. FEA is very popular for determining theoretical responses of systems to given inputs, this can be compared to experimental results to validate the accuracy of the model. Popular FEA software includes ANSYS, Autodesk NASTRAN, and Solidworks. Dynamic simulations of the system which analyze the kinematics of systems can be performed. These simulation can give insight into the various velocities, forces, and stresses experienced through a range of motion as well as given insight into possible conflicts or collisions. Popular kinematic software is often included in popular CAD platforms such as Inventor and Solidworks. Siemens also offers a comprehensive simulation platform called mechatronic concept designer (MCD) which can also interface with simulation PLC program simulation. The response of various mathematical physics-based models can be simulated to determine their response as well. Software such as Matlab can be used to simulate these models and understand their response to various inputs and conditions.

Digital Twin Platforms

In recent years there has been booming interest in DTs. As a result, many companies have developed and are now offering DT building software. This software is often offered as add-ons or modules to existing software platforms, or as stand alone packages. CAD platforms offer their own DT platforms. Dassault offers 3DEXPERIENCE and Autodesk offers Autodesk platform services. Large tech companies such as Amazon and Microsoft offer their own DT and Iot platforms, with AWS IoT and Azure IoT

respectively. Siemens offers a DT suite for their machine tools and other mechanical systems with their Sinumerik One CNC platform and their NX MCD modeling and simulation software.

3.3 Design Process and Manufacturing

After examining the design considerations and what has previously been done in the literature, this information and knowledge can be synthesized with the design criteria and constraints to form an initial design plan. There are two main design components in this system, the mechanical system, and the electronic control system.

3.3.1 Synthesizing Criteria with Design Considerations

Both the industry sponsor and academics interests needed to be taken in to account when determining the final constraints and criteria. After evaluated the previously discussed constraints and criteria a final set was determined which would drive the design.

For the physical system it would be driven by a 7% preloaded double nut ball screw with a stroke of approximately 800 mm. This is less than the 1000 mm stroke of the screws used on the production machines but still allow for adequate stroke to achieve high acceleration and velocities. This would allow it to fit on the allowable footprint. A 7% preloaded ball screw is loaded similar to what would be expected in a machine tool. The diameter of the selected ball screws was 20 mm and they had a 20 mm lead. This is smaller than lead screws on the machine tools which was 40 mm but was within the allowable range for the lead screw. The other components

such as the bearings, motors, and linear guides would be sized appropriately for the expected loads and velocities. Servo motors with equal or greater maximum speeds would be used to ensure the same table velocities could be achieved. They would also need adequate torque to quickly accelerate the system.

The primary interest for simulating faults and wear was in ball screw wear. In anticipation of testing multiple faults and degrees of wear, multiple ball screws were purchased. Before any faults are implemented using the methods in section 3.2.2 baseline data would be collected to determine the "healthy" state. The linear guides and bearing were of secondary interest. Because the linear guides and bearings are common standardized sizes additional ones can be purchased and wear and faults induced at a later date. The system would be designed to allow some misalignment so that the effect could be observed.

The tests and movements developed on the test bench would need to be easily applied to the production equipment. To easily facilitate this the same CNC control system would be used as the production equipment. Siemens CNC equipment was used as that is what was used on the industry sponsors machine tools. Analysis performed for the industry sponsor could only use the integral sensors described in section 3.2.3. These sensors were prioritized but an additional I/O module would be included which would allow the addition of digital and analogue sensors described in section. Additional sensors could be added for other types of analysis such as vibration monitoring and machine learning. To summarize:

- 7% preloaded ball screw with stroke of 800 mm, lead of 20 mm, and diameter of 20 mm
- Servo motors capable of high torque and up to 6000 RPM rotational speed

- Focus on ball screw with multiple ball screws to test various faults and wear states.
- Focus on analysis using integral sensors but include module to attach external sensors
- Same control system as Ford so tests and analysis is easily transferable

3.3.2 Mechanical Design

For the mechanical system the primary design challenge would be to create an external loading system to simulate disturbance forces such as milling and drilling. It would also be important to design components which could withstand the expected forces experienced during operation while also be sufficiently inexpensive, easily manufactured, and assembled. It would also be important to design a worktable which could hold and enclose the system to ensure safety given that there would be moving components moving at high speeds with high force capacity.

External Loading

The basic structure of the feed drive was relatively simple as most feed drives consist of a platform with a ball screw centered between two linear guides. The more difficult process was determining how to do the external loading of the ball screw. There were a few options for loading externally: a magnetic brake, linear motors, or additional ball screws. One issue with magnetic brakes is that it would be difficult to control the applied force. Ideally any external loading system would involve an easily controllable motor, for this reason the magnetic brake option was eliminated. Early versions of this

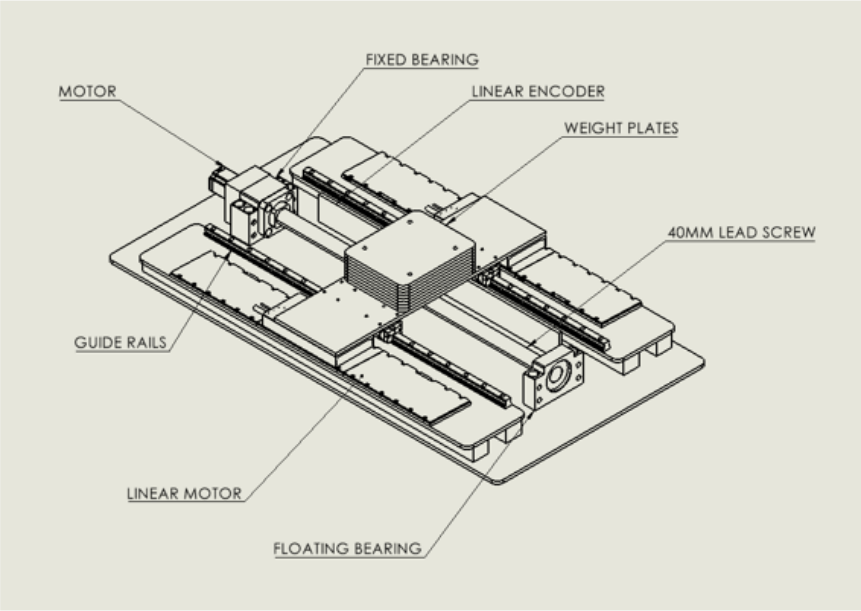

Figure 3.5: Early design with linear motor

design involved the use of a linear motor to function as the external force generator as seen in Figure 3.5. A few issues arose from this design. The primary issue was the large size of the linear motors, using linear motors would are substantially increased the footprint of setup in both width and length. A side effect of this is also a decrease in effective stroke. Linear motors also generate a great deal of heat and require an external cooling system, this would increase the cost and complexity of the system. So with these options eliminated the last of the original considerations was an additional ball screw controlled by another servo motor. After discussing with Siemens, they had made it known that their control systems was capable of having two motors driving against each other in a "master-slave" arrangement. With this in mind there needed to be a design to incorporate a second motor to act as a disturbance force. Multiple instances in the literature had utilized an additional servo motor to simulate external forces. The two discussed earlier the primary issue was the location of the applied

force. In [107, 106] the motor was coupled to the end of the end of a shaft connected to the motor, and in [165] the secondary motor was connected to a second stage which was coupled to the primary platform. Initially it was considered of connecting one or two additional ball screws underneath the platform to apply the external force. However, there is issues with either of these approaches. With one additional screw you would either need to offset both screws from the mid-line, or you would need to offset one. This would cause a torsional force to occur as the force isn't being transmitted down the mid-line. The issue with using two screws is that you would need to either use two motors to drive them or some sort of force distribution like gearing or belts and pulleys. To solve all of these potential issues the external force screw can be placed above the platform. In addition to not interfering with the driving screw it more closely resembles the direction force would normally be applied in which is demonstrated in Figure 3.6. Once the issue of applying an external disturbance force was resolved, the next step would be a system for adding additional weight. Originally the plan was to have loadable weight plates in the middle of the platform, but with the external force screw design, this would not be possible. Instead loadable weight plates were added to each side. Three weight plates of 0.25, 0.5 and 0.75 kg were designed so the system could be loaded an additional 10 kg. This allows the system mass to be modified so that the effect on the system can be observed.

System Platform and Guarding

One important consideration when designing the system was how to align and secure all of the components together. Given the relatively large footprint required for the setup it would be difficult to machine a single base plate for all the components to

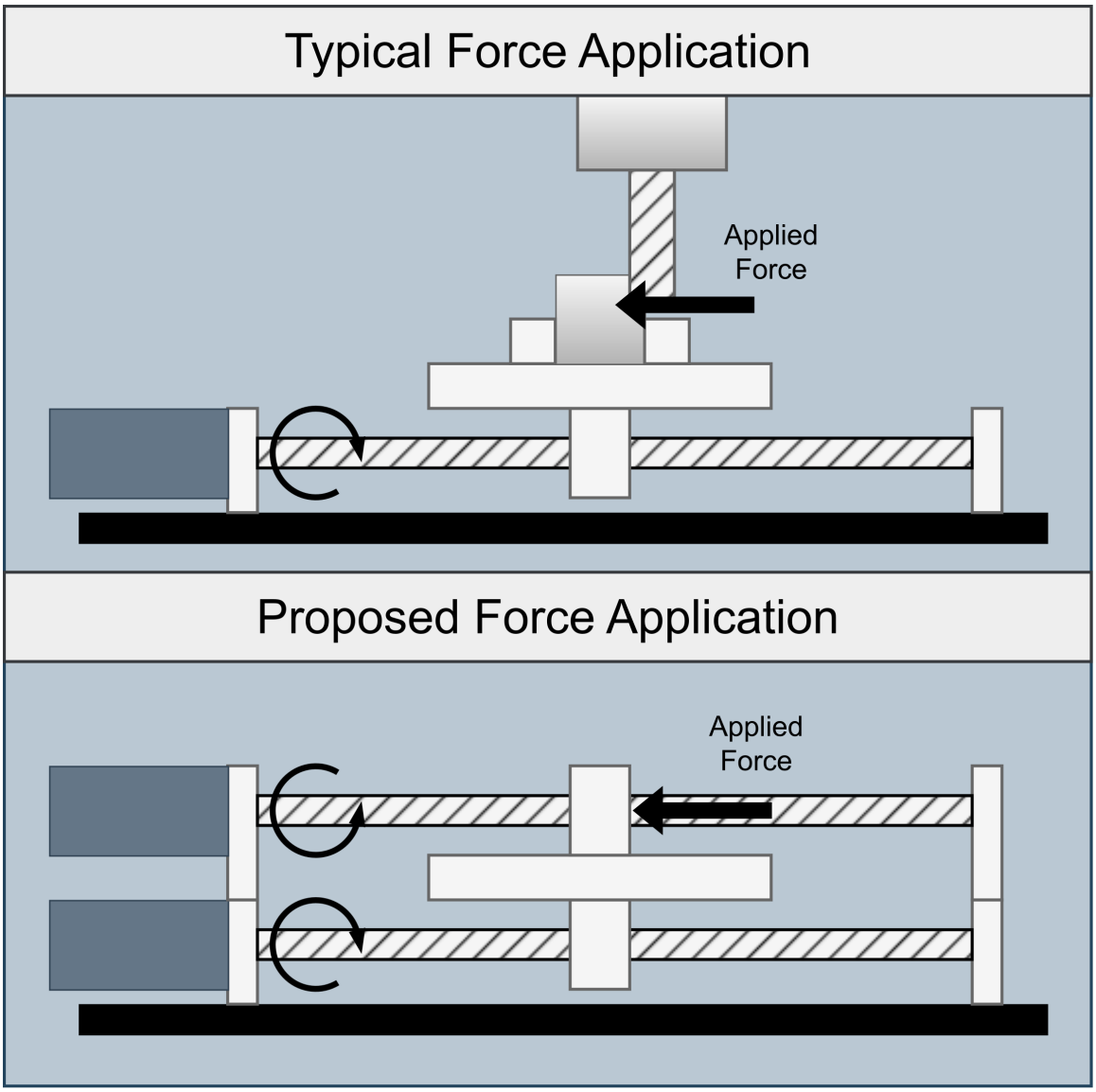

Figure 3.6: Proposed design of external force application

secure to. The original plan was to use large sections of plate steel which would be machined for mounting all other components. This solution would have been costly and require a great deal of time to machine, and any error in machining would likely result in substantial misalignment of the components. Fortunately there are devices called optical breadboards which precision manufactured plates. These plates have threaded mounting holes located every 25mm and a very flat top. They are often used for precise scientific measurement and experimentation. This would be an ideal solution to the issue of precisely positioning and securing all the components together. A large 600 x 1200 mm optical bread board was selected and used as the base plate for the workbench. This base plate was mounted onto a steel topped workbench. The original workbench was not rigid enough along the axis of movement of the platform. So an additional full steel sub frame was added to the workbench to increase rigidity, vibration damping, and weight. After adding this sub-frame the workbench was very rigid in each direction. Vibration damping pads were added beneath each of the eight feet of the workbench. These will help isolate the system from any external vibration.

A cabinet was constructed to act as shielding for the mechanical equipment to ensure there would be no safety issues. The cabinet would need to be see through to ensure that any tests could be observed. There were two obvious choices for the materials for the material for this application: Acrylic, and polycarbonate glass. Polycarbonate glass is known as being more shock resistant, and is therefore more often used in shielding applications. Polycarbonate panels were affixed to an aluminum extrusion frame to create the cabinet guarding the moving parts.

Figure 3.7: Optical breadboard used to mount components

Component Selection and Design

One of the important parts when designing the system was to ensure that each of the components that were manufactured or purchased could withstand the expected loads that would occur during operation. For manufactured parts FEA was performed to ensure that the safety factor of the components was at least 3 for an applied load that was equal to the maximum expected applied load. The maximum load was determined based on the maximum load rating of the ball screw. For the primary ball screws used in this investigation the maximum rated load was 7000N. One of the primary objectives of the design would be re-configurability. This would allow easy adjustment of the system, and to easily replace components such as the ball screws or linear guides. To achieve this most of the individual components would be bolted together. Bolted connections can provide a large clamping force between two objects. If looking at the equation below where F_{clamp} is the clamping force, T_{tight} is

Bolt Size	Tightening torque (N·M)	Clamping force (N)
M5	10	10,000
M6	17	14,000
M8	41	25,000
M12	143	60,000

Table 3.1: Tightening torque and clamping force for grade 10.9 metric bolts

the tightening torque, K the friction coefficient (assumed to be 0.2 for steel on steel), and D the nominal diameter of the bolt.

$$F_{clamp} = \frac{T_{tight}}{K \cdot D} \tag{3.3.1}$$

It can be seen in Table 3.1 that the clamping forces for bolted connections is very high, even for small M5 bolts. This allowed for larger clearance holes to be used. With larger clearance holes there is more possibility to adjust components and to allow for the purposeful introduction of misalignment if desired. For purchased parts it was ensured that the components were rated to loads greater than the expected maximum load. Full details on the purchased components and their specifications can be seen in the appendix.

Part Manufacturing

Most components were manufactured using 1018 mild steel. This material was chosen for its machinability, rigidity, and low cost and ease of availability. The majority of the parts were manufactured from plate steel, and rectangular or square bar. Manufacturing these parts from simple shapes allows low cost manufacturing using tools such as the mill, drill press and water jet. Most of the parts that were designed using square or rectangular bar stock were manufactured on the mill to allow for precise

dimensions with easy manufacturing. The parts that were designed with plate metal or had complex geometries such as the the nut mount were cut from plate steel using the water jet. The water jet can cut fairly complex shapes at a fairly high precision. Certain parts of water jet cut components were completed on the mill where final hole geometries or hole threading could be completed. Parts were then checked with micrometers, vernier calipers, and other measurement devices to ensure conformity to design specifications. Component drawings can be seen in the appendix.

3.3.3 Electrical Drive and Control System Design

Part of designing this system involved designing an electrical control system and cabinet. The primary electrical components include a CNC controller, motor drives, an I/O system. Selection of the components was done using a combination of Siemens design manuals as well as recommendations from Siemens based on the constraints and requirements of the project. Once each of the critical component were selected design of the electrical cabinet could begin. The primary considerations would be selecting proper wire gauges, heat dissipation, electromagnetic interference, and safety. Originally the intention was to include all of the electrical components into a single electrical cabinet. However after some consideration, it was decided that two separate cabinets would be used. One for the high voltage motor control equipment, and one for the lower voltage control equipment. The reasoning behind this decision was to keep the control and I/O equipment, which would regularly need to be accessed, separate from the high voltage equipment which could pose a potential hazard.

One important consideration when designing electrical equipment is heat dispersion. Given the large electrical loads expected with the motor drive equipment it was

important that there was adequate cooling. Cooling can be accomplished several ways but the most common is via fans. An estimate of required air displacement due to heat dissipation can be estimated using the formula (3.3.2) below which uses and estimate of approximately 5% of the rated power of the active line module [124]. Using an ambient temperature of 20°C and an estimated power loss of $900\,W$ $(18,000 \cdot 0.05)$

$$\dot{V}\frac{m^3}{h} = \frac{3.1 \cdot P_L[W]}{40°C - T_{AMB}[°C]} = \frac{3.1 \cdot 900}{40°C - 20°C} = 140\frac{m^3}{h} \tag{3.3.2}$$

With the required air flow an appropriate fan could be selected for the system. In addition to considerations of heat dissipation it was important to consider possible electro-magnetic interference. It was important to lay signal cables as far away as possible from power cables. Siemens produced a manual for design around this interference which recommended separating the 400V power cables from any signal cables approximately 20cm away. The cables could cross or come in near proximity if needed but it should be minimized. In addition to the above consideration proper electrical safety precautions were taken such as ensuring appropriate grounding connections, ground fault detection, and appropriate circuit breakers were used.

3.4 Final Design

The overview of the complete final design of the system can be seen in Figure 3.8. There are a few main components which are described in the sub-sections below. The electro-mechanical system has 6 primary components: the LFD workbench, the operator interface, the low-voltage control cabinet, the high voltage motor control cabinet, the computer workstation and the motor control panel.

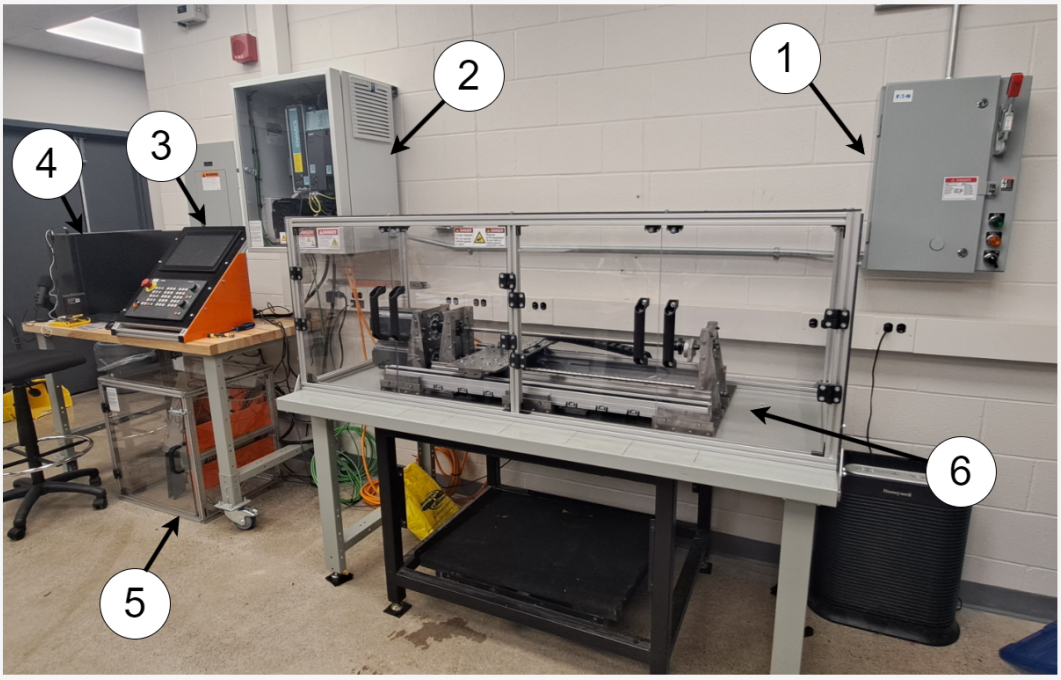

1. Motor Control Panel
2. Motor Drive Cabinet
3. Machine Interface
4. Computer Workstation
5. Control Cabinet
6. Mechanical System

Figure 3.8: Full system overview

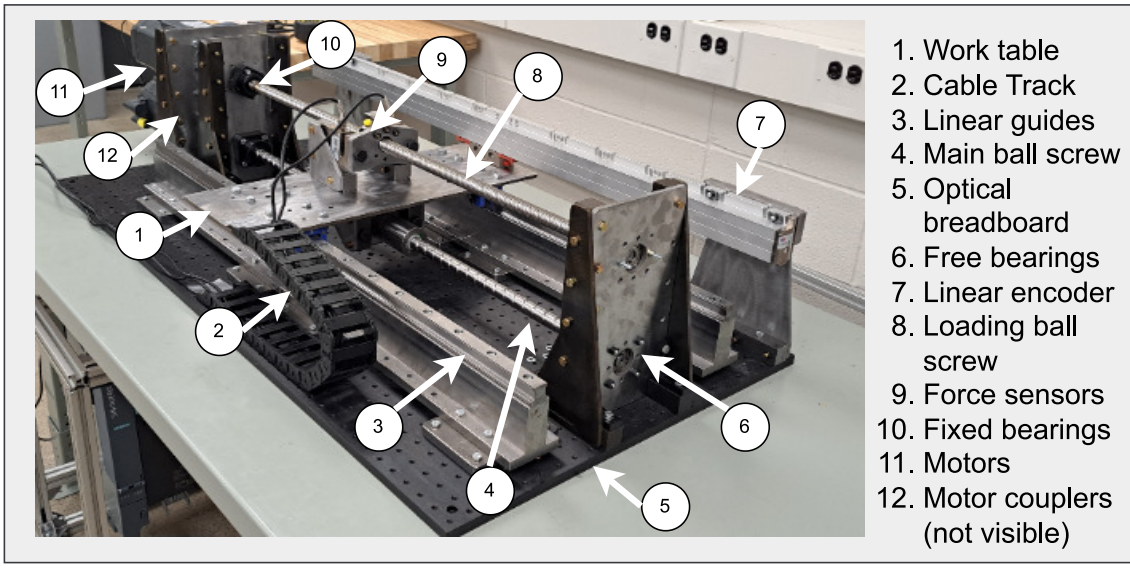

Figure 3.9: Full mechanical system overview

3.4.1 Linear Feed Drive Workbench

An overview of the key components of the mechanical system can be seen in figure 3.9. The system is very similar to other LFD experimental setups in the literature which can be seen in Figure 3.1 with a few key novel design features. Similar to most other linear feed drives, the system is primarily composed of a work table (1) which moves along a track guided via linear guides (3). The table is moved via a main ball screw (4) which is mounted via an axially fixed bearing (10) and a free bearing (6). The ball screw is rotated using a AC servo motor (11) which is connected using motor couplings (12). These parts are connected to an optical breadboard (5) which allows easy alignment and connection of each of the parts.

Similar to many MTs the system is also equipped with a linear encoder (7). Linear encoders are useful for accurate linear position measurement. Most servo motors contain a rotary encoder which is coupled to the motor rotor to measure the angular

displacement which can be translated to a linear displacement measurement. The issue with only using only rotary encoder is that it does not take into account the fact that the system is not perfectly rigid, a linear encoder coupled to the worktable will give a more accurate position measurement. There is also a cable track (2) attached to the system. Cable tracks ensure proper cable management for any cables mounted to the worktable. The linear encoder and force sensors (9) both have cables which need to be routed to the control cabinet. The primary unique part of this system is the loading ball screw (8) which was discussed in section 3.3.2. The secondary loading ball screw allows for simulation of an external disturbance force using a second servo motor. This force is measured using the two force sensors and through the motor torque in the control system.

One of the primary design factors for this system was adjustability and reconfigurability. To achieve this each of the parts was to be bolted together and easily assembled together. It is important to be able to easily be able to swap in different ball screws of different wear, lead, diameter, and preload to examine the effect on the system dynamics. A bolted design with some clearance in the bolted holes would allow for the introduction of some misalignment to examine the effect.

3.4.2 Electronic Control Components

There are 5 primary components of the electrical system. An overview of the electrical system can be seen in Figure 3.10 more detailed drawings and diagrams can be found the appendix. The first component is the motor controller panel which can be seen in Figure 3.11a. The building primary high voltage line is 3 phase 600 VAC, this is above the range of the motor control equipment. The first component is a step

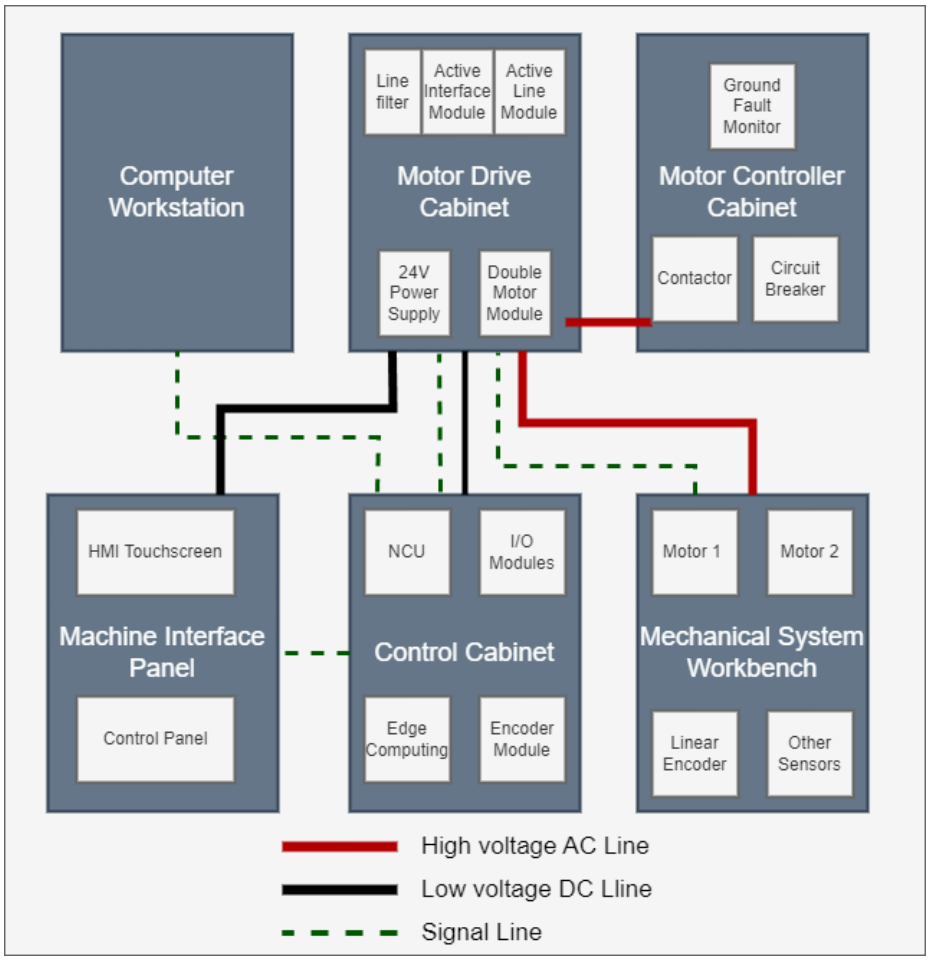

Figure 3.10: Overview of electronic components

down transformer to 415 VAC, which is within the allowable operating range of the motor control equipment. The system has a 40amp circuit breaker which is operated via a large lever. There is ground fault monitoring equipment installed to detect any current leakage that could be dangerous to both operators or equipment. Finally, there is a contactor which is activated via a switch on the panel and can be interrupted via the ground fault monitor if a fault is detected.

Once the motor controller is activated current can flow to the high voltage motor drive cabinet as seen in Figure 3.11b. The high voltage motor drive cabinet has two

primary purposes, to power and control the motors, and to supply 24 VDC power to the control equipment. The 3PH 415VAC power enters the cabinet and is distributed to two components. The first of these is a 24 VDC power supply which steps down the voltage and converts it from AC to DC current. 24 VDC is the power supply used by most of the control equipment for the rest of the system. The second destination for the current is the line filter. The line filter is designed to attenuate conducted interference emissions. After the fine filter the current travels to the active interface module which filters the power input and ensures a steady voltage supply to the next components the active line module. The active line module converts the 415 VAC power to 600 VDC. It ensures a constant regulated DC voltage will be supplied to any attached motor modules. Active line modules can also feed back energy into the supply line during motor breaking. The attached motor module converts the supplied 600 VDC back to AC voltage. It can run up to two AC servo motors. Communication within the system is handled via Drive-CliQ cables which are RJ45 cables. These cables transfer data between components within the high voltage control cabinet and to other control equipment in the control panel and control cabinet.

The control cabinet contains all the lower voltage equipment required to control and operate the system which can be seen in Figure 3.12b. The primary component of this cabinet is the Numerical control unit (NCU). The Sinumerik ONE NCU 1500 is the "brain" of the system and the main computing and control system. All of the communication within the system converges on the NCU. In addition there is an I/O system which contains both digital and analogue I/O. This enables the connection of both analogue and digital sensors such as accelerometers, temperature sensors, and force sensors. Additionally the interface for the linear encoder is connected in this

cabinet. The Sinumerik Edge industrial PC is also located here. This industrial PC is used for edge computing functionality.

The final part of the electric components is the operator interface which can be seen in Figure 3.12a. The control panel has two key components: the touch screen display, and the control panel. This is the interface that will be used to control the linear feed drive such as to jog each of the axis, select which program to run, check for any error codes etc. There is also a computer workstation next to the setup. This computer is equipped with the software provided by Siemens for commissioning the setup. The main software is Siemens total integrated automation (TIA) portal. This software is used for configuring the CNC system and creating PLC programs to run on the NC system. Additionally the system is equipped with Siemens NX and MCD, which is used for simulating the movements of a machine. This software is advertised as a DT software as it can be used to create a virtual replica of the equipment along with the processes.

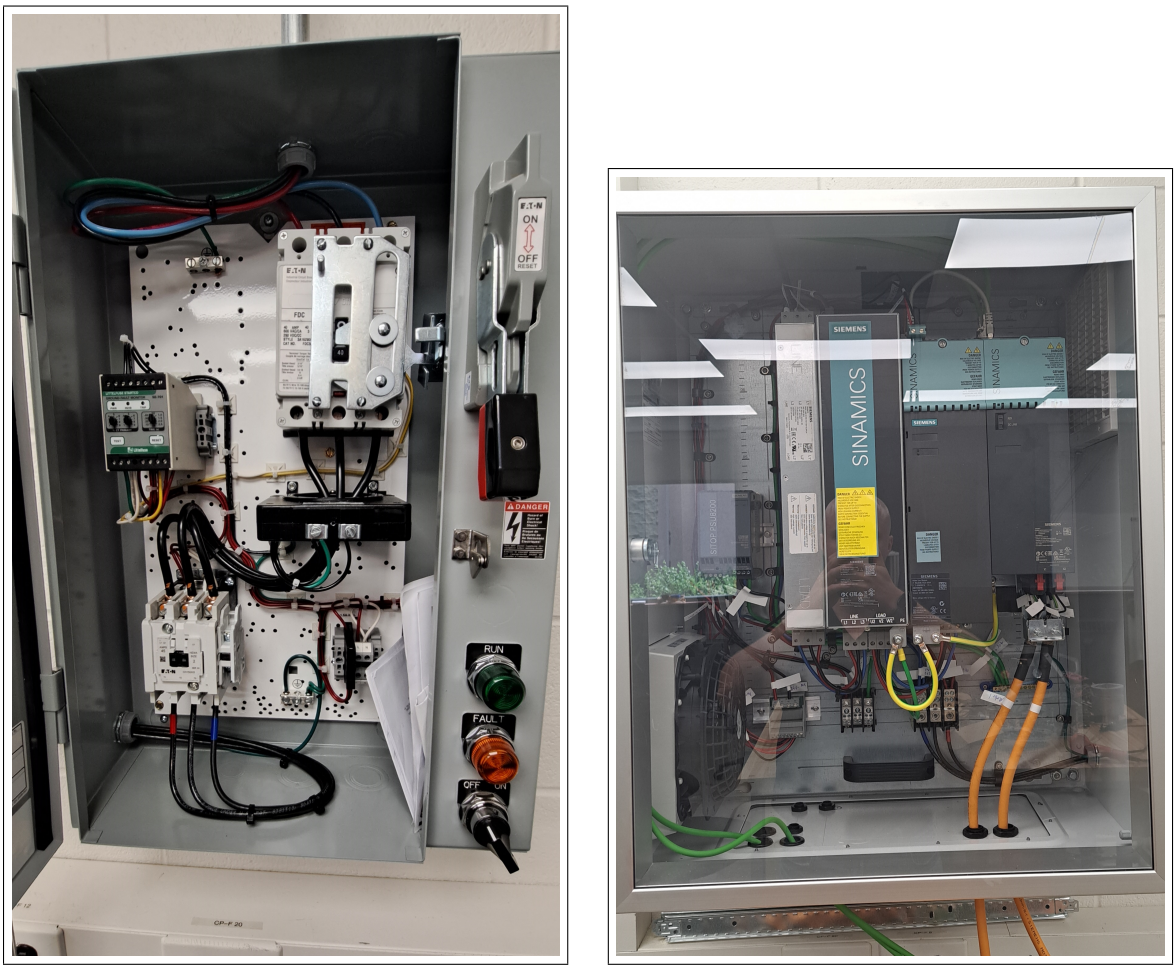

(a) Motor control panel (b) High voltage motor drive cabinet

Figure 3.11: High voltage electrical components

(a) HMI and computer with Siemens control software

(b) Control cabinet containing NCU, I/O, and Edge computing devices

Figure 3.12: Low voltage control components

3.5 System Integration and Programming

Once the final design was complete it was necessary to assembly an connect the entire system. On the mechanical side it would be important to assemble and align all the components. For the electrical side it was important that the system was safe given the high voltages and current. It would also be necessary to program the system.

3.5.1 Mechanical Assembly and Alignment

Given the nature of the many bolted connections and the limits on space it was necessary to assemble the setup in the correct order to ensure access to each of the fasteners. One other important consideration when assembling the system was ensuring alignment. To ensure the system was aligned a combination of 1-2-3 blocks, calipers, and dial indicators were used to align the system. First the sub assemblies for the free and fixed bearings and motor mounts were assembled and aligned. 1-2-3 blocks were used as a flat edge to align the each of the components. The components were then clamped in place, doubled checked for alignment and then fastened together. Once the sub assemblies were complete there were placed on the mounting plate. First the two bearing mount sub-assemblies were mounted, they were initially positioned using the micrometer, once approximately in position they were moderately tightened in place. Next, alignment was checked by using the dial indicators. The edge of the mounting plate was used as a straight reference and the displacement from the edge from each side was measured. If noticeable misalignment was measured ($>\pm$ 0.25mm) the component was adjusted into place using a rubber mallet. Once adjusted it it was double checked for alignment and fully secured. This process was repeated for the

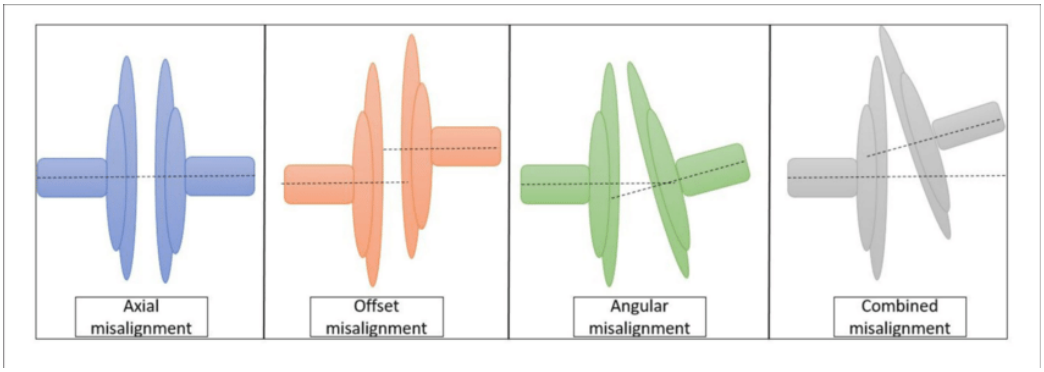

(a) Types of misalignment [5]

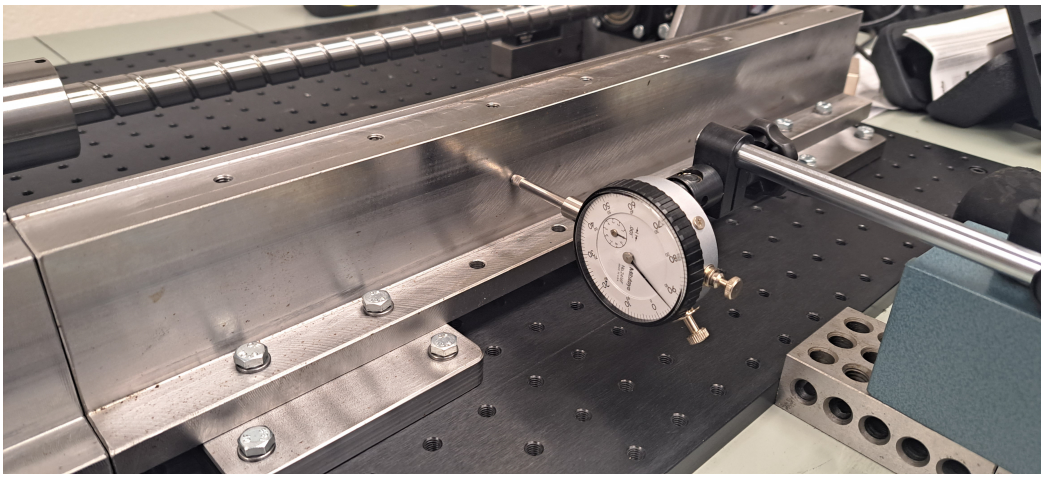

(b) Alignment using a dial indicator

Figure 3.13: Alignment of the workbench components

motor mounts and the linear guide mounts. The most important parts to align were the ball screws and the linear guides, there is some allowable misalignment allowable but it was desirable to keep it below about $>\pm$ 0.1mm per meter of stroke which is a common threshold among moderate to high accuracy equipment. There are multiple types of misalignment possible including radial offset misalignment where the center axis of the shaft is parallel to the guides, but offset the center some distance, or angular misalignment where the center of the axis isn't parallel to the linear guides. A similar approach as was used with the bearing mounts was used for alignment of the ball screw. The main difference this time is that both the vertical and horizontal directions needed to be considered. To adjust the position of each end of the ball screw the bearing mounting bolts were loosened and moved into position. After the ball screw shaft was sufficiently aligned the linear guides were installed. A similar alignment process was used to align the linear guides but only in the horizontal direction. The linear guides had a reference edge to press up against, the shaft was adjusted as needed to properly align. The final component to align was the linear encoder. The linear encoder needed to be aligned in both the vertical and horizontal directions to ensure there would be no damage during operation. Once all the components were aligned and the workbench was moved into place it would need to be leveled. It is necessary to level the workbench because the floor was uneven. If the workbench were to be uneven it would result in increased or decreased torques in one direction or another as now the platform may need to move against or with gravity. To adjust the level of the workbench a long level was placed at various positions and the eight leveling feed equipped to the legs of the workbench were adjusted until the system was sufficiently level.

3.5.2 Electrical Assembly and Programming

Another key point for preparing the system was the electrical part of the system. This primarily included checking the electrical components for safety and for programming the system. For checking the parts for safety it was important to ensure that each of the wired connections used an appropriate sized wire to carry the current, was the proper colour for its purpose, and was not frayed or had any exposed connection. Additionally it was important to check the integrity of the ground connection so the continuity of each of the ground connections was ensured. Additionally proper labeling was used to ensure proper warning of high voltage and risk of electric shock or arc flash was given. Once the electrical system was double checked for safety, it was inspected for electrical safety authority (ESA) and Canadian standards association (CSA) for compliance. After passing these inspections the commissioning process could begin.

The electrical commissioning process is outlined in Siemens manuals. It primarily involves commissioning the individual components that make up the CNC system including the NC unit, the human machine interface and the motor drives. This would all need to be complete before the system could be used. The primary part of this involved establishing connection between each of the components. The NCU needs to be able to communicate with the HMI, the control panel, the motor drives, and the I/O module. Once connection is established the motor drives can be commissioned. This involves assigning encoders to axes, determining travel limits, and an original determination of the controller gains. Once these steps are complete a PLC program can be created. These PLC programs control the movements and behaviour of the system.

Chapter 4

Fault Detection in Ball Screw Preload

The following results were publish in the IEEE Open Journal of Instrumentation and Measurement (OJIM) on August 4, 2023 [123].

Nomenclature

A	State-transition model.
B	Input model.
C	Observation model.
C^+	Pseudoinverse of measurement matrix.
$\bar{c}, c$	Normalized factor.
d	Diameter.
d_p	Preload disturbance torque.
D_e	Damping coefficient.
F_p	Force of Preload.
h_p	Screw lead.
I	Identity matrix.
J	Inertia.
K	Kalman gain.

m	Mass.
p	Mode transition matrix.
P	State error covariance.
Q	State noise covariance.
R	Measurement noise covariance.
R_t	Transmission ratio.
S	Innovation covariance.
sat	Saturation of a value (result between -1 and +1).
$\overline{sat}$	Diagonal of saturation term.
T	Time step length.
u	Input force.
v	State noise.
w	Measurement noise.
x	State matrix.
$\hat{x}$	State estimate matrix.
z	Measurement matrix.
$\tilde{z}$	Predicted innovation.
α	Lead angle.

δ Sliding boundary.

η Efficiency.

θ Angular position.

$\dot{\theta}$ Angular velocity.

$\ddot{\theta}$ Angular acceleration.

Λ Likelihood function.

μ Mixing probabilities.

ρ Density.

4.1 Introduction

The manufacturing world has entered the fourth industrial revolution, often referred to as Industry 4.0. The fourth industrial revolution builds upon the automation and digitization of the third industrial revolution. It includes the implementation of the Internet of Things, machine to machine communication, and condition monitoring (CM). Part of CM is the implementation of predictive maintenance (PM). PM is an evolution of the current prevailing maintenance paradigm of preventative maintenance. PM utilizes signals from the machine, wear models, and historic data to predict wear and remaining useful life. By utilizing PM machine components can be replaced when necessary, rather than at set intervals, or after failure has occurred. Using PM can optimize machine availability and minimize costs associated with maintenance and wear.

Effective maintenance management is essential for machine tools which are an integral component to modern manufacturing. Computer numerical control (CNC) machine tools make up most of modern manufacturing. They enable the fast and precise manufacture of millions of parts. CNC machine tools are essential components of the automotive, aerospace, and heavy equipment industries to name a few. The value of a machine tool relies upon it being in good working condition and having minimal down time. Ball screws are the most common mechanism for linear motion in machine tool feed drives. They convert the rotational motion of a servo motor into linear motion. Ball screws function similarly to lead screws, moving a nut which is connected to the worktable, up and down a screw. However, ball screws possess certain characteristics that make them more desirable than lead screws for machine tool feed drives. These include their extremely high efficiency (>90%), the ability to run at continuous duty with large loads, having high load capacities, and low wear properties. To improve the rigidity and repeatability of ball screw feed drives, they are often preloaded.

Preloading a ball screw is the process of eliminating internal clearance between the ball nut and ball screw. Preload is applied primarily in two ways: by using oversized balls, or by using a double nut to create a tension or compression force between the two nuts. Preload is normally designated as a percentage of the dynamic load capacity of the ball screw. Preloads typically range from 2% to 10% of the dynamic load capacity. A higher preload of 10% is most often used for machine tools to maintain high rigidity and repeatability with high cutting loads and vibrations. Maintaining high preload is important not only to manufacture parts to tight tolerances, but also because preload loss is often a symptom of degradation of the raceway of a ball screw.

The importance of preload necessitates the ability to effectively measure it. Several studies to measure and detect preload loss exist in the literature. They can broadly be categorized as sensor-based or sensor-less as has been presented in a paper by Butler et al. [20]. Sensor-based solutions require external sensors such as accelerometers and thermometers to measure vibrations and temperature, respectively. One downside of sensor-based solutions is that it requires the purchase of additional sensors along with their calibration, the need for external infrastructure for data collection and storage, as well as issues surrounding routing wires and dealing with cable management, especially if sensors are installed on moving parts. A sensor-less solution uses built-in signals of CNC machine tools, and is often ideal as it requires no additional cost or complexity to implement. The majority of existing methods for measuring preload or identifying preload loss that currently exist in the literature are sensor-based.

This paper proposes a sensor-less method to monitor and quantify the preload level of a ball screw using the mode probability of an interacting multiple models (IMM) system. IMM has been previously used in the literature for fault detection but there is currently a limited scope of applications, with most dealing with actuator and sensor faults. This method is a novel implementation of IMM for fault detection in preloaded ball screws. Additionally, most IMM based fault detection methods identify faults, but do not quantify them. There is a similar issue in the literature on preload monitoring and loss detection, where many methods simply identify that preload loss has occurred, rather than quantifying the current level of preload. The proposed method predicts the current level of preload using a weighted sum of the mode probabilities of the models making up the IMM, an activation function, and a weighing factor based on the model's preload designation. As will be demonstrated

in the results section of this work, the proposed method will be shown to be robust by maintaining accurate estimates under a number of different circumstances. The proposed method will also be shown to have equal or better predictive capabilities compared to other preload monitoring methods in the literature. The method is sensor-less, while most current methods are sensor-based. This can reduce the cost, complexity, and time of implementation compared to sensor-based methods. The IMM based method can be a cost effective solution that can be utilized on its own, or with other methods using model fusion, to provide real-time accurate estimates of the level of preload in a system.

The remainder of this paper is organized into the following sections. Section 4.2 will cover existing literature on preload measurement and the application of estimation theory to fault detection and CM. Section 4.3 covers modeling of the ball screw feed drive system and preload loss. Section 4.4 covers estimation and filtering methods. Section 4.5 explains how the method is formulated and how it is used to predict preload. Section 4.6 covers the methodology and results of computer simulations used to validate the effectiveness of the method, and a comparison to the results of other methods in the literature. Section 4.7 is the conclusion and future recommendations.

4.2 Literature Review

The following review of the literature examines both the application of estimation theory to fault detection and CM, as well as other methods that have been used to measure levels of preload, or to detect loss of preload.

4.2.1 Preload Detection

As previously mentioned, sensor-based methods involve external sensing or measurement apparatuses installed onto the system. Sensor-less methods use data already collected by the numerical controller [20]. Sensor-based methods are more common in the literature, often utilizing sensors such as force sensors and accelerometers [118]. In a study by Frey et al. a force sensor was inserted between the nuts in a system preloaded with a double nut. Doing this they were able to determine the preload force and measure changes over time and over the stroke of the screw [42]. Studies by Feng and Pan used accelerometers and temperature sensors to diagnose preload using frequency analysis [40, 39]. In one study they analyzed the peak frequency shift and the magnitude variation of the peak frequency to diagnose preload [40]. In two papers they utilized acceleration [39, 155] and temperature [39] data to predict preload where a support vector machine method was used to classify levels of preload. Tsai et al. used ball pass frequency to predict levels of preload. A decrease to the order of the ball pass frequency, and appearance of side bands, were used to detect changes in preload [135]. Nguyen et al. used motor current and vibration signals to diagnose preload in real time based on the calculated axial natural frequency of the system [100]. Benker et al. utilized a neural network to identify faults in a ball screw system. They used data from an accelerometer placed on screw nut. They classified screws based on preload loss, pitting damage, and indistinct defect and used mechanical power, and acceleration in three axes as features. They found up to a 92% classification accuracy when using mechanical power as the signal during direction changes [16]. Zhou et al. ran three ball screws for 7.2 million cycles and measured preload every 240 thousand cycles. They measured force using a tension-compression

sensor and calculated experimental preload based on contact load and sliding speed and compared their calculated values versus experimental results. Their method was based on calculating the estimated depths of the raceway which could be used to calculate contact load of the ball bearings and raceway and therefore preload [167]. Denkena et al. utilized an accelerometer as well as linear position and error to estimate preload. They ran their screw until complete preload degradation. Preload was classified based on error signal and acceleration data [34].

In contrast to sensor-based methods, the following sensor-less methods use signals that are built-in to the system for diagnosing preload loss. Built-in signals include the position, velocity, and acceleration of the various axes, and the motor current and torque for the feed drive and spindle motors are the other most commonly used built-in signals. Chang et al.[27] and Huang et al.[64] used decomposed motor current and torque signals to diagnose preload loss using the Hilbert-Huang transform. These methods seem to be effective at estimating levels of preload without the need for the implementation of additional sensors .

Other methods may require taking measurements of the ball screw beforehand to estimate future degradation. Shen et al. developed a 2 stage model for predicting wear. They compared their model to experimental results and found their model tracked the actual results fairly accurately. The first stage of the wear model uses geometric errors such as pitch errors, ball radius errors to predict wear, then the second stage uses fractal theory which was adopted to characterize contact between the balls and raceway using an adhesive and abrasive wear model [115].

There are a variety of methods that exist in the literature for detecting and measuring preload loss. Some methods classify the system as either being healthy or at

a certain level of degradation. Others methods measure and quantify the estimated level of preload in the system. Quantifying the level of preload is generally preferable as it is useful to quantify the level of preload as well as track its degradation. There are many more sensor-based methods which utilize external sensors than those which are sensor-less.

4.2.2 Estimation for Fault Detection

The field of estimation theory has often been applied to problems such as improving the accuracy of measurements and for effective target tracking. Many different types of Kalman filters (KF) and other estimation methods exist. The extended Kalman filter (EKF) and unscented Kalman filter (UKF) are extensions which are useful for nonlinear systems. Newer filters such as the smooth variable structure filter (SVSF) [53, 14, 44] and sliding innovation filter (SIF) [45, 77] have shown to be robust to changing system dynamics. IMM is a method that has been used in the literature for several different types of applications. Many studies have used IMM for improved target tracking where the object has multiple modes of system dynamics to describe its motion [73, 74, 113]. It was found that as the process error increases relative to the measurement error, the performance of IMM relative to a regular KF increases substantially [73]. In addition to these applications there are examples in the literature of estimation methods being applied to fault detection.

A popular use for IMM is that it can be used to detect faults by observing the mode probability of each filter. In addition to detecting faults, many of these studies implemented fault tolerant control (FTC). A popular application case for these studies involve the failure of aircraft actuators and sensors. Mohan et al. created a method

for fault detection for stuck air craft actuators using IMM. They used 25 states, with 3 fault states for each actuator for being stuck in various positions [98]. Kim et al. created a fuzzy tuned IMM filter to apply FTC to aircraft actuators, they found their method had improved performance to regular IMM FTC by reducing the incidences of false fault detection and control input discontinuities [72]. Zhang et al. utilized IMM to implement FTC for a longitudinal vertical takeoff and landing aircraft. They modeled sensor, actuator and a system faults in their IMM [164]. Another popular implementation of IMM for fault detection and FTC is quadcopters and unmanned aerial vehicles (UAV). In one study Lee et al. predicted fault sizes of actuator and sensor faults in quadcopters using IMM. Their method could identify whether a sensor or actuator fault had occurred, then identify which of the actuators had failed based on the fault probability [78]. Zhang et al. identified actuator faults in a quadcoptor using IMM. Their method utilized error residuals to estimate actuator faults and their amplitude [161]. Cork and Walker created a method of sensor FTC and found that their method had improved target tracking by decreased positioning and attitude error compared to a single UKF filter method [31]. Rago et al implemented FTC using IMM. Their method was able to identify faults in several sensors and actuators. By identifying the faults they could compensate and control a UAV under these failure conditions. Other studies examined IMM in relation to electro-hydrostatic actuators where leakage and friction faults were detected [1, 46]. Several types of filtering methods were used within the IMM, including: IMM-EKF, IMM-UKF, and IMM-SVSF. Each of these studies found the IMM to be an effective method of detecting faults and implementing FTC. One study by Huang et al. [60] used a KF based method for detecting faults in a ball screw system and were able to detect both

measurement and mechanical failures. They used residual signals from the KF for fault detection and identification and also implemented FTC in their system.

IMM has proven to be an effective method for fault detection and FTC. However, the scope of applications is small in the literature. Most studies have investigated its application to only electro-hydrostatic actuators, aircraft actuators, and UAV or quadcopter navigation. Most methods, with the exception of Zhang et al. [161], identified faults but did not quantify the magnitude of the fault. An application of IMM to preload loss in ball screw feed drives which can identify preload loss, as well as quantify it, would be a novel application to IMM literature.

4.3 Ball Screw Modeling

The first step in creating a method of preload detection is modeling the ball screw feed drive system. One possible representation of a ball screw system was proposed by Altinas et al. as seen in Figure 4.1 [7]. This model can simplify analysis relative to more complex models that separate the components into multiple interacting masses. This representation lumps the motor, screw, nut, table, and workpiece masses together as shown in (4.3.1)-(4.3.3). The system is represented by the differential equation (4.3.4) below.

$$J_{bs} = \rho l \pi \frac{d^4}{32} \tag{4.3.1}$$

$$J_t = (m_t + m_{wp}) \frac{h_p}{2\pi}^2 \tag{4.3.2}$$

$$J_e = J_{bs} + J_t + J_m \tag{4.3.3}$$

$$J_e\ddot{\theta} + D_e\dot{\theta} = u(t) - d_p(t) \tag{4.3.4}$$

The distance the worktable travels linearly along the screw for a given rotation is determined by the ball screw's transmission ratio, which is calculated using

$$R_t = \frac{h_p}{2\pi}. \tag{4.3.5}$$

The second important consideration is modeling the loss of preload in the system. Preload has a few effects on system dynamics. First, increasing preload increases the drag torque [27]. Second, increasing preload increases the positional repeatability of the system [42]. Third, increasing preload increases the stiffness of the system. The preload can also affect the efficiency value, where decreasing preload increases mechanical efficiency as long as the applied load is greater than the preload [145]. There are a few different methods to calculate preload disturbance torque [166, 133, 100]. Some calculate it using the system stiffness and the radius of the balls, but the

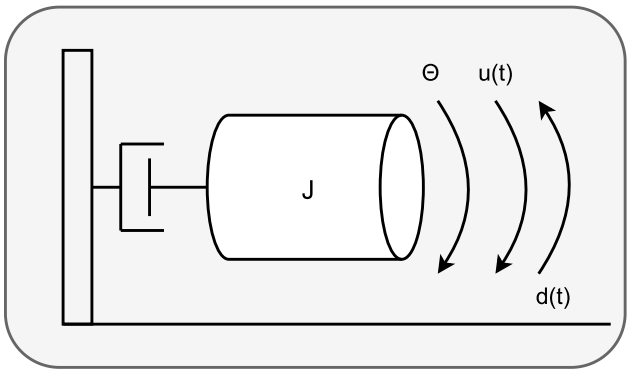

Figure 4.1: A simple lumped model of the ball screw as seen in [7].

most common method is the following equation

$$d_p(t) = \frac{0.05}{\sqrt{\tan \alpha}} \cdot \frac{F_p h_p}{2\pi\eta}. \tag{4.3.6}$$

Preload will fluctuate over the stroke of the screw due to manufacturing error resulting in variation in the width of the raceway. This variation decreases as the precision grade of the ball screw increases [133]. Over time with the degradation of the balls, raceway, and nut, the preload will decrease in a somewhat linear fashion over the life of the ball screw [167]. In the Zhao et al. study they noticed a period of steeper degradation followed by a long period of linear degradation [165]. The rate of preload degradation depends on the initial preload [167]. Larger initial preloads degrade at a higher rate than lower preloads. Degradation also causes an increase in travel variation. For the purpose of the experimentation that was performed, the decrease in drag torque due to a decrease in preload will be the method in which a loss of preload was modeled.

4.4 Estimation and Filtering

Each method of filtering discussed in Section 4.2 has its own advantages and use cases which have been examined in the literature. The KF and the SIF are the chosen filters that will be examined for their application for preload loss detection using IMM. The KF was chosen due to its widespread use across the literature and industry, and the SIF due to its improved performance in faulty systems.

4.4.1 Kalman Filter

The KF is an optimal solution to the linear estimation problem [70]. It uses a prediction and update stage to recursively estimate the system state. The KF is used for linear systems and is an accurate predictor for these models. However, it is not very robust for nonlinear systems or systems with faults. To overcome these issues, many derivations and extensions of the KF have been developed for estimation with nonlinear systems or systems with changing dynamics. The formulation for the KF will be shown below. The KF has two stages: the prediction stage

$$\hat{x}_{k+1|k} = A_k \hat{x}_{k|k} + B_k u_k \tag{4.4.1}$$

$$P_{k+1|k} = A_k P_{k|k} A_k^T + Q_k \tag{4.4.2}$$

followed by an update stage

$$S_{k+1} = C_{k+1} P_{k+1|k} C_{k+1}^T + R_{k+1} \tag{4.4.3}$$

$$K_{k+1} = P_{k+1} C_{k+1}^T S_{k+1}^{-1} \tag{4.4.4}$$

$$\hat{x}_{k+1|k+1} = \hat{x}_{k+1|k} + K_{k+1}(z_{k+1} - C_{k+1}\hat{x}_{k+1|k}) \tag{4.4.5}$$

$$P_{k+1|k+1} = (I - K_{k+1}C_{k+1})P_{k+1|k}(I - K_{k+1}C_{k+1})^T + K_{k+1}R_{k+1}K_{k+1}^T. \tag{4.4.6}$$

4.4.2 The Sliding Inovation Filter

Unlike the KF, the SIF is a sub-optimal solution to the linear estimation problem. The SIF is an estimation strategy that makes use of a switching gain and innovation term which bounds state estimates [45]. The SIF performs similarly to the KF for normal linear systems, but performs much better in linear systems with faults. The adaptive version of the SIF offers a slight performance improvement compared to the standard SIF in both regular operation and faulty operation linear systems due to the inherent robustness of the switching gain [77]. The SIF is formulated similarly to the KF with a prediction stage

$$\hat{x}_{k+1|k} = A_k \hat{x}_{k|k} + B_k u_k \tag{4.4.7}$$

$$P_{k+1|k} = A_k P_{k+1|k} A_{k+1}^T + Q_k \tag{4.4.8}$$

$$\tilde{z}_{k+1|k} = z_{k+1} - C\hat{x}_{k+1|k} \tag{4.4.9}$$

followed by an update stage

$$K_{k+1} = C_{k+1}^{+} \overline{sat}(|\tilde{z}_{k+1}|/\delta) \tag{4.4.10}$$

$$\hat{x}_{k+1|k+1} = \hat{x}_{k+1|k} + K_{k+1}\tilde{z}_{k+1} \tag{4.4.11}$$

$$P_{k+1|k+1} = (I - K_{k+1}C_{k+1})P_{k+1|k}(I - K_{k+1}C_{k+1})^T + K_{k+1}R_{k+1}K_{k+1}^T. \quad (4.4.12)$$

4.4.3 Interacting Multiple Models

Most systems have several different models to describe their behaviour. Because of this, a single filter is often inadequate to accurately estimate such systems. To overcome the limitation of using a single filter, the IMM method uses several models to more accurately estimate a system. IMM can be used with several different types of estimation methods and many different numbers of models. Increasing the number of models in an IMM system can increase estimation accuracy at the cost of computing performance. The first two steps of the IMM involves calculating the mixing probabilities

$$\mu_{i|j,k|k} = \frac{1}{\bar{c}_j} p_{ij}\mu_{i,k} \quad (4.4.13)$$

$$\bar{c}_j = \sum_{i=1}^{r} p_{ij}\mu_{i,k}. \quad (4.4.14)$$

The next stage of the IMM is the mixing and interaction stage. Here the mixed initial conditions for each mode are calculated

$$\hat{x}_{0j,k|k} = \sum_{i=1}^{r} \hat{x}_{i,k|k}\mu_{i|j,k|k} \quad (4.4.15)$$

$$P_{0j,k|k} = \sum_{i=1}^{r} \mu_{i|j,k|k}\{P_{i,k|k} + (\hat{x}_{i,k|k} - \hat{x}_{0j,k|k})(\hat{x}_{i,k|k} - \hat{x}_{0j,k|k})^T\}. \tag{4.4.16}$$

The next stage calculates the likelihood function for each mode matched filter

$$\Lambda_{j,k+1} = N(z_{k+1}; \hat{z}_{j,k+1|k}, S_{j,k+1}) \tag{4.4.17}$$

$$\Lambda_{j,k+1} = \frac{1}{\sqrt{|2\pi S_{j,k+1}|_{Abs}}} exp(\frac{-\frac{1}{2} e_{j,z,k+1|k}^T e_{j,z,k+1|k}}{S_{j,k+1}}). \tag{4.4.18}$$

After calculating the likelihood function for each mode matched filter, the mode probability can be updated and the normalizing constant calculated

$$\mu_{j,k} = \frac{1}{c} \Lambda_{j,k+1} \sum_{i=1}^{r} p_{ij} \mu_{i,k} \tag{4.4.19}$$

$$c = \sum_{j=1}^{r} \Lambda_{j,k+1}. \tag{4.4.20}$$

The output state and state error covariance of the IMM system are then determined

$$\hat{x}_{k+1|k+1} = \sum_{j=1}^{r} \mu_{j,k+1|k+1} \hat{x}_{j,k+1|k+1} \tag{4.4.21}$$

$$P_{k+1|k+1} = \sum_{i=1}^{r} \mu_{j,k+1|k+1}\{P_{j,k+1|k+1} + (\hat{x}_{j,k+1|k+1} - \hat{x}_{k+1|k+1})(\hat{x}_{j,k+1|k+1} - \hat{x}_{k+1|k+1})^T\}. \tag{4.4.22}$$

4.5 Proposed Method

The proposed method utilizes a weighted sum of the mode probabilities of various filters which represent different levels of preload. Five KF models representing preload levels 10%, 7.5%, 5%, 2.5%, and 0% were used to create the IMM system. If there were more models the system may not be able to correctly transition between models and therefore could not correctly identify the levels of preload. If there were fewer models there would be too large a gap of preload between models and it would be too difficult to accurately determine the current level. The mode transition matrix used in the IMM model is given below

$$p_{ij} = \begin{bmatrix} 0.8 & 0.08 & 0.06 & 0.04 & 0.02 \\ 0.07 & 0.8 & 0.07 & 0.04 & 0.02 \\ 0.04 & 0.06 & 0.8 & 0.06 & 0.04 \\ 0.02 & 0.04 & 0.07 & 0.8 & 0.07 \\ 0.02 & 0.04 & 0.06 & 0.08 & 0.8 \end{bmatrix}. \tag{4.5.1}$$

The model is more likely to switch to an adjacent model (i.e from 7.5% to 5% or 10%) than to one further away in level of preload (i.e from 10% to 2%) as this is the more likely scenario to occur.

Each time step the IMM system produces mode probabilities for each of the five KF models, which is the probability that a system model matches the measured system. The probabilities sum up to 1, with models more representative of the system having probabilities approaching 1 and less representative systems having a probability closer to 0. For each of the models the weighted estimate can be calculated using

$$Act(\mu_{ij}) \cdot Weight. \tag{4.5.2}$$

Where $Act(\mu_{ij})$ is the activation function and the weights are equal to the level of preload of each model. Generally IMM uses a linear activation function. These weighted estimates can be summed together to equal an estimate of the current level of preload. A diagram showing the proposed method can be seen in Figure 4.2. For example, if looking at Table 4.2 when actual preload is at 5%, the estimated preload calculated from the IMM system using a linear activation function $Act(\mu_{ij}) = \mu_{ij} \cdot (1)$ is

$$\begin{aligned} 0.04 \cdot 1 \cdot 10 + 0.05 \cdot 1 \cdot 7.5 + 0.85 \cdot 1 \cdot 5 + 0.04 \cdot 1 \cdot 2.5 + 0.03 \cdot 1 \cdot 0 \\ = 5.125\%. \end{aligned} \tag{4.5.3}$$

The issue with using a linear activation function is that the prediction accuracy for the upper (10%) and lower (0%) bounds was comparatively less accurate than the predictions in the middle of the bounds. This is due to the fact that since there will be residual mode probability for the other models, and there is no model above 10% and none below 0%, it will skew the measurement low for the 10% prediction and high for the 0% prediction. To address this issue the exponential activation function can be used where

$$Act(\mu_{ij}) = \frac{\mu_{ij}^2}{\sum_{j=1}^{r} \mu_{ij}^2}. \tag{4.5.4}$$

Using an exponential activation function can further decrease the residual mode probability to close to zero. This method of activation had improved prediction capabilities near the end of the prediction range but encountered the issue that the prediction

would oscillate about the true value. Using an exponential value of 1.33 rather than 2 yielded improved results. From examining the literature this seems to be a novel approach to dealing with residual mode probabilities which often decreases prediction accuracy. The results of these changes to weighing can be seen in Figure 4.6. and Table 4.2. All the simulations were conducted using an exponent of 1.33.

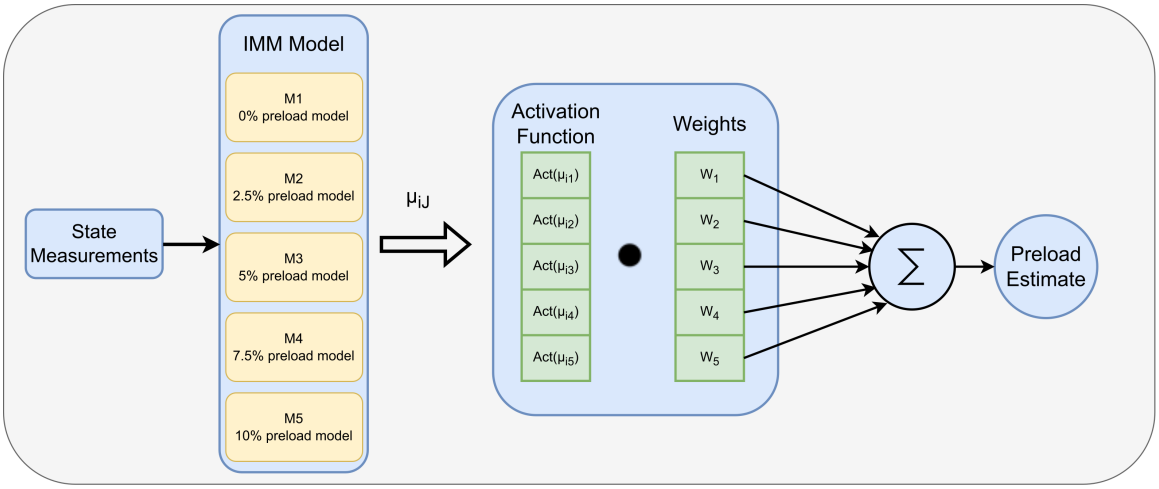

Figure 4.2: Diagram of proposed method.

4.6 Computer Simulation and Results

Table 4.1: Parameters and values.

Parameter	Meaning	Value
D_e	Damping coefficient	1.98×10^{-2} $\frac{\text{kg}\cdot\text{m}^2}{\text{s}}$
d	Average diameter of the ball screw	0.02 m
$d_p(0)$	Initial disturbance torque	0.3 N $\cdot$ m
F_p	Force of preload	1×10^3 N

h_p	Screw lead	0.02 m
J_{bs}	Ball screw inertia	1.26×10^{-4} kg $\cdot$ m^2
J_e	Lumped inertia	3.3×10^{-3} kg $\cdot$ m^2
J_m	Motor inertia	3×10^{-3} kg $\cdot$ m^2
J_t	Table inertia	2×10^{-4} kg $\cdot$ m^2
l	Length of ball screw	1 m
m_t	Mass of table	10 kg
m_{wp}	Mass of workpiece	10 kg
R_t	Transmission ratio	1.59×10^{-3} $\frac{\text{m}}{\text{r}}$
t_f	Total time	100 s
T	Time step length	0.1 s
α	Lead angle	0.31 rad
η	Efficiency	90%
ρ	Density of the ball screw material (steel)	8.05×10^3 $\frac{\text{kg}}{\text{m}^2}$

To test the IMM method for detecting preload loss, a computer simulation was created which tested multiple scenarios to display the robustness and accuracy of the model. The simulated system is an open loop single axis feed drive. The value of all parameters used in the simulation can be found in Table 4.1. The various parameters were calculated using equations (4.3.1)-(4.3.6) Efficiency was assumed to be 90% and the damping coefficient which was used was the same as the Y-axis from the paper by Altinas et al. [7]. The screw is a steel 20 mm lead, 20 mm nominal diameter, 1 m long screw. The system transition and measurement models are defined below in

(4.6.1) and (4.6.2) where k is the current time step, and $k+1$ is the next time step.

$$x_{k+1} = Ax_k + Bu_k + w_k \tag{4.6.1}$$

$$z_{k+1} = Cx_{k+1} + v_{k+1} \tag{4.6.2}$$

Using (4.3.4), the state space representation for the continuous system is found

$$\begin{bmatrix} \dot{x}_1 \\ \dot{x}_2 \end{bmatrix} = \begin{bmatrix} 0 & 1 \\ 0 & -\frac{D_e}{J_e} \end{bmatrix} \begin{bmatrix} x_1 \\ x_2 \end{bmatrix} + \begin{bmatrix} 0 \\ \frac{1}{J_e} \end{bmatrix} \hat{u}(t). \tag{4.6.3}$$

A third state x_3 which represents the linear position of the system is added using the transmission ratio of the system. The system is then discretized and the following equations are found

$$\begin{bmatrix} x_1 \\ x_2 \\ x_3 \end{bmatrix}_{k+1} = \begin{bmatrix} 1 & T & 0 \\ 0 & 1 - \frac{D_e \cdot T}{J_e} & 0 \\ R_t & R_t \cdot T & 0 \end{bmatrix} \begin{bmatrix} x_1 \\ x_2 \\ x_3 \end{bmatrix}_k + \begin{bmatrix} 0 \\ \frac{T}{J_e} \\ 0 \end{bmatrix} \hat{u}(t) + w_k. \tag{4.6.4}$$

The measurement equation is seen below where measurements are taken of both the angular and linear position, which is common for most machine tool feed drives which use both rotary and linear encoders

$$\begin{bmatrix} z_1 \\ z_2 \end{bmatrix}_{k+1} = \begin{bmatrix} 1 & 0 & 0 \\ 0 & 0 & 1 \end{bmatrix} \begin{bmatrix} x_1 \\ x_2 \\ x_3 \end{bmatrix}_{k+1} + v_{k+1}. \tag{4.6.5}$$

The state noise covariance and measurement noise covariance matrix are given below in (4.6.6) and (4.6.7), respectively. The measurement noise was determined based on typical measurement error of precision linear and rotary encoders. Positioning error was based on some allowances for backlash or clearances in the system, these would be small in a rigid precision machine tool.

$$Q = \begin{bmatrix} 1 \times 10^{-3} & 0 & 0 \\ 0 & 1 \times 10^{-2} & 0 \\ 0 & 0 & R_t \cdot 1 \times 10^{-3} \end{bmatrix} \tag{4.6.6}$$

$$R = \begin{bmatrix} 1 \times 10^{-4} & 0 \\ 0 & 2 \times 10^{-5} \end{bmatrix} \tag{4.6.7}$$

The system input can be seen in (4.6.8). The disturbance due to preload was subtracted from the system input to get the true system input $\hat{u}(t)$. The piecewise function to determine this value is given in (4.6.9).

$$u(t) = 2 \cdot \sin(t) \tag{4.6.8}$$

$$|\hat{u}(t)| = \begin{cases} |u(t)| - |d_p(t)| & |u(t)| > |d_p(t)| \\ 0 & |u(t)| \leq |d_p(t)| \end{cases} \tag{4.6.9}$$

A time step of 0.1s was chosen, as with smaller time steps the system was unable to correctly identify the level of preload. This likely occurred because the difference in the filters used for the IMM model was too small to correctly identify the correct model. In practical terms this means that down sampling would need to occur in an

actual application as CNC systems sample at much higher frequencies.

Four simulations representing different possible scenarios were tested to determine the robustness of the model. These first four simulations utilize a KF-IMM. The first is a simulation testing gradual preload loss from full 10% preload to 0% preload. The second is a simulation where preload is decreased from 7.5% preload to 2.5% preload. The third simulation is one where the preload remains at the full 10% the entire simulation. The fourth simulation tests for the proposed methods ability to account for a rapid change from 10% preload to 0% preload. A fifth simulation was conducted using SIF-IMM rather than using KF-IMM so that the performance could be compared. Performance of the IMM will be determined by comparing the estimated preload compared to the actual preload.

4.6.1 Simulation 1: Gradual Loss Over Time

The first simulation represents a situation in which the preload gradually degrades over time. This is the most common type of degradation that is observed as it would occur due to regular wear on the components. Over the course of the simulation the disturbance value decreased linearly from the initial value of 10% preload ($d_p(0) = 0.3$) to a final value of 0% ($d_p(t_f) = 0$) preload which can be seen in Figure 4.6.

The actual system input $\hat{u}(t)$ increased over time as a result of decreased disturbance torque due to preload as can be seen in Figure 4.3. Due to the increase in actual input, the system moved further each period of the sin wave input. Using the constructed IMM model the following mode probabilities were found as seen in Figure 4.4. There is a great deal of noise in the mode probabilities, however it is clear that there is a pattern which correctly identifies the level of preload. Using a

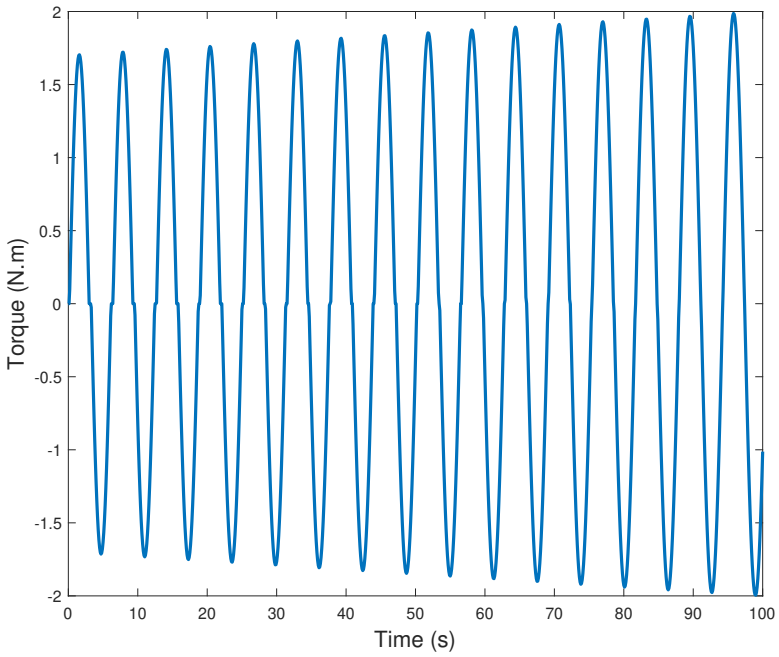

Figure 4.3: Simulation 1 system input.

moving average, the mode probabilities were smoothed and the trend is clearer which can be seen in Figure 4.5. The mode probability for all simulations used a moving average to account for the noise.

The results of the first simulation can be seen in the confusion matrix in Table 4.2 and Figure 4.6. The model with the greatest mode probability is shown in bold font. The predicted preload level was calculated using the method demonstrated in section 4.5. From these results it has been demonstrated that the IMM model was able to accurately and reliably estimate the levels at preload throughout this simulation.

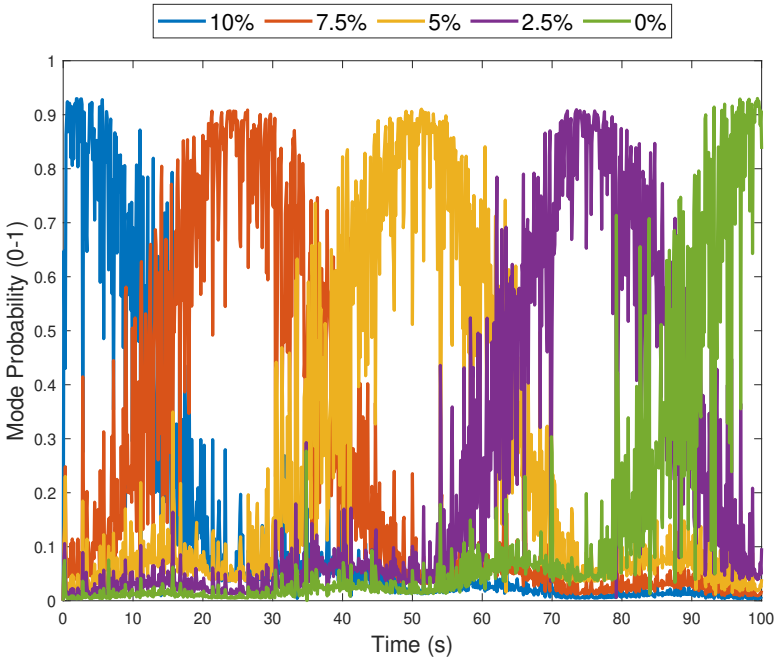

Figure 4.4: Simulation 1 preload predictions using mode probabilities.

Table 4.2: Predicted preload versus actual preload confusion matrix.

Actual preload	Mode					Prediction	
	10%	7.5%	5%	2.5%	0%	Linear	Exp
10%	**0.85**	0.07	0.04	0.03	0.02	9.3%	9.7%
7.5%	0.04	**0.88**	0.04	0.02	0.02	7.3%	7.5%
5%	0.04	0.05	**0.85**	0.04	0.03	5.1%	5%
2.5%	0.02	0.02	0.04	**0.89**	0.03	2.7%	2.5%
0%	0.02	0.02	0.03	0.05	**0.87**	0.6%	0.3%

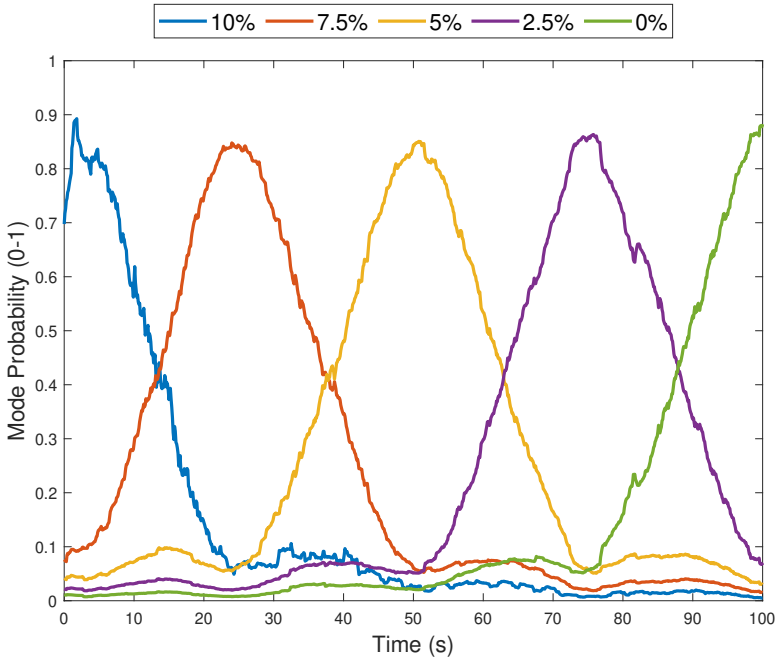

Figure 4.5: Simulation 1 smoothed preload predictions using mode probabilities.

4.6.2 Simulation 2: Alternate Starting and Ending Preload

The second simulation involves different starting and ending levels of preload. Over the course of the simulation, the preload was gradually reduced from 7.5% ($d_p(0) = 0.225$) to 2.5% ($d_p(t_f) = 0.075$). This shows that the model can start at different points of initial preload and end at different points of preload and still be able to correctly predict the current level of preload. This is important as there is a wide variety of different preloads used across different applications. Running the IMM method yielded the following results as seen in Figure 4.7. This simulation shows the robustness of the proposed method. The method continued to work in this condition and it could correctly identify the level of preload over the course of the simulation.

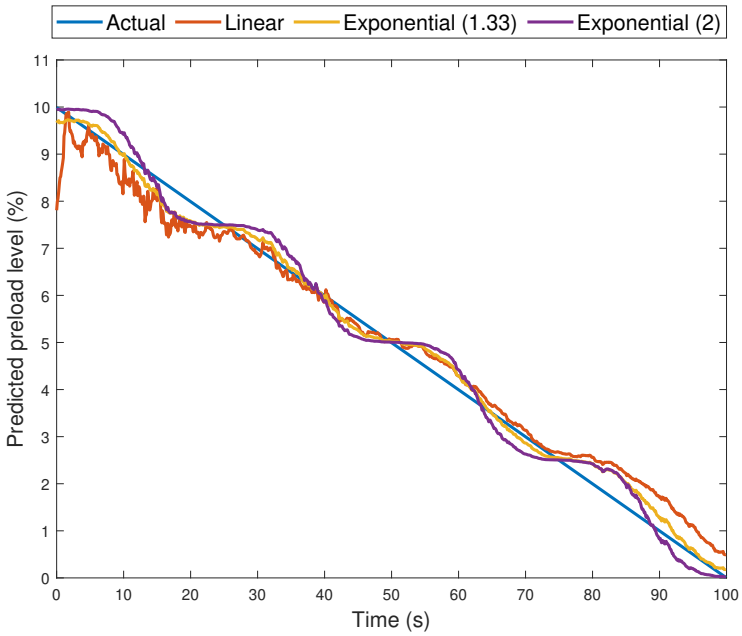

Figure 4.6: Simulation 1 preload predictions using different weighing factors.

4.6.3 Simulation 3: No Change to Preload

The third test for the method involved maintaining full preload the entire simulation. This simulation showed that the model will not give false positives and show a decrease in preload. Given that preload degradation will normally occur very slowly this simulation emulates the most common operating condition. Running the IMM model yielded the following results as seen in Figure 4.8. As can be seen, the model was able to accurately predict that the system had maintained full preload throughout the simulation.

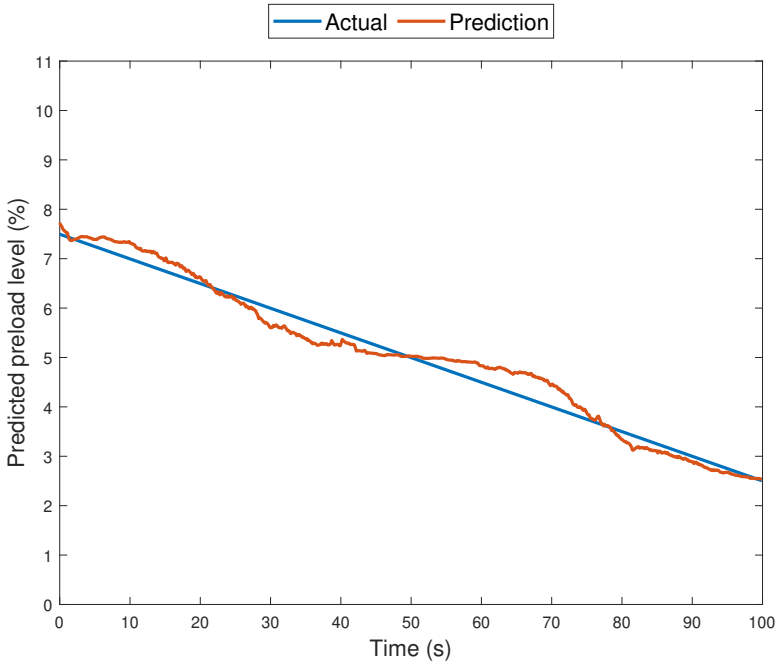

Figure 4.7: Simulation 2 preload prediction using weighted sum versus actual preload.

4.6.4 Simulation 4: Sudden Drop in Preload

The fourth test for the proposed method involved a sudden drop from full 10% preload to 0% preload at the midpoint of the simulation. This test will determine if the model is capable of responding to sudden and rapid changes to preload. This test simulated a scenario in which the preloading method (a spacer nut for examples) suddenly fails, resulting in a complete loss in preload. Running the IMM method yielded the results seen in Figure 4.9. Within 3 time steps the IMM method was able to accurately detect the level of preload. This test demonstrated the method's quick reaction to large changes in the system.

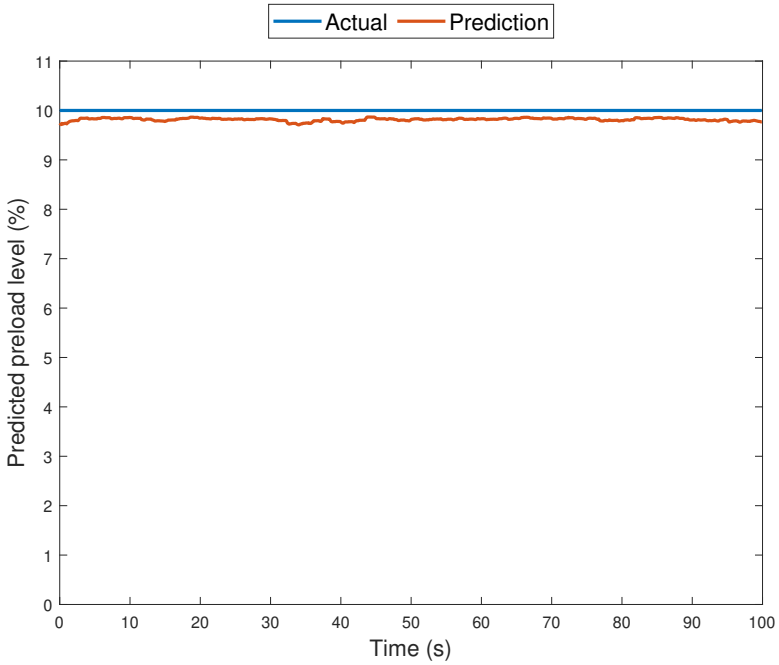

Figure 4.8: Simulation 3 preload prediction using weighted sum versus actual preload.

4.6.5 Simulation 5: Comparison of Estimation Methods

It is possible that other estimation methods may yield better or worse results compared to the KF based model. An SIF-IMM was tested using the same parameters as the first method. The sliding boundary layer was calculated to be

$$\delta = \begin{bmatrix} 0.05 \\ 0.07 \end{bmatrix}. \tag{4.6.10}$$

The same conditions as the first simulation with gradual loss of preload were used in this test. After running the simulation and examining the results, it can be seen that they are similar to that of the regular KF based IMM as seen in Figure 4.10. The results are very similar to the KF based IMM seen in the first simulation,

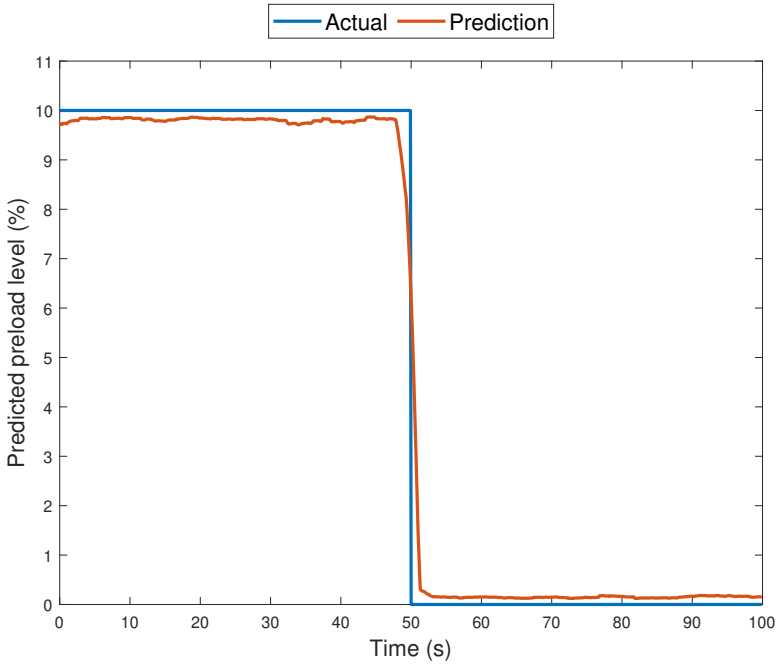

Figure 4.9: Simulation 4 preload prediction using weighted sum versus actual preload.

with the predicted preload tracking the actual preload very closely. As noted in the original SIF paper, the SIF performs similarly to the KF in no fault conditions[45]. Because the IMM switches models to one representative of the current level of preload it essentially is in a no-fault condition, which explains the similarity in results. From these results it can seen that the proposed IMM method for preload measurement can be constructed using both the regular KF and the SIF.

4.6.6 Comparison to Other Methods in the Literature

After examining the results of the five performed simulations, it is clear that the proposed method is robust under a variety of circumstances. In addition to being robust, the proposed method was able to obtain an average accuracy of approximately

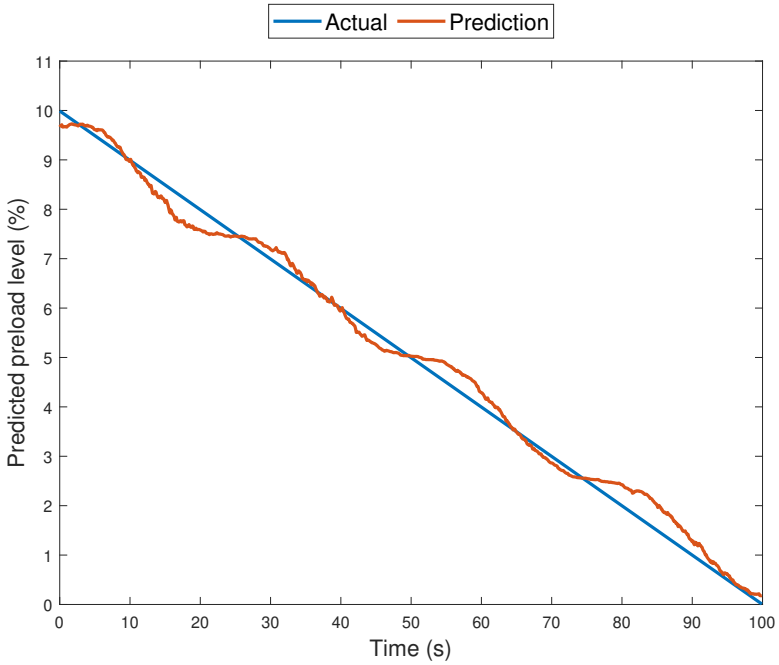

Figure 4.10: Simulation 5 preload prediction using weighted sum versus actual preload.

95% to 98% in predicting the levels of preload.The results of the previous preload measuring or preload loss identification methods have been compared to the method proposed in this work. It is difficult to directly compare results for a few reasons. Some papers predict the level of preload, while others seek to classify into states of preload. This work seeks to quantify preload so it is best to be compared to the papers which quantified preload in Table 4.3. Additionally, it is difficult to compare as the experiments or simulations used to validate the results is different for each work. Many papers also present a method to identify preload loss but do not directly quantify their method's ability to quantify or classify preload. In the table these are marked as "N/A" in the accuracy column. For some papers it was also necessary to estimate prediction accuracy based on graphs they provided which showed predicted preload compared to actual preload, as they did not provide accuracy estimates. As

can be seen the proposed method has similar accuracy to other preload quantifying methods seen in the literature. One advantage it has over other methods is that it is sensor-less, the two other preload quantification methods that were able to obtain 95% prediction accuracy were sensor-based methods.

Table 4.3: Comparison of results to other preload estimation methods.

Paper	Sensor-based / sensor-less	Type	Accuracy
Proposed	**Sensor-less**	**Quantified**	**95%**
[167]	Sensor-based	Quantified	95%
[100]	Sensor-based	Quantified	95%
[34]	Sensor-based	Classification	94%
[16]	Sensor-based	Classification	92%
[115]	Other	Quantified	77%
[155]	Sensor-based	Classification	50%
[42]	Sensor-based	Quantified	N/A
[40]	Sensor-based	Quantified	N/A
[39]	Sensor-based	Quantified	N/A
[135]	Sensor-based	Classification	N/A
[27]	Sensor-less	Classification	N/A
[64]	Sensor-less	Classification	N/A

4.7 Conclusion and Future Work

Maintaining preload is an important factor in a machine tool feed drive's ability maintain rigidity and repeatability as it helps ensure accurate, high-quality parts are manufactured. The proposed method provides a novel sensor-less method for accurately measuring preload and detecting loss of preload in a ball screw feed drive system. Sensor-less methods are advantageous to sensor-based methods due to not requiring the installation and any related additional costs and complexity of additional external sensors. Sensor-based and sensor-less methods can also be used in conjunction via model fusion to create an even more accurate estimate of preload than one method alone. The proposed method using IMM, and activation function, and a weighted sum of the mode probabilities was found to be robust and accurate across multiple testing scenarios and while using different types of filters. The accuracy of this method in estimating preload was comparable or better than other methods in the literature. In addition to the contribution to preload detection, this work also contributes to the literature in regards to filtering and estimation. The proposed method is a novel implementation of IMM which currently has a limited scope of applications to fault detection in the literature. The use of an activation function in IMM is a novel modification of the method. In summary the primary contributions and advantages of the proposed method are the following:

1. High degree of predictive accuracy and robustness.

2. Novel implementation of IMM for fault detection, it has never been applied to estimating preload before.

3. Sensor-less method, there is much fewer sensor-less based methods than sensor-based methods.

4. IMM based method that quantifies fault rather than just classification, the majority of IMM fault detection methods classify and identify fault states rather than quantify the fault.

5. Preload method that quantifies level of preload, many other preload identify that preload loss has occurred or categorize wear into several levels of wear rather than quantifying the fault or wear.

6. Utilizing an activation function for predictions using IMM, which is a novel modification and not seen in the literature.

Further work on this method could go in a few different directions. First, the method could be modified to work with closed loop control. Most, if not all, feed drive systems, especially in CNC machine tools, operate in a closed loop control system. Therefore, it would be necessary to implement the method with closed loop control in order to be viable to actual implementation. By implementing closed loop control the method could be used to develop a FTC scheme to improve control accuracy. Second, the system could be tested on a real industrial machine tool. Although the method has demonstrated benefits on our computer simulation, the method should be applied and proven to work in a real world environment. To properly test this method experimentally, there would need to be an adjustable preload nut with force measurements to accurately measure preload in real time. Finally, other faults could be tested using the IMM framework. Faults such as misalignment, lack of lubrication, or a number of other faults would be interesting to examine using a similar method.

Chapter 5

Data Analysis and Modeling

This chapter covers the analysis of data collected from the experimental setup. Data collected from the CNC system can be used for modeling and CM purposes. Data analysis from the system will be used towards achieving both the industry sponsor and academic goals.

5.1 Digital Twin Modeling Strategy

One key characteristic of DTs is the use of multiple models to model the physical system. The advantage of this approach is certain models may provide certain knowledge of the system better than other types of models or that other models cannot provide. One other advantage of using multiple models is that their estimates or results can be fused together for model fusion. This means more accurate estimations of the systems current state and parameters can be obtained than a single model alone. The general process for analyzing the system is the following:

1. Create and run tests which can be used to extract useful information

2. Collect and parse the heterogeneous data generated via the system

3. Analyze data and create models to represent useful parameters and qualities of the system

4. Create a model to represent the "healthy" or base case

5. Modify operating parameters and repeat steps 1 to 3 and evaluate effects on models

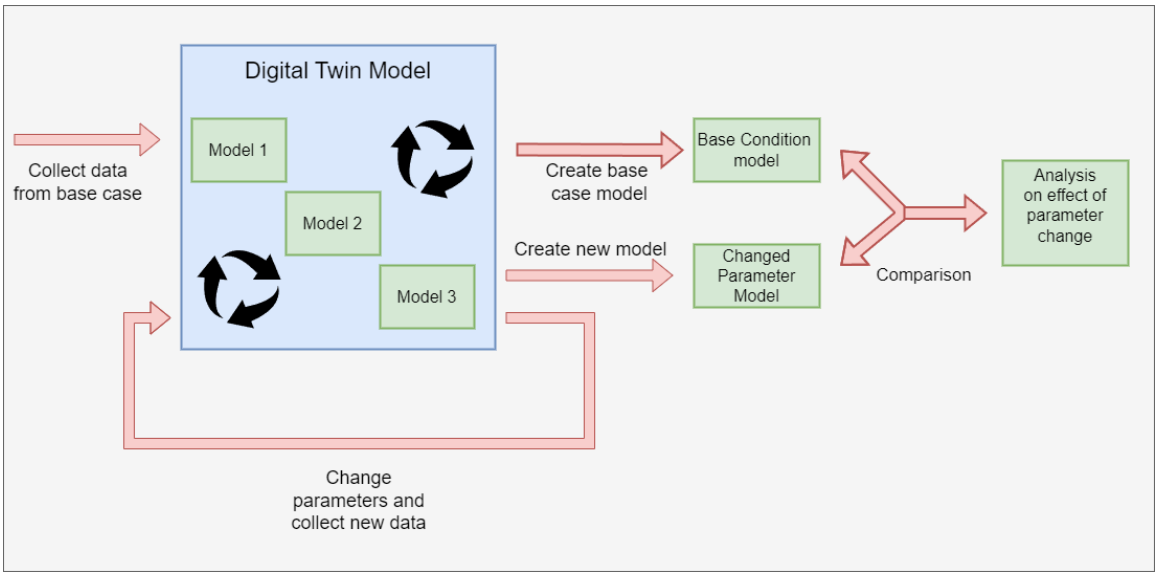

Figure 5.1: Overview of DT modeling and analysis process

An overview of this process can be seen in Figure 5.1. In this case a "healthy" model for the LFD workbench will be developed by using new components in proper alignment. With this state several tests will be ran which are described in section 5.2 which will be used to create several models, some of which are described in section 5.3. Several changes to the system parameters will be changed to observe the effect.

After changing the parameters the system will be re-modeled to observe the effect as will be shown for the effect of a warm up cycle in section 5.3.2.

5.2 Data Generation and Collection

An important step in CM and modeling is the collection of data. Collected data can be used to fit parameters and create relationships and models between the input and outputs of the system.

5.2.1 Test Programs

To collect data to evaluate the system it is important to generate movements which can be used to extract the parameters and qualities of the system. In this case, some relevant parameters are friction, stiffness, preload, backlash, and inertia. One important consideration is that the parameters, specifically friction and inertia, will both vary based on a few factors. Stiffness will tend to decrease the further from an axially fixed bearing, so this might be near the far end in the case of a single fixed bearing, or in the middle in the case of two fixed bearings. It may also have some variation along the axis based on wear or manufacturing defects which lead to lead variations or increased groove radius. The lead and groove radius variations as well as other types of wear such as pitting and spalling can also lead to increased or decreased friction along the stroke. Knowing that friction varies with velocity and there is substantially different friction profiles at low and high speeds. It is important when designing movements that these variations of parameters are taken in to account. Several tests were designed for the purpose of extracting estimates of

Rotational speed (RPM)	Linear velocity (mm/min)
15	300
30	600
60	1200
120	2400
150	3000
300	6000
600	12000
1200	24000
1500	30000
3000	60000

Table 5.1: Speeds used for the friction test

the stiffness, inertia, and friction. The tests were designed after the tests Siemens uses for their proprietary software.

For the friction tests several speeds were used to create a full friction profile. This involved moving the axis at 10 different speeds both forwards and back as seen in table 5.1. Moving the axis at several different constant velocities would allow the creation of a friction profile which can be seen in section 5.3.2. An overview of the friction test can be seen in Figure 5.2. Another test used constant acceleration over different sections of the stroke to estimate the stiffness by taking the difference of the rotary encoder and linear encoder. Using this stiffness estimates could be taken at different points along the axis.

5.2.2 Data Collection

The data generated by the CNC are called "trace files". When generating trace files you can select which variables are included. These variables can be sensor readings, such as from the encoders, or it can be data from the control loop such as velocity

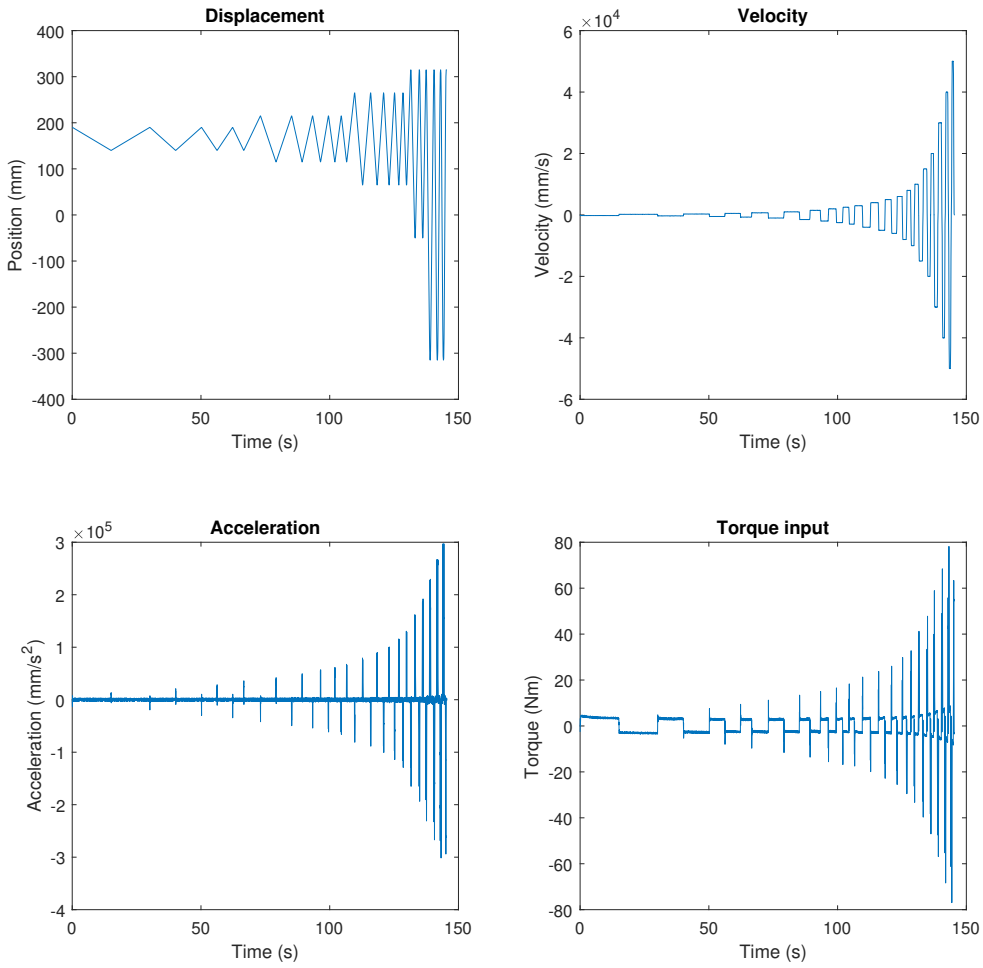

Figure 5.2: Overview of friction test

and position error. These files are generated as a XML file. To effectively analyze this data, the first step would be to load the data, or convert it to a data form which can be used. The primary modeling software being used for analysis has been MATLAB. To easily load this data into MATLAB it is first converted to a table in a CSV data file. For the trace files used for data analysis the primary variables of interest are the measured positions and velocity at each encoder and the command torque. These variables can be used to create the estimates of stiffness and friction seen in sections 5.3.1 and 5.3.2. The torque command and position of the axis are also useful for modeling of the system. An input-output set of data is necessary for validating any model and for any parameter estimation of those models.

5.3 Modeling the System

Modeling the system is important for several different purposes. For the industry partner it is valuable to model the system and understand how different conditions can affect the system. For research purposes it is valuable for research into other topics such as ML, control, and estimation. Modeling of the systems parameters and models used to predict and understand the systems behaviour are discussed below.

5.3.1 Modeling Stiffness

One point of analysis would be examining the stiffness of the system. A LFD consists of multiple connected competent which each contribute to the overall stiffness of the system. An overview of a typical LFD and the components that contribute to its stiffness can be seen in figure 5.3. These components are connected in series meaning

the overall stiffness K_{eq} can be expressed as:

$$K_{eq} = \{\frac{1}{K_1} + \frac{1}{K_2} + ... + \frac{1}{K_n}\}^{-1} = \{\sum_{i=1}^{n} \frac{1}{K_i}\}^{-1} \tag{5.3.1}$$

For a ball screw specifically, if looking at the various stiffness's that make up to equivalent stiffness it may look like this:

$$K_{eq} = \{\frac{1}{K_{coupling}} + \frac{1}{K_{screw}} + \frac{1}{K_{nut}} + \frac{1}{K_{bearings}} + \frac{1}{K_{Supports}}\}^{-1} \tag{5.3.2}$$

Because this system uses a fixed-free arrangement for the bearings only the fixed bearing and support would be considered, not the free bearing and support. Given this relationship the equivalent stiffness will be most affected by smaller values of stiffness than by larger values of stiffness. For instance given 4 springs in series with a stiffness of 1000 NM. the equivalent stiffness would be:

$$K_{eq} = \{\frac{1}{1000} + \frac{1}{1000} + \frac{1}{1000} + \frac{1}{1000}\}^{-1} = 250 \tag{5.3.3}$$

If one of the elements stiffness was doubled to 2000 the resulting stiffness would be:

$$K_{eq} = \{\frac{1}{2000} + \frac{1}{1000} + \frac{1}{1000} + \frac{1}{1000}\}^{-1} = 285 \tag{5.3.4}$$

Which is an increase of 14% If one of the elements stiffness was halved to 500 the resulting stiffness would be:

$$K_{eq} = \{\frac{1}{500} + \frac{1}{1000} + \frac{1}{1000} + \frac{1}{1000}\}^{-1} = 200 \tag{5.3.5}$$

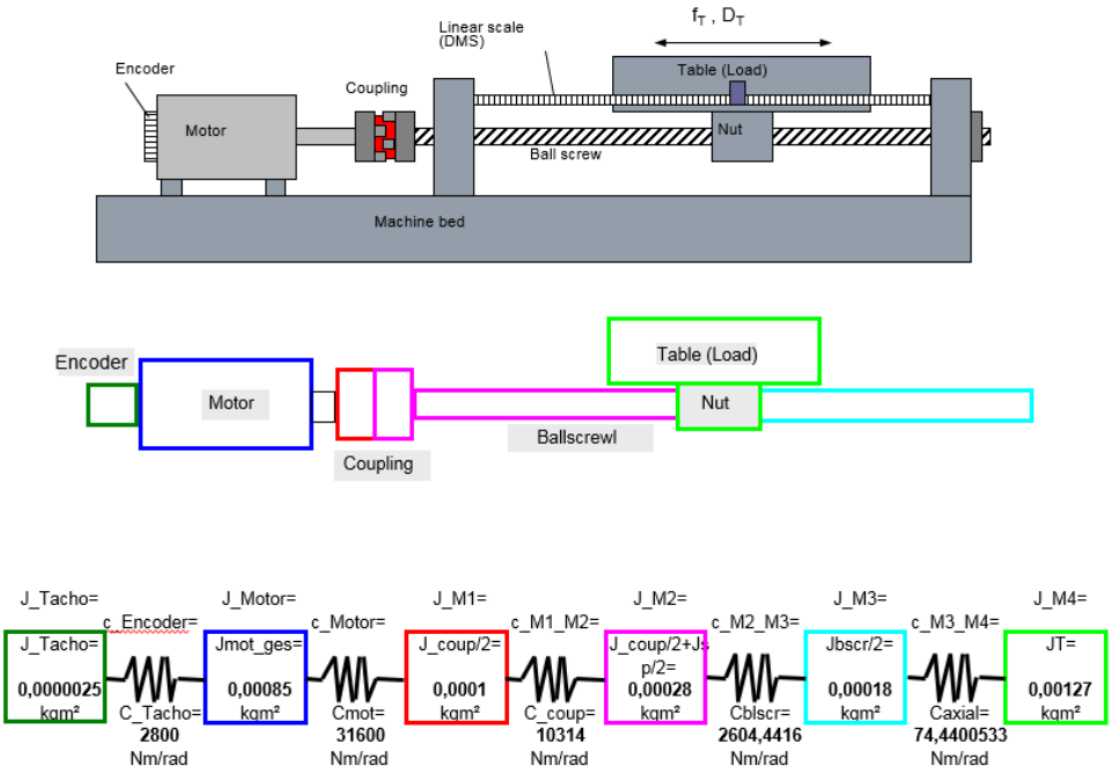

Figure 5.3: Multiple components of a linear feed drive contributing to overall stiffness [125]

Which represents an increase of 20%. The results are even more drastic with larger changes in stiffness. With a 10 times increase or decrease to stiffness results in a 29% increase or decrease 70% respectively. From this we can see that lower component stiffness has a larger effect on overall stiffness than high stiffness.

While it may be useful to individually examine each of the stiffness and their contribution to the overall stiffness as well as the instantaneous position of various components along the system, modeling each of these components separately can increase system complexity exponentially. For example the transfer function for the last mass unit and the input for a system with a single mass, two masses connected

via one spring, and 3 masses each connected via a spring can be seen in equations (5.3.6)-(5.3.8) below. As can be seen each additional level of complexity increases the order of the transfer function by 2.

$$\frac{x_1}{u} = \frac{1}{(m_1 s^2)} \tag{5.3.6}$$

$$\frac{x_2}{u} = \frac{k_1}{(m_1 m_2)s^4 + (m_1 k_1 + m_2 k_1)s^2} \tag{5.3.7}$$

$$\frac{x_3}{u} = \frac{k_1 k_2}{m_1 s^2 k_1 \begin{vmatrix} m_2 s^2 + k_1 + k_2 & -k_2 \\ -k_2 & m_3 s^2 + k_2 \end{vmatrix} + k_1 \begin{vmatrix} -k_1 & -k_2 \\ 0 & m_2 s^2 + k_2 \end{vmatrix}}$$
$$= \frac{b_1}{a_1 s^6 + a_2 s^4 + a_3 s^2 + a_4} \tag{5.3.8}$$

As can be seen complexity of the system and resulting transfer functions increases substantially for each additional sub-stiffness being examined. This is not ideal as it will increase computational complexity, increase the chance of instability, and increase the number of parameters that need to be estimated. Given this information it is ideal to simply choose a lower level approximation such as the one or two mass model to model the system. Often the single mass model has been applied for many control applications. One issue with this model is that it does not account for the stiffness within the system.

In addition to the difficulty in modeling many stiffness in series there is also the issue with the fact that the stiffness of at least some of these objects is non-linear.

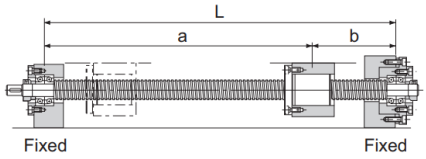

(a) Fixed-fixed bearing arrangement

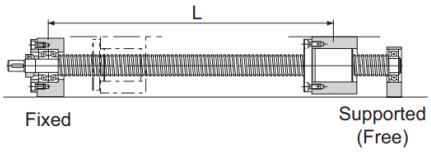

(b) Fixed-free bearing arrangement

Figure 5.4: Two different types of bearing arrangements

For the ball screw for instance the ball screws stiffness will vary along the length of the screw, it will also depend on bearing support configuration. There are two common bearing arrangements as seen in Figure 5.4. For a fixed-free configuration the following formula is used to estimate the stiffness of of the ball screw:

$$\frac{A \cdot E}{L} \tag{5.3.9}$$

And for a fixed-fixed the following equation is used

$$\frac{A \cdot E \cdot L}{a \cdot b} \tag{5.3.10}$$

In the fixed-free configuration the stiffness decreases linearly from if the nut is positioned near the fixed side to the free side. As can be seen in the experimental results in Figure 5.5 the stiffness decreases from one end to the other. The change is relatively modest from one end to another, this is due to the fact that with several stiffness in series the change in one will have a modest overall effect especially if the ball screw is the stiffest component compared to others. It is also known that the preload will increase the stiffness of the system, specifically at lower axial loads. Higher levels of preload result in high levels of stiffness. Once the applied axial load

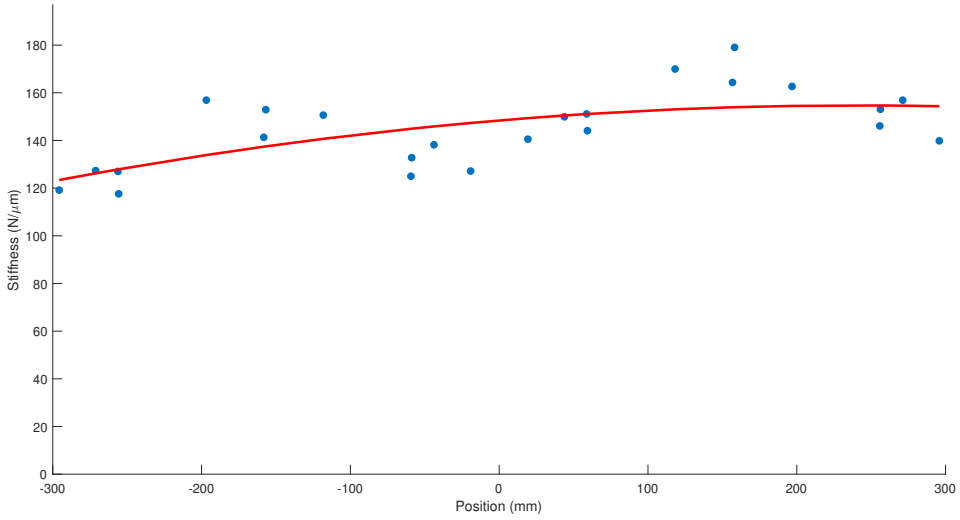

Figure 5.5: Stiffness estimation from experimental data

reached a certain value the difference between a preloaded screw and non preloaded screw become negligible as seen in Figure 5.6. One approximation for the stiffness due to preloading is given as [133]:

$$K_n = K(\frac{F_a}{0.1C_a})^{\frac{1}{3}} \cdot 0.8 \tag{5.3.11}$$

Where F_a is the true nut stiffness, K is the nominal nut stiffness F_a if the force due to preload and F_a is the dynamic load rating. Given this relationship it can be seen that preloading has an effect of increasing stiffness. If looking at Figure 5.6. It can be seen that the stiffness curve of different preloads seems to be approximately flat for lower axial loads.

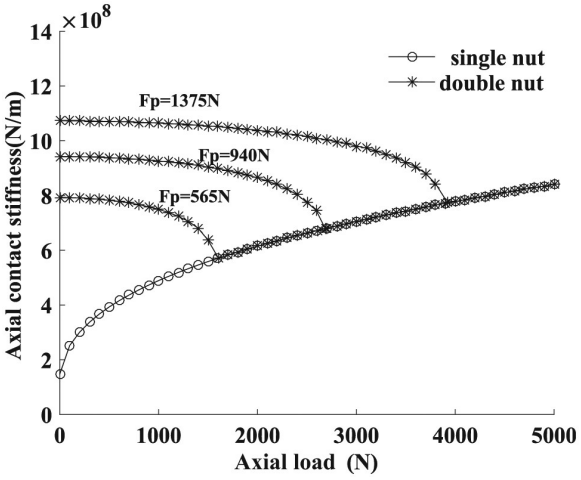

Figure 5.6: Stiffness due to preload at multiple different levels of preload [87]

5.3.2 Friction Modeling

Normally friction in linear system modeling used for estimation and control only considers the velocity dependent component of viscous friction, unfortunately this is inadequate for accurately modeling the system dynamics. When modeling the friction between two lubricated surfaces, a a non-linear relationship between the friction force/torque and the velocity of the system is observed as seen in Figure 5.7. This relationship for the friction force can be given by equations. (5.3.12)-(5.3.15).

$$F_{Friction} = F_{Stribeck} + F_{Coulomb} + F_{Viscous} \tag{5.3.12}$$

$$F_{Stribeck} = \sqrt{2e}(F_{brk} - F_c) \cdot exp(-(\frac{v}{v_{st}})^2) \cdot \frac{v}{v_{st}} \tag{5.3.13}$$

$$F_{Coulomb} = F_c \cdot tanh(\frac{v}{v_{Coul}}) + f_{offset} \tag{5.3.14}$$

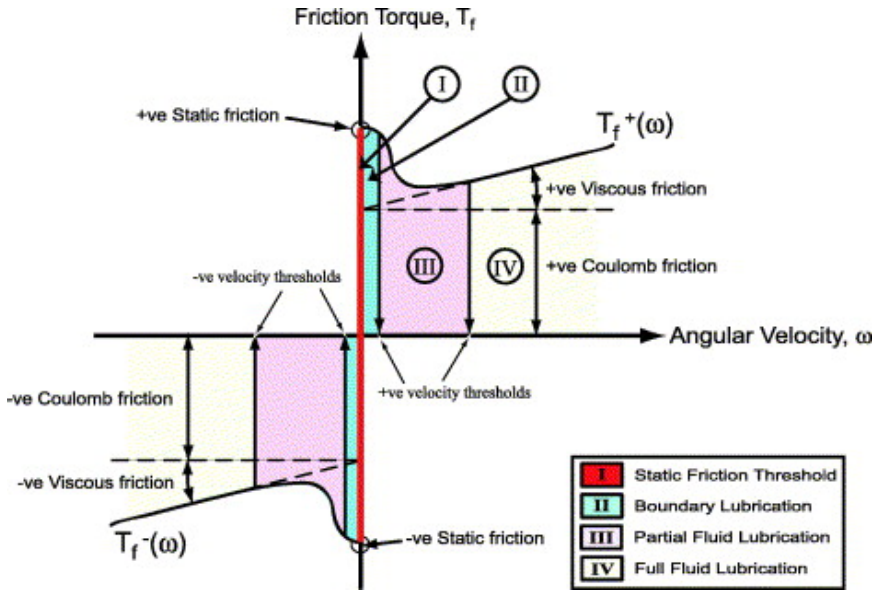

Figure 5.7: Friction profile [154]

$$F_{Viscous} = Dv \tag{5.3.15}$$

Where F_{brk}, F_c, f_{offset} v, v_{st}, v_{Coul}, D are the breakaway friction, Coulomb friction amplitude, Coulomb force offset, velocity, Stribeck velocity threshold, Coulomb velocity threshold, and viscous friction coefficient respectively. The individual frictions as well as their sum can be seen in Figure 5.8. Looking at the results obtained from experimental tests seen in Figure 5.9. Using the model and the equations above the parameters of each of the friction component can be estimated and the model can be fit to the data using non-linear regression as seen in Figure 5.10.

One point of interest that was brought up by our industry partner was the effect of a warm-up cycle on the performance of their MTs. They had noticed that after a machine was down for service it would have odd performance for a while after being brought into use. To examine the effect this might have five sets of tests

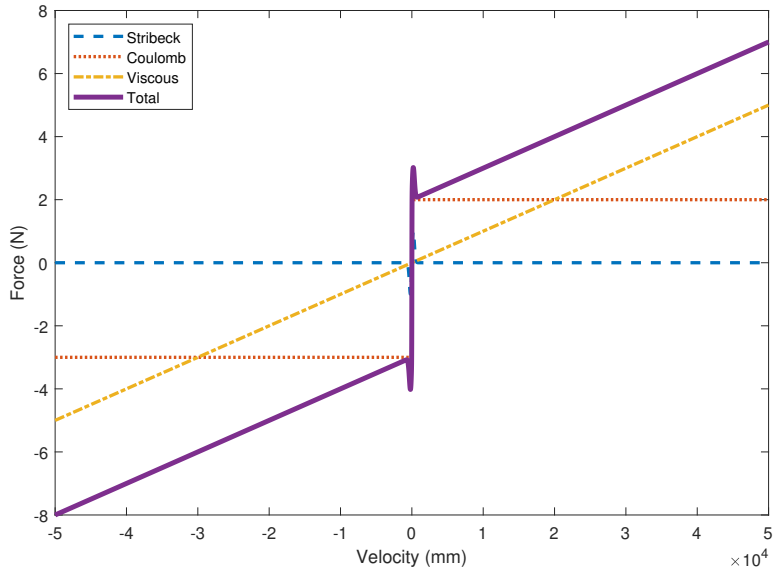

Figure 5.8: The different components that make up friction

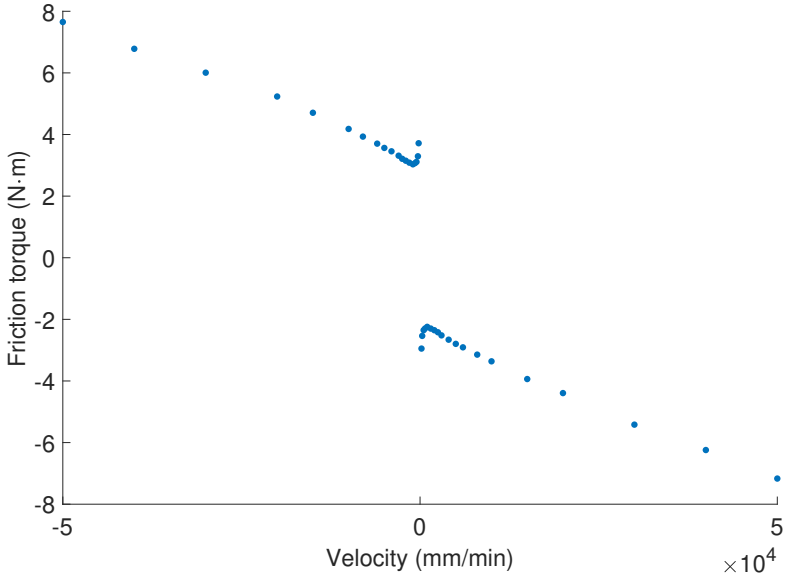

Figure 5.9: Experimental results for friction

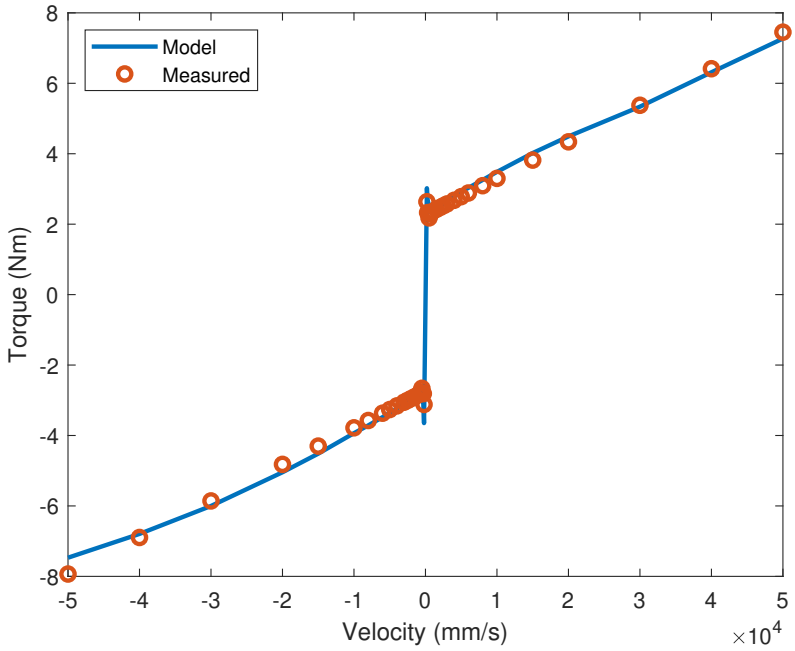

Figure 5.10: Model estimate of friction

were conducted. After each test a warm-up cycle was run. So each successive test would represent a more "warmed up" state. After examining the data and using the parameter estimation of the friction model the following results were found in Figure 5.11. As can be seen the warmup cycle had relatively minimal effect on the high speed portion of the friction. The primary difference was at lower speeds. With the exception of the fourth warm-up cycle which seemed to be an outlier, more warmed up systems seemed to have a lower coulomb and stribeck friction at lower speeds. This makes sense as the Stribeck friction is affected by the viscosity of the lubrication [37]. As the lubrication increases in temperature its viscosity tends to decrease. This decrease in viscosity will decrease the overall Stribeck friction.

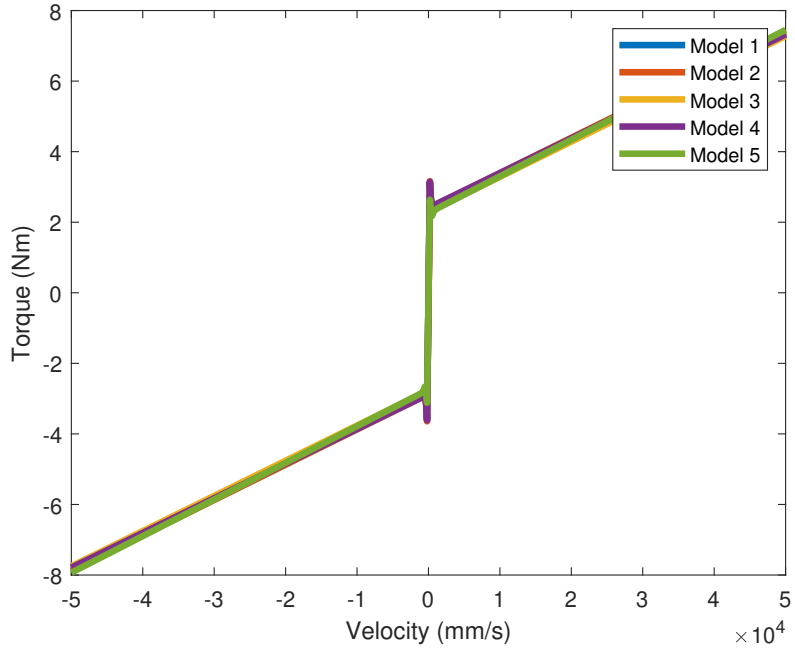

(a) Friction results with different levels of warmup

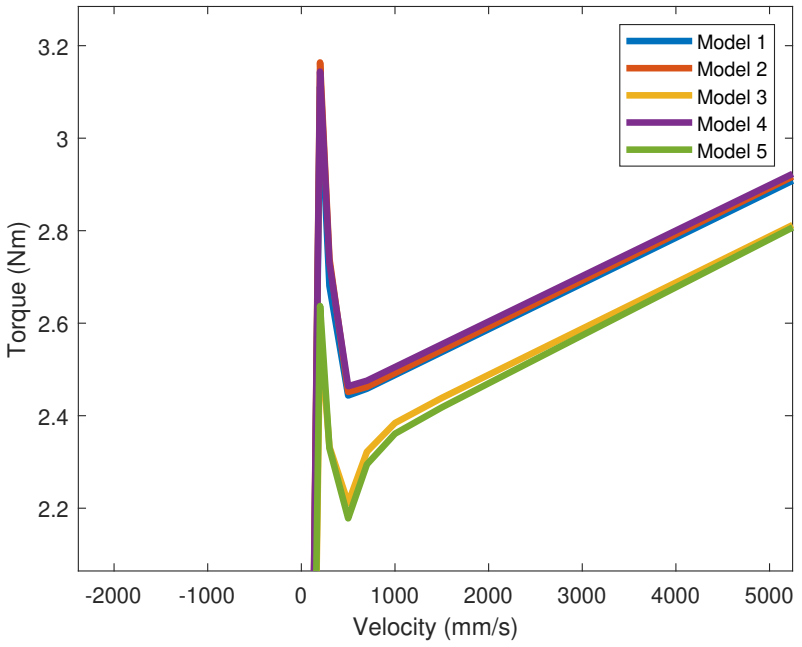

(b) Friction results with different levels of warmup zoomed in on stribeck portion

Figure 5.11: Effect of system warm-up cycle on friction

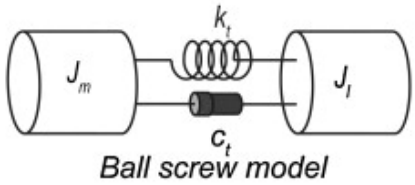

(a) First type of common model which accounts for stiffness between motor and moving components [9]

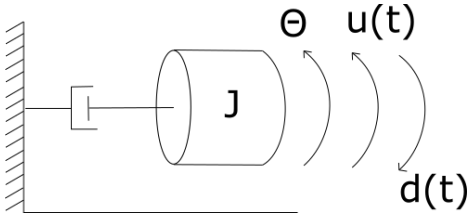

(b) Second type of popular system which lumps all masses [123]

Figure 5.12: Two types of Lagrangian lumped mass models

5.3.3 Modeling the Linear Feed Drive

Creating a model of the system is very important. One of the stated goals of this experimental test bench is the development and testing of control and estimation methods. Both of these, especially estimation, require a system model which can accurately predict its behaviour. Two modeling solutions were utilized to attempt to model the system. The first is a Lagrangian lumped mass model, and the second is a Simulink Simscape model.

Lumped Mass Modeling

There has been several previous works which have modeled the system using a Lagrangian lumped mass model. This is the most common model for control and estimation seen in the literature. Two common Lagrangian lumped mass models describing the system modified from the one seen in figure 5.12. For the simpler of the two models the transfer function relating the input to the output is the following:

$$G(s) = \frac{\theta}{u} = \frac{1}{Js^2 + Ds} \tag{5.3.16}$$

Taking the z transform of this transfer function yields the following form:

$$G(z) = \frac{\theta}{u} = \frac{b_1}{a_1 z^2 + a_2 z} = \frac{b_1 z^{-2}}{a_1 + a_2 z^{-1}} \tag{5.3.17}$$

and a state space representation of the following:

$$\begin{bmatrix} \dot{x}_1 \\ \dot{x}_2 \end{bmatrix} = \begin{bmatrix} 0 & 1 \\ 0 & -\frac{D}{J} \end{bmatrix} \begin{bmatrix} x_1 \\ x_2 \end{bmatrix} + \begin{bmatrix} 0 & 0 \\ \frac{1}{J_m} & \frac{1}{J_m} \end{bmatrix} \begin{bmatrix} u(t) \\ d(t) \end{bmatrix} \tag{5.3.18}$$

For the second model with the two lumped masses the transfer function for the input to the output of the table can be given as:

$$G(s) = \frac{\theta_2}{u} = \frac{D_1 s + k}{(J_m + J_{fd})s^4 + (D_1 J_m + D_1 J_{fd} + D_2 J_m)s^3 + (J_m K + J_{fd} K + D_1 D_2)s^2 + (D_2 K)s} \tag{5.3.19}$$

Which can also be given as a z transform of this transfer function which gives:

$$G(z) = \frac{\theta_2}{u} = \frac{b_1 z + b_2}{a_1 z^4 + a_2 z^3 + a_3 z^2 + a_4 z} = \frac{b_1 z^{-3} + b_2 z^{-4}}{a_1 + a_2 z^{-1} + a_3 z^{-2} + a_4 z^{-3}} \tag{5.3.20}$$

and finally the state space of this system can be given as:

$$\begin{bmatrix} x_1 \\ x_2 \\ x_3 \\ x_4 \end{bmatrix} = \begin{bmatrix} 0 & 1 & 0 & 0 \\ -\frac{K}{J_{fd}} & -\frac{D_1}{J_{fd}} & \frac{K}{J_{fd}} & \frac{D_1}{J_{fd}} \\ 0 & 0 & 0 & 1 \\ \frac{K}{J_m} & \frac{D_1}{J_m} & -\frac{K}{J_m} & -\frac{D_1+D_2}{J_m} \end{bmatrix} \begin{bmatrix} \dot{x}_1 \\ \dot{x}_2 \\ \dot{x}_3 \\ \dot{x}_4 \end{bmatrix} + \begin{bmatrix} 0 & 0 \\ \frac{1}{J_m} & 0 \\ 0 & 0 \\ 0 & \frac{1}{J_{fd}} \end{bmatrix} \begin{bmatrix} u(t) \\ d(t) \end{bmatrix} \tag{5.3.21}$$

Some initial parameter estimation was done using these models and the system identification toolbox in Matlab. However this did not yield very promising results as seen in Figure 5.13. This is expected due to the clear non-linear behaviour for the friction of this system. One typical solution is to use a Taylor series approximation of the system [12]. One issue with this approach is that since it is creating a linear approximation about a certain point it may only be valid within a certain range. And given the system experienced movements at a variety of velocities this will be inadequate.

Simscape Modeling

Another type of model that can be used to represent the system is a Simulink Simscape model. As previously mentioned, Simscape models use relations such as springs, shafts, and masses to model the system. Using previous work which has modeled LFDs [105] the following model seen in Figure 5.14 was created to model the LFD. There are several key components in the model. First is a flexible shaft to represent the flexibility of the system which creates a discrepancy between the rotary encoder measurement and the linear encoder measurements. The second components is the

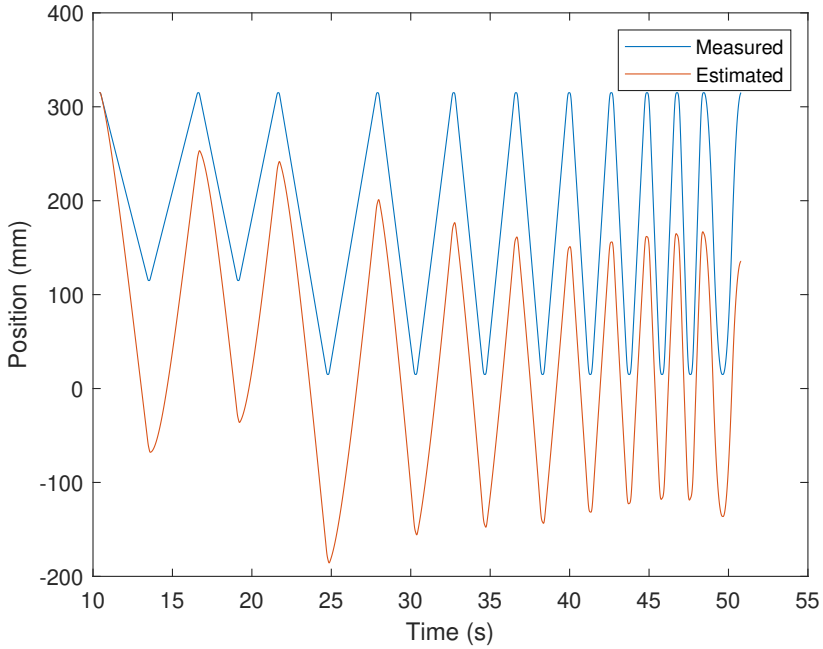

Figure 5.13: Results of system identification using first model

lead screw components which transfers rotary motion into linear motion. The translation friction component models the three friction components which make up the friction force. And finally, the platform mass represents the mass of the moving platform. There is two inputs to the system, the input torque which acts on the shaft and a disturbance force which acts on the platform. There are four system outputs. The rotational position and speed measured from the shaft input, and the linear position and velocity measured from the table. This model can be used to simulate the dynamics of the system as well as estimate the parameters of the system for a given input-output relationship.

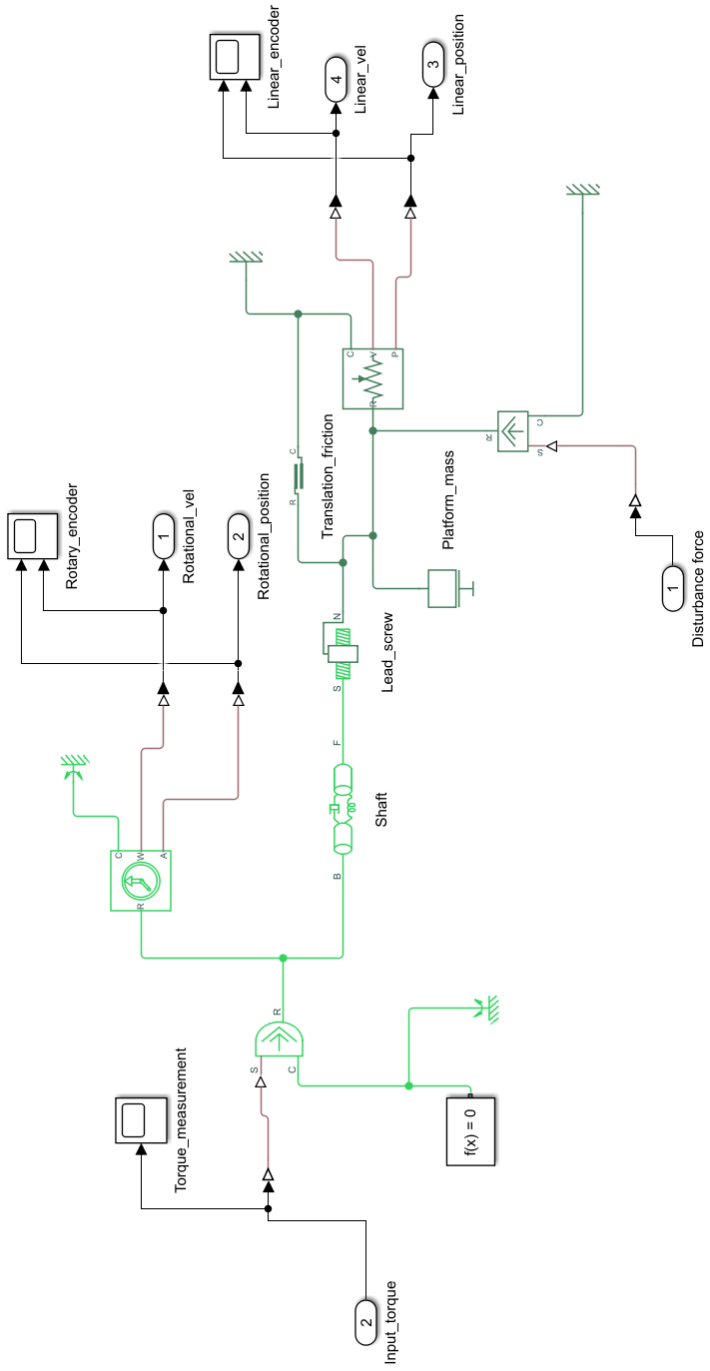

Figure 5.14: Simscape model of the LFD

Chapter 6

Conclusion

MTs form the backbone of modern manufacturing. They enable the fast and accurate manufacture of complex parts. In order to keep them in good working order it is ideal to apply CM. CM can improve the performance and reliability of these machines to maximize throughput and return on investment. One possible strategy for implementing CM is the use of a DT. DTs use multiple data streams and multiple models for up to date system modeling. These predictive capabilities can be used for various useful functionality.

This work involved the design, manufacture, assembly, and integration of a MT LFD workbench. To design the workbench previous work in the literature was examined. Factors such as how wear was implemented, how external force was applied as well as which sensors and data streams were examined. Combining knowledge of previous work with the constraints and criteria of the stakeholder were combined to form a design. The research performed on the workbench will be used both for industrial purposes as well as improving the theory and application of various smart technologies such as ML, estimation theory, mechanical modeling, and control. The

MT LFD has a novel method of implementing external disturbance force which is more realistic and controllable compared to other methods seen in the literature.

A IMM method was introduced which can be used for fault detection and condition monitoring. This method is a novel implementation of IMM. It has been shown through simulation to be able to accurately predict levels of preload levels in the test scenarios. A novel method of calculating the mode probability by introducing an activation function has also been introduced. This modification improved the fault detection accuracy compared to regular IMM.

The final contribution was an analysis of the data gathered from the MT LFD which provides insight into modeling of the friction and stiffness with the associated difficulties. Two modeling strategies, one using Lagrangian lumped mass modeling and one using Simulink Simscape were used to model the system and estimate parameters. Additionally, a DT strategy of model fusion for improved modeling and CM was introduced. This modeling method can provide improved modeling certainty and accuracy over a single model.

This work has already produced published notable results as described in the section 6.2. A great deal of other research can be built off of this work as discussed below in section 6.1.

6.1 Future Work

Future work on this research can be divided into 3 sections, future work involving adding additional sensors and capabilities to the workbench, improving on the IMM fault detection strategy, and continued analysis on system modeling.

Future work on the physical LFD workbench would primarily involve the inclusion

of additional sensors such as accelerometers, temperature sensors, and an IMU. This would allow the collection of additional data streams which would allow more types of analysis and easier implementation of data driven modeling and condition monitoring. Additionally, it would be ideal to design and implement a ball screw with a modifiable preload. This would enable easier analysis of the effects of decreased preload.

For additional work on the IMM fault detection strategy it would be advantageous to implement a more complex model of the system as well as implementing the method for fault tolerant control. It would also be advantageous to implement a modifiable preload screw as mentioned above to gather experimental validation of the method.

In addition to continue to work on the existing implemented modeling methods, other modeling methods such as FEM, or dynamic simulations using Siemens MCD could provide more useful information. The more modeling strategies and the more accurate and complex they become the more refined the DT of the system becomes. This test bench and various modeling can be used for future research into more advanced types of modeling such as physics informed machine learning.

6.2 Summary of Contributions

The primary contributions of this work are the following.

1. Machine tool workbench
    (a) The design, manufacture, assembly, and integration of a MT LFD test bench
    (b) Novel method of implementing external disturbance force
2. IMM based preload loss detection method

   (a) Novel implementation of IMM

   (b) Novel method for fault detection of preload loss in ball screws

   (c) Novel modification of IMM mode probability calculation

3. Data analysis and modeling for LFD

   (a) Introduction of DT based modeling method for the LFD

   (b) Analysis of modeling stiffness and friction in LFD

   (c) Traditional Lagrangian and Simscape modeling of LFD

Several papers and conference proceeding over the course of this work were published as seen below:

1. Preload Loss Detection in a Ball Screw System using Interacting Models [123]
2. Predictive Maintenance and Condition Monitoring in Machine Tools: An IoT Approach [118]
3. Experimental Setups for Linear Feed Drive Predictive Maintenance: A Review [121]
4. Cognitive dynamic digital twin: enhancements for digital twin platforms based on human cognition [122]
5. IIoDT: Industrial Internet of Digital Twins for Hierarchical Asset Management in Manufacturing [120]
6. Design Considerations for Building an IoT Enabled Digital Twin Machine Tool Sub-System [119]

Appendix A

Component Drawings and Specifications

Table A.1: Main ball screw specifications

Specification	Value	Unit
Dynamic load rating	7450	N
Static load rating	17000	N
Lead	20	mm
Diameter	20	mm
Preload	510	N
Ball diameter	3.175	mm
Drag torque	1.18-1.77	Nm
Lead angle	17.17	degree
Total length	998	mm
Maximum stroke	880	mm

Table A.2: Ball screw support bearing specifications

Specification	Value	Unit
Dynamic load rating	21.9	kN
Max axial load	26.6	kN
Allowable speed	6000	RPM

Table A.3: Loading screw specifications

Specification	Value	Unit
Dynamic load rating	10800	N
Static load rating	18000	N
Lead	20	mm
Diameter	20	mm
Preload	Clearance	
Total length	985	mm
Maximum stroke	905	mm

Table A.4: Motor specifications

Specification	Value	Unit
Static torque	16	Nm
Static current	42.3	A
Maximum torque	42	Nm
Maximum current	44	A
Maximum speed	6000	rpm
Rotor inertia	10.4	kg-cm^2
Rated speed	3000	rpm
Rated torque	10.6	Nm
Rated current	9.7	A
Rated power	3.3	kW

Table A.5: Motor coupling specifications

Specification	Value	Unit
Dynamic torque	19.8	Nm
Static torque	39.6	Nm
Torsional stiffness	67.2	Nm/Deg
Maximum speed	10,000	RPM
Moment of inertia	9.95E-05	kg-m^2

Table A.6: Linear guide specifications

Specification	Value	Unit
Length	1000	mm
Dynamic load rating	21,100	N
Preload	1680	N
Maximum speed	5	m/s

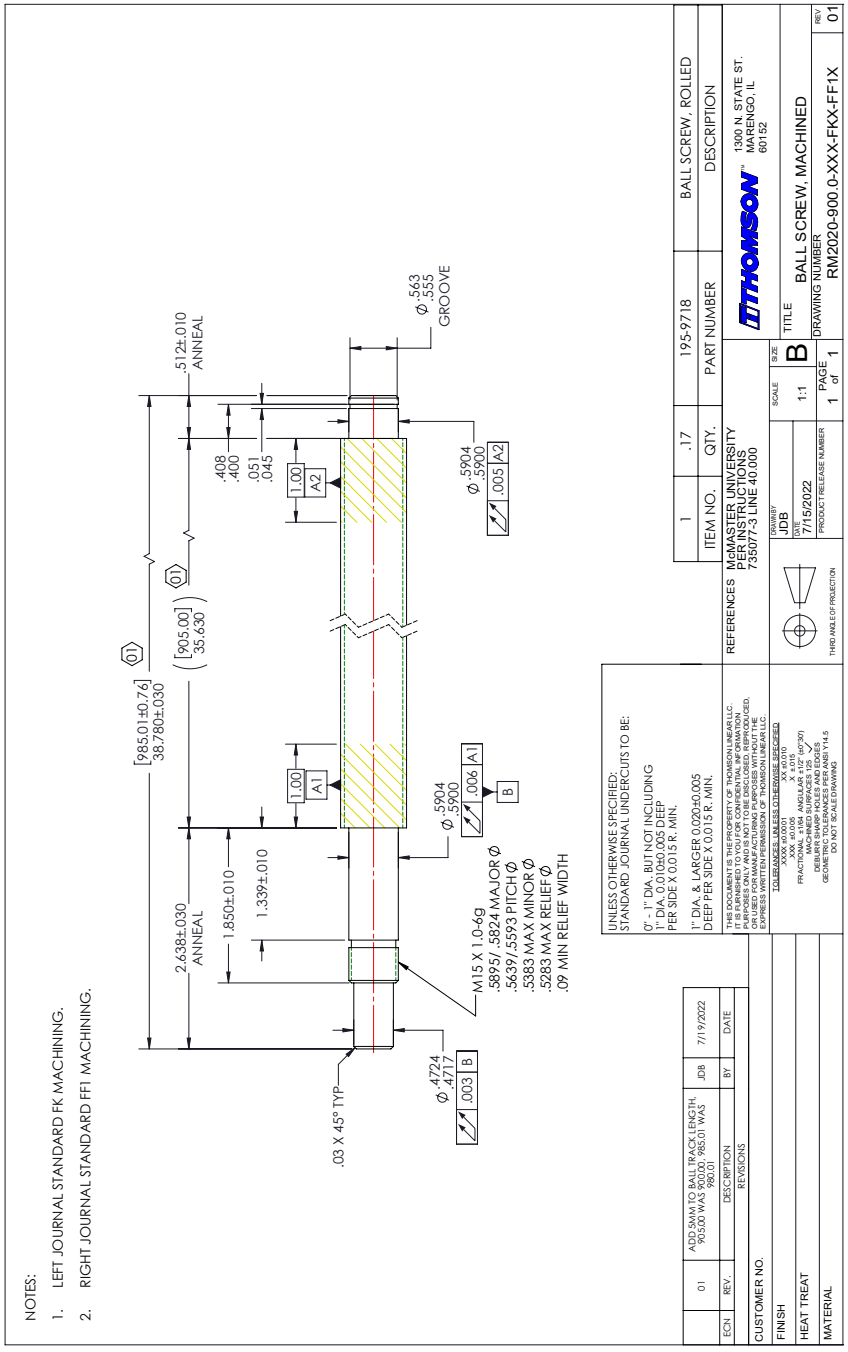

Figure A.1: Secondary external load ball screw drawing

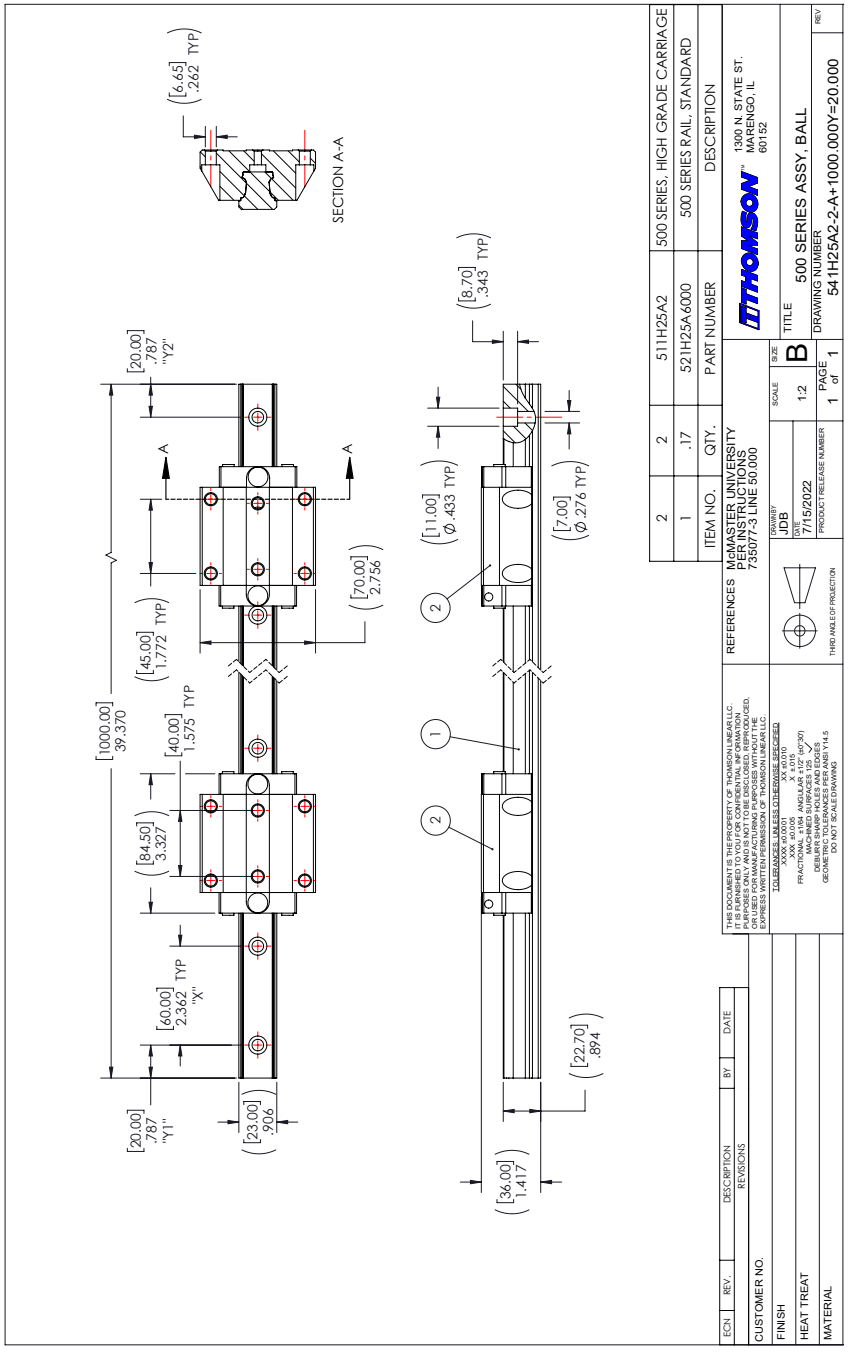

Figure A.2: Linear guides drawing

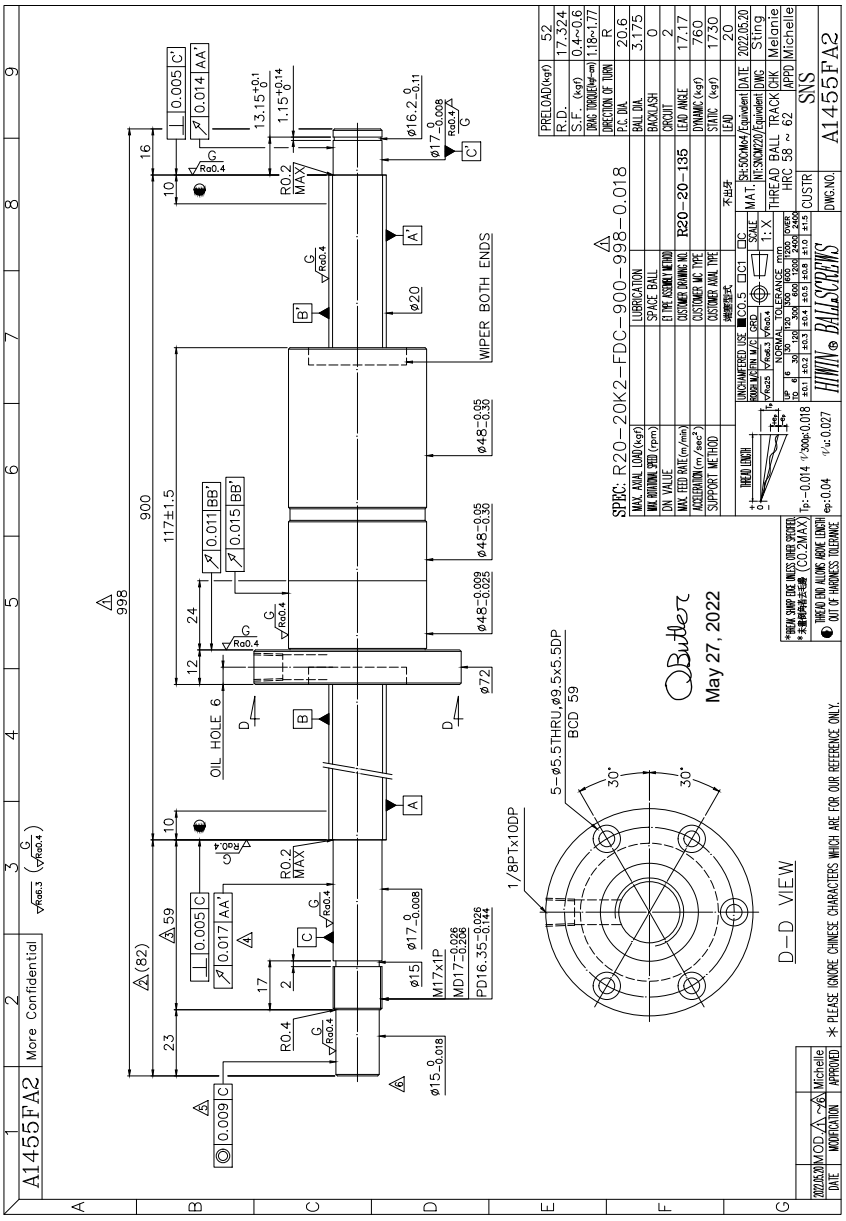

Figure A.3: Main ball screw drawing

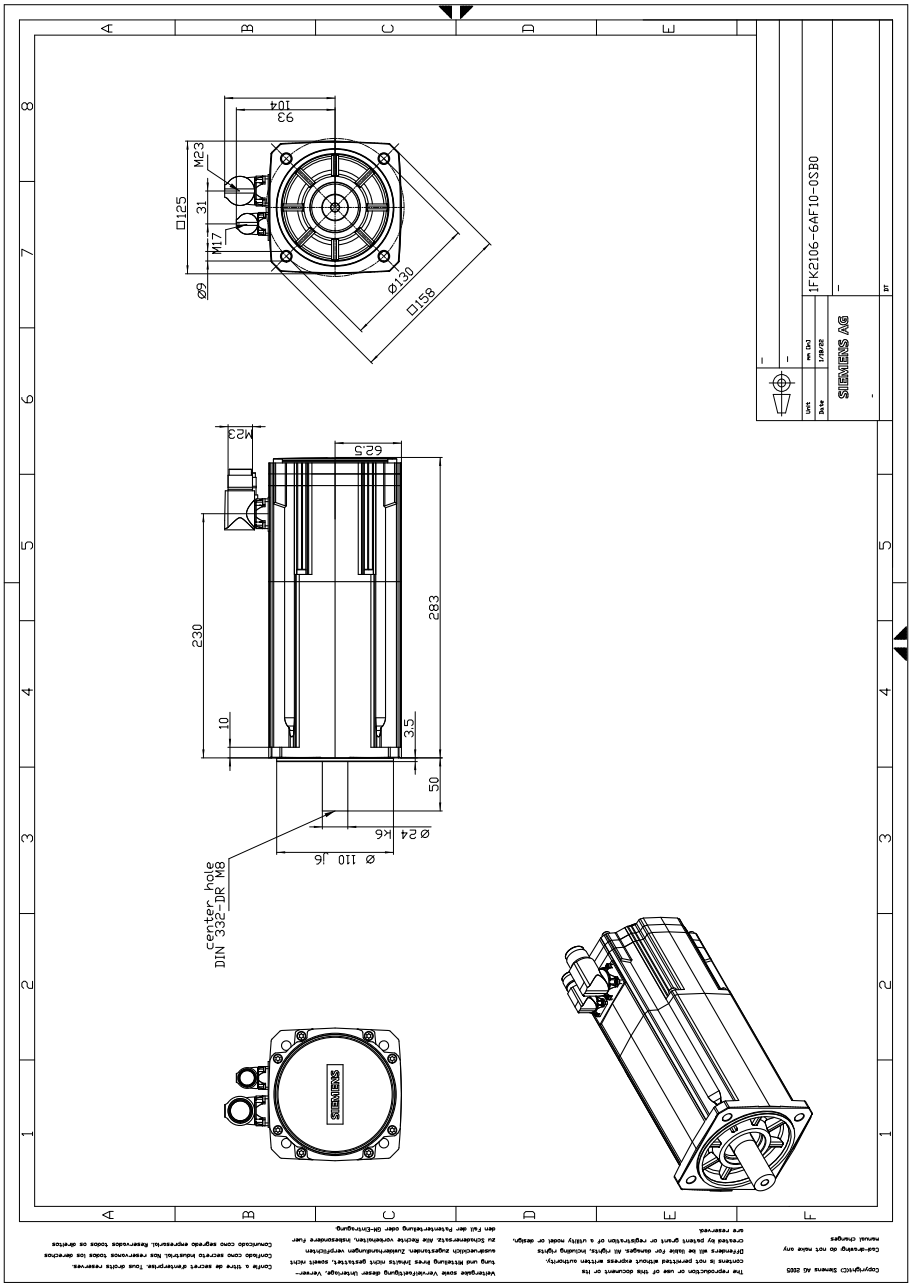

Figure A.4: Servo motor

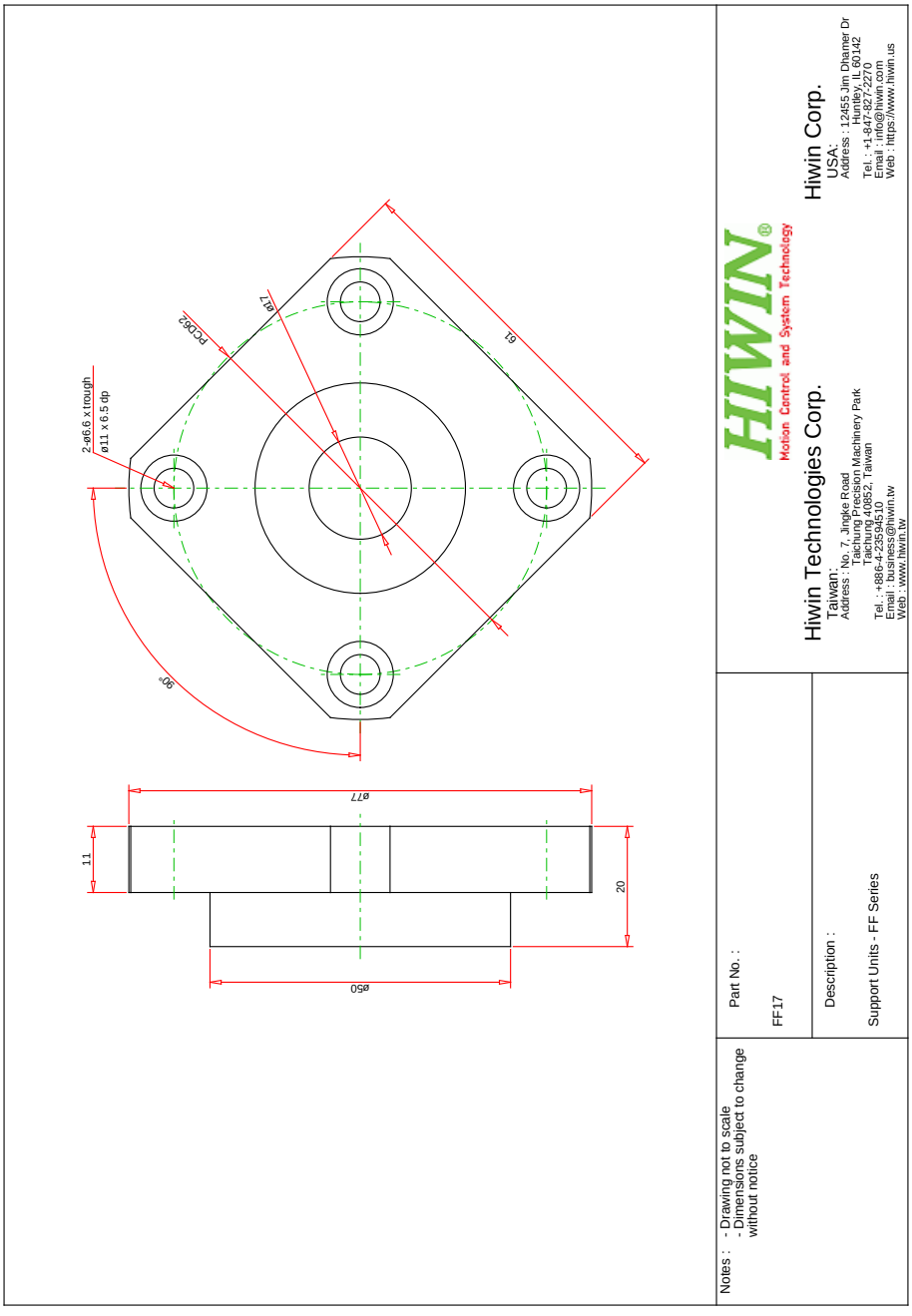

Figure A.5: Free ballscrew bearing

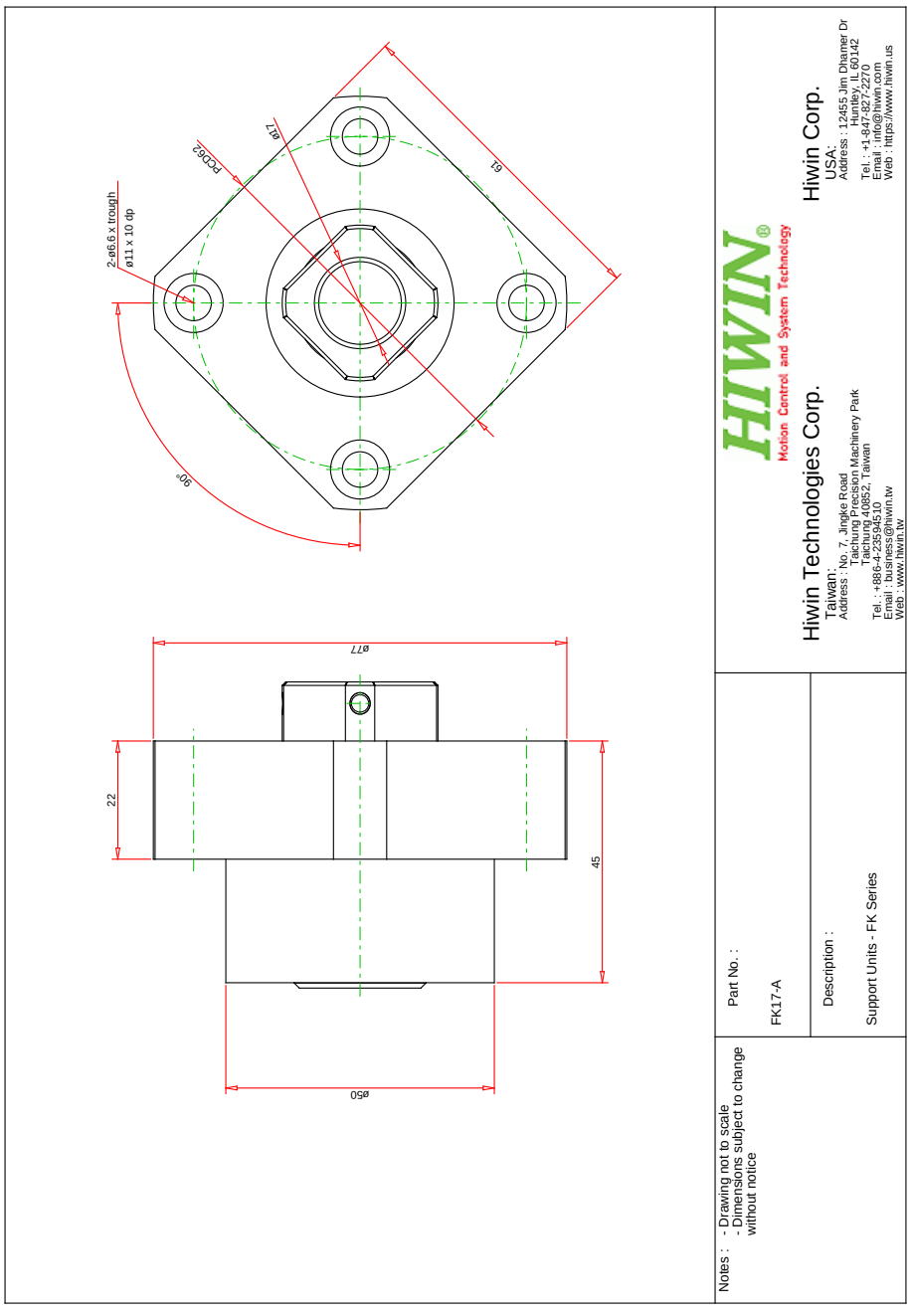

Figure A.6: Fixed ballscrew bearing

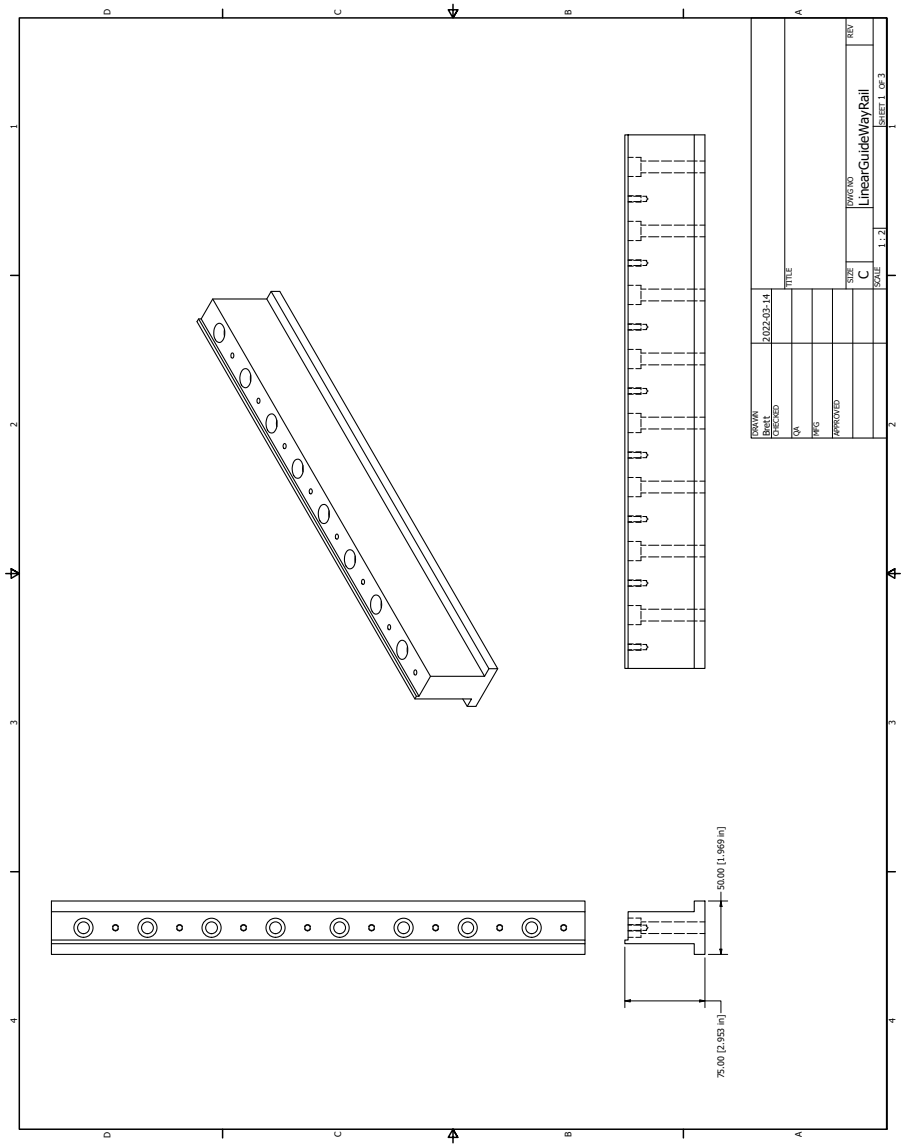

Figure A.7: Linear guide-way mount drawing page 1

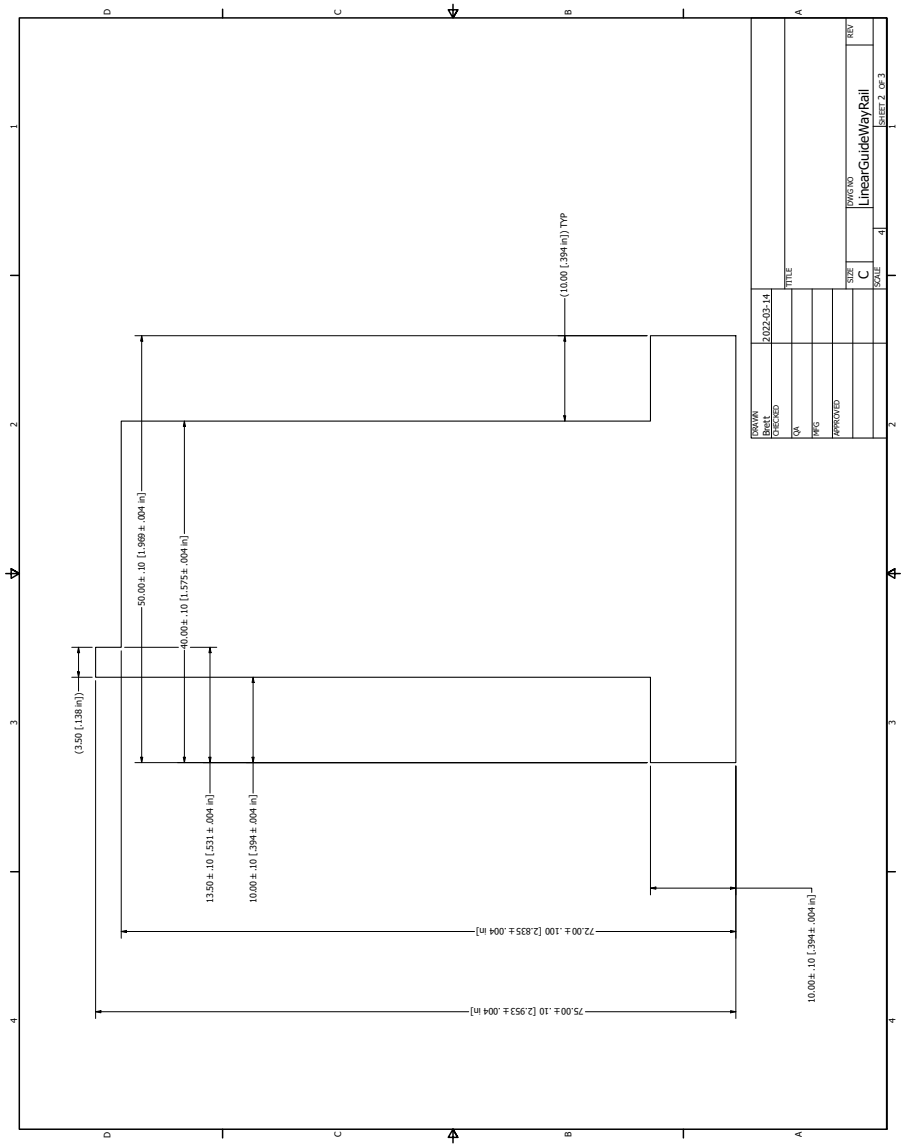

Figure A.8: Linear guide-way mount drawing page 2

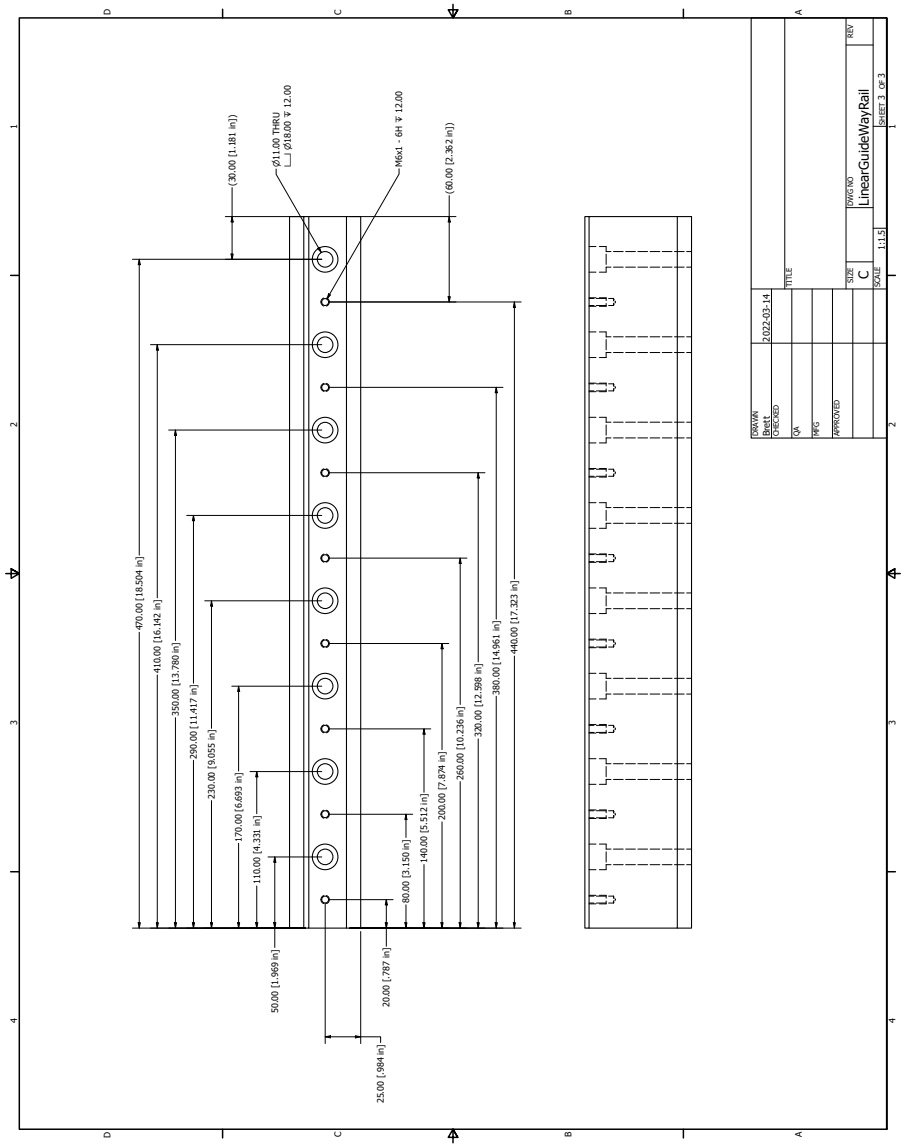

Figure A.9: Linear guide-way mount drawing page 3

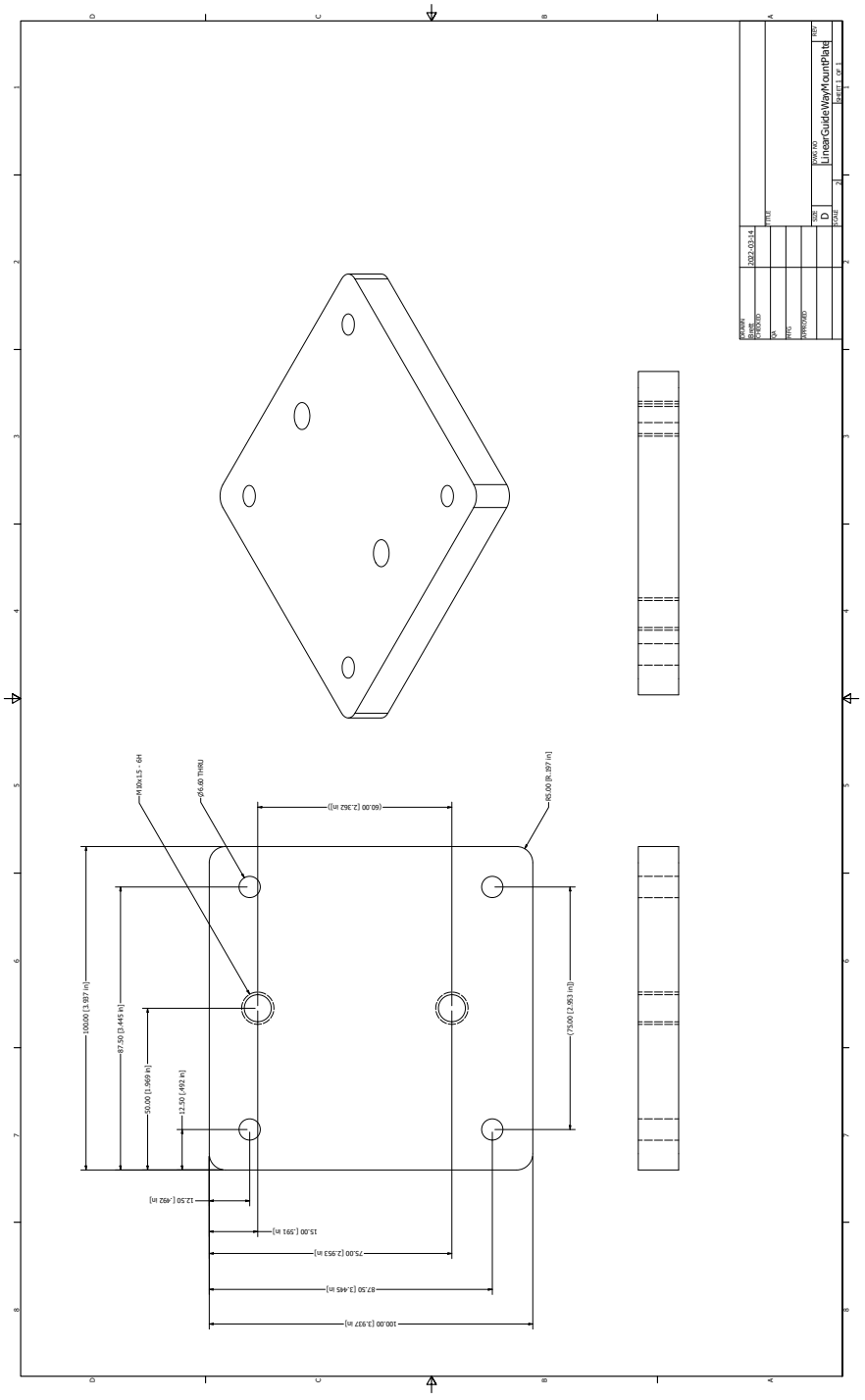

Figure A.10: Linear guide-way mount drawing plates

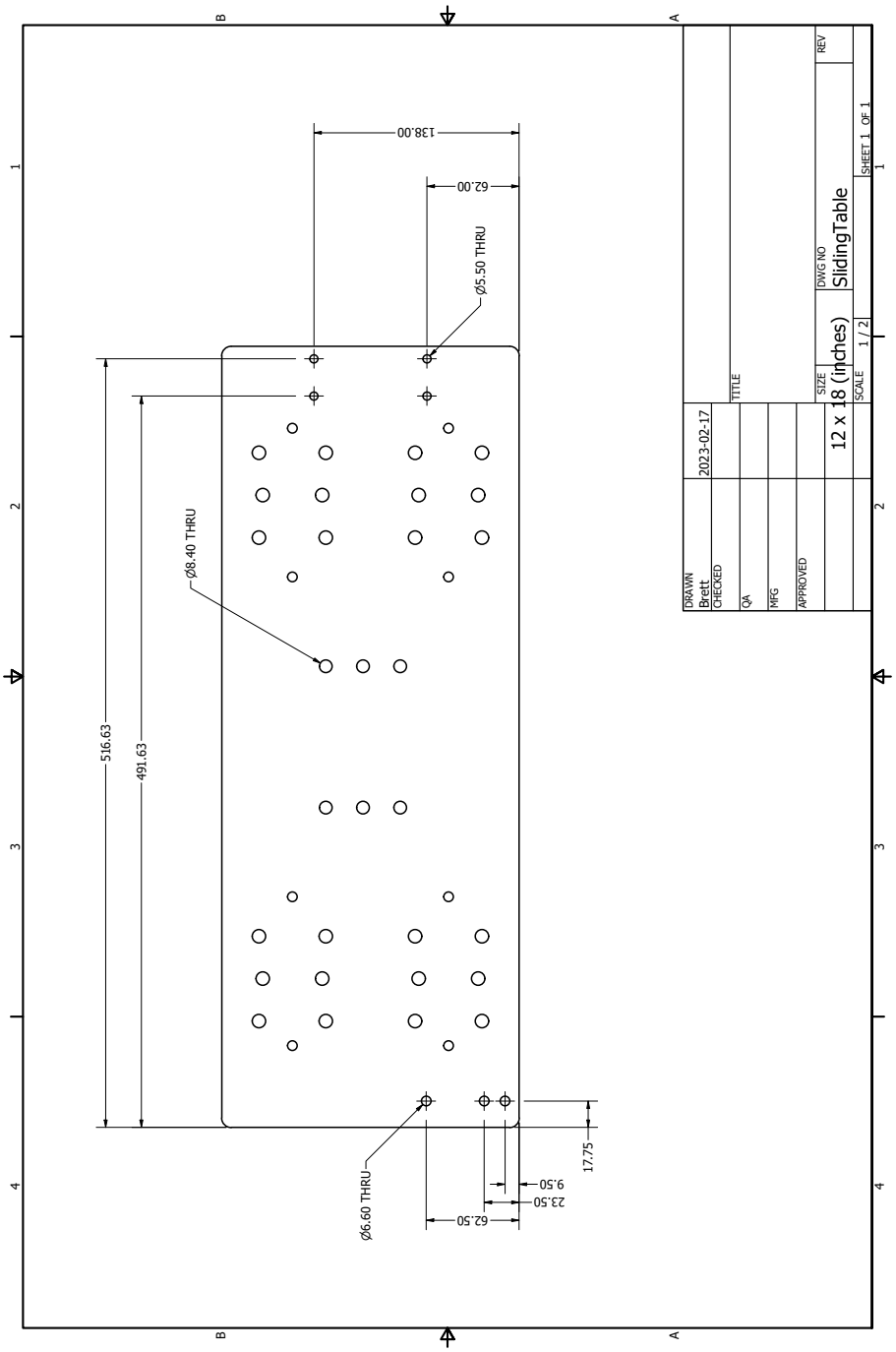

Figure A.11: Work platform drawing

Appendix B

Electrical Drawings

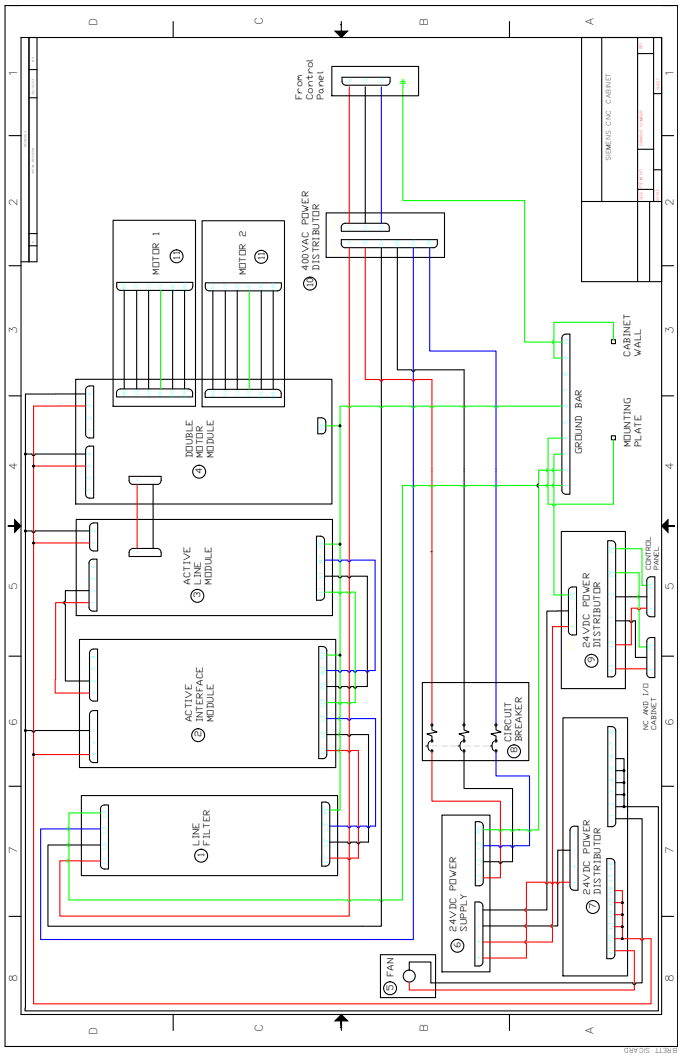

Figure B.1: Electrical drawing for motor drive cabinet

Table B.1: Electrical components bill of materials

Item Number	Description	Part #	Quantity
1	SINAMICS Line Filter	6SL3000-0BE21-6DA0	1
2	SINAMICS Active Interface Module	6SL3100-0BE21-6AB0	1
3	SINAMICS Active Line Module	6SL3130-7TE21-6AA4	1
4	SINAMICS Double Motor Module	6SL3120-2TE21-8AD0	1
5	24V Cabinet Fan	K1G165-AA03-06	1
6	24VDC SITOP Power Supply	6EP3436-8SB00-0AY0	1
7	24VDC Power Distributor	2315256	1
8	Circuit Breaker	3RV2711-1JD10	1
9	24VDC Power Distributor	LFD14003Z	1
10	400 VAC Power Distributor	16220-3	1
11	SIMOTICS S-1FK2 HD Servo motor	1FK2106-6AF10-0SB0	2

Bibliography

[1] H. H. Afshari, S. A. Gadsden, and S. R. Habibi. Robust fault diagnosis of an electro-hydrostatic actuator using the Novel dynamic second-order SVSF and IMM strategy. *International Journal of Fluid Power*, 15(3):181–196, 2014. ISSN 1439-9776. Publisher: Taylor & Francis.

[2] F. Aghazadeh, A. Tahan, and M. Thomas. Tool condition monitoring using spectral subtraction and convolutional neural networks in milling process. *The International Journal of Advanced Manufacturing Technology*, 98(9):3217–3227, Oct. 2018. ISSN 1433-3015. doi: 10.1007/s00170-018-2420-0. URL `https://doi.org/10.1007/s00170-018-2420-0`.

[3] F. Akhavan Niaki, M. Michel, and L. Mears. State of health monitoring in machining: Extended Kalman filter for tool wear assessment in turning of IN718 hard-to-machine alloy. *Journal of Manufacturing Processes*, 24:361–369, Oct. 2016. ISSN 1526-6125. doi: 10.1016/j.jmapro.2016.06.015. URL `https://www.sciencedirect.com/science/article/pii/S152661251630072X`.

[4] K. M. Al-hussain and I. Redmond. DYNAMIC RESPONSE OF TWO ROTORS CONNECTED BY RIGID MECHANICAL COUPLING WITH PARALLEL MISALIGNMENT. *Journal of Sound and Vibration*, 249(3):483–498,

Jan. 2002. ISSN 0022-460X. doi: 10.1006/jsvi.2001.3866. URL https://www.sciencedirect.com/science/article/pii/S0022460X01938660.

[5] A. Al-Shdifat, C. Emmanouilidis, M. Khan, and A. Starr. Ontology-Based Context Modeling in Physical Asset Integrity Management. *Frontiers in Computer Science*, 2, Oct. 2020. doi: 10.3389/fcomp.2020.578673.

[6] A. W. A. Ali, F. A. A. Razak, and N. Hayima. A Review on The AC Servo Motor Control Systems. *ELEKTRIKA- Journal of Electrical Engineering*, 19(2):22–39, Aug. 2020. ISSN 0128-4428. doi: 10.11113/elektrika.v19n2.214. URL https://elektrika.utm.my/index.php/ELEKTRIKA_Journal/article/view/214. Number: 2.

[7] Y. Altintas, K. Erkorkmaz, and W.-H. Zhu. Sliding mode controller design for high speed feed drives. *CIRP Annals*, 49(1):265–270, 2000. doi: https://doi.org/10.1016/S0007-8506(07)62943-6. Publisher: Elsevier.

[8] Y. Altintas, C. Brecher, M. Weck, and S. Witt. Virtual Machine Tool. *CIRP Annals*, 54(2):115–138, Jan. 2005. ISSN 0007-8506. doi: 10.1016/S0007-8506(07)60022-5. URL https://www.sciencedirect.com/science/article/pii/S0007850607600225.

[9] Y. Altintas, A. Verl, C. Brecher, L. Uriarte, and G. Pritschow. Machine tool feed drives. *CIRP Annals*, 60(2):779–796, Jan. 2011. ISSN 0007-8506. doi: 10.1016/j.cirp.2011.05.010. URL https://www.sciencedirect.com/science/article/pii/S0007850611002125.

[10] M. Armendia, F. Peysson, and D. Euhus. Twin-Control: A New Concept Towards Machine Tool Health Management. *PHM Society European Conference*, 3 (1), 2016. ISSN 2325-016X. doi: 10.36001/phme.2016.v3i1.1584. URL http://www.papers.phmsociety.org/index.php/phme/article/view/1584. Number: 1.

[11] M. Armendia, F. Cugnon, L. Berglind, E. Ozturk, G. Gil, and J. Selmi. Evaluation of Machine Tool Digital Twin for machining operations in industrial environment. *Procedia CIRP*, 82:231–236, Jan. 2019. ISSN 2212-8271. doi: 10.1016/j.procir.2019.04.040. URL https://www.sciencedirect.com/science/article/pii/S2212827119306547.

[12] M. Asghari, A. M. Fathollahi-Fard, S. M. J. Mirzapour Al-e hashem, and M. A. Dulebenets. Transformation and Linearization Techniques in Optimization: A State-of-the-Art Survey. *Mathematics*, 10(2):283, Jan. 2022. ISSN 2227-7390. doi: 10.3390/math10020283. URL https://www.mdpi.com/2227-7390/10/2/283. Number: 2 Publisher: Multidisciplinary Digital Publishing Institute.

[13] A. Automation. Ball Screw Guide, 2021. URL https://www.anaheimautomation.com/manuals/forms/ball-screw-guide.php.

[14] M. Avzayesh, M. Abdel-Hafez, M. AlShabi, and S. A. Gadsden. The smooth variable structure filter: A comprehensive review. *Digital Signal Processing*, 110:102912, Mar. 2020. doi: 10.1016/j.dsp.2020.102912. Publisher: Elsevier.

[15] R. U. Baig, S. Javed, M. Khaisar, M. Shakoor, and P. Raja. Development of an ANN model for prediction of tool wear in turning EN9 and EN24 steel alloy. *Advances in Mechanical Engineering*, 13(6):16878140211026720, June

2021. ISSN 1687-8132. doi: 10.1177/16878140211026720. URL https://doi.org/10.1177/16878140211026720. Publisher: SAGE Publications.

[16] M. Benker and M. F. Zaeh. Condition monitoring of ball screw feed drives using convolutional neural networks. *CIRP Annals*, 71(1):313–316, 2022. doi: 10.1016/j.cirp.2022.03.017. Publisher: Elsevier BV.

[17] J. M. Bossio, G. R. Bossio, and C. H. De Angelo. Angular misalignment in induction motors with flexible coupling. In *2009 35th Annual Conference of IEEE Industrial Electronics*, pages 1033–1038, Nov. 2009. doi: 10.1109/IECON.2009.5414696. URL https://ieeexplore.ieee.org/abstract/document/5414696?casa_token=0Cua0rP6_b8AAAAA:IQzvMLgj1rqBsszL9ATYQ68yF6YTBlGIXCyUR-ir2J1m_NjfTm0O2GKeN6HI90XCyAG_1l4Y434. ISSN: 1553-572X.

[18] D. Botkina, M. Hedlind, B. Olsson, J. Henser, and T. Lundholm. Digital Twin of a Cutting Tool. *Procedia CIRP*, 72:215–218, Jan. 2018. ISSN 2212-8271. doi: 10.1016/j.procir.2018.03.178. URL https://www.sciencedirect.com/science/article/pii/S2212827118303378.

[19] Q. Butler, B. Sicard, E. Hughey, Y. Ziada, D. Stephenson, and S. A. Gadsden. Rapid parameter estimation of CNC feed drive systems. In *Signal Processing, Sensor/Information Fusion, and Target Recognition XXXI*, volume 12122, pages 344–351. SPIE, June 2022. doi: 10.1117/12.2626801. URL https://www.spiedigitallibrary.org/conference-proceedings-of-spie/12122/121221B/Rapid-parameter-estimation-of-CNC-feed-drive-systems/10.1117/12.2626801.full.

[20] Q. Butler, Y. Ziada, D. Stephenson, and S. Andrew Gadsden. Condition Monitoring of Machine Tool Feed Drives: A Review. *Journal of Manufacturing Science and Engineering*, 144(100802), June 2022. ISSN 1087-1357. doi: 10.1115/1.4054516. URL https://doi.org/10.1115/1.4054516.

[21] Q. Butler, W. Hilal, B. Sicard, Y. Ziada, and S. A. Gadsden. Generalizing the unscented Kalman filter for state estimation. In *Signal Processing, Sensor/Information Fusion, and Target Recognition XXXII*, volume 12547, pages 13–26. SPIE, June 2023. doi: 10.1117/12.2664227. URL https://www.spiedigitallibrary.org/conference-proceedings-of-spie/12547/1254703/Generalizing-the-unscented-Kalman-filter-for-state-estimation/10.1117/12.2664227.full.

[22] W. Cai, W. Zhang, X. Hu, and Y. Liu. A hybrid information model based on long short-term memory network for tool condition monitoring. *Journal of Intelligent Manufacturing*, 31(6):1497–1510, Aug. 2020. ISSN 1572-8145. doi: 10.1007/s10845-019-01526-4. URL https://doi.org/10.1007/s10845-019-01526-4.

[23] Y. Cai, B. Starly, P. Cohen, and Y.-S. Lee. Sensor Data and Information Fusion to Construct Digital-twins Virtual Machine Tools for Cyber-physical Manufacturing. *Procedia Manufacturing*, 10:1031–1042, Jan. 2017. ISSN 2351-9789. doi: 10.1016/j.promfg.2017.07.094. URL https://www.sciencedirect.com/science/article/pii/S2351978917302767.

[24] R. Caracciolo and D. Richiedei. Optimal design of ball-screw driven servomechanisms through an integrated mechatronic approach. *Mechatronics*, 24(7):819–832, Oct. 2014. ISSN 0957-4158. doi: 10.1016/j.mechatronics.2014.01.004. URL https://www.sciencedirect.com/science/article/pii/S0957415814000051.

[25] K. Chaiprabha and R. Chancharoen. A Deep Trajectory Controller for a Mechanical Linear Stage Using Digital Twin Concept. *Actuators*, 12(2):91, Feb. 2023. ISSN 2076-0825. doi: 10.3390/act12020091. URL https://www.mdpi.com/2076-0825/12/2/91. Number: 2 Publisher: Multidisciplinary Digital Publishing Institute.

[26] P. Chandrasekar and K. Srinivasan. Inferential based measurement of backlash in servo system. *Materials Today: Proceedings*, 46:9766–9770, Jan. 2021. ISSN 2214-7853. doi: 10.1016/j.matpr.2020.09.552. URL https://www.sciencedirect.com/science/article/pii/S2214785320372680.

[27] J.-L. Chang, J.-A. Chao, Y.-C. Huang, and J.-S. Chen. Prognostic experiment for ball screw preload loss of machine tool through the hilbert-huang transform and multiscale entropy method. In *The 2010 IEEE international conference on information and automation*, pages 376–380. IEEE / IEEE, June 2010. doi: 10.1109/icinfa.2010.5512064.

[28] S.-L. Chen and Y. W. Jen. Data fusion neural network for tool condition monitoring in CNC milling machining. *International Journal of Machine Tools and Manufacture*, 40(3):381–400, Feb. 2000. ISSN 0890-6955.

doi: 10.1016/S0890-6955(99)00066-8. URL https://www.sciencedirect.com/science/article/pii/S0890695599000668.

[29] C. Cimino, E. Negri, and L. Fumagalli. Review of digital twin applications in manufacturing. *Computers in Industry*, 113:103130, Dec. 2019. ISSN 0166-3615. doi: 10.1016/j.compind.2019.103130. URL https://www.sciencedirect.com/science/article/pii/S0166361519304385.

[30] H. Coprporation. Ballscrews & Supports | HIWIN, 2023. URL https://www.hiwin.us/products/ballscrews-supports/.

[31] L. Cork and R. Walker. Sensor fault detection for UAVs using a nonlinear dynamic model and the IMM-UKF algorithm. In *2007 information, decision and control*, pages 230–235. IEEE / IEEE, Feb. 2007. doi: 10.1109/idc.2007.374555.

[32] Y. Deng, D. Shichang, J. Shiyao, Z. Chen, and X. Zhiyuan. Prognostic study of ball screws by ensemble data-driven particle filters. *Journal of Manufacturing Systems*, 56:359–372, July 2020. doi: 10.1016/j.jmsy.2020.06.009. Publisher: Elsevier BV tex.readstatus: skimmed.

[33] B. Denkena, J.-K. Park, B. Bergmann, and P. Schreiber. Force sensing linear rolling guides. Proceedings of the Euspen's 18th International Conference & Exhibition, Venice, Italy, pages 4–8, 2018.

[34] B. Denkena, B. Bergmann, and A. Schmidt. Preload monitoring of single nut ball screws based on sensor fusion. *CIRP Journal of Manufacturing Science and*

Technology, 33:63–70, May 2021. doi: 10.1016/j.cirpj.2021.02.006. Publisher: Elsevier BV.

[35] Y. Ding, L. Ma, J. Ma, M. Suo, L. Tao, Y. Cheng, and C. Lu. Intelligent fault diagnosis for rotating machinery using deep Q-network based health state classification: A deep reinforcement learning approach. *Advanced Engineering Informatics*, 42:100977, Oct. 2019. ISSN 1474-0346. doi: 10.1016/j.aei.2019.100977. URL https://www.sciencedirect.com/science/article/pii/S1474034619305506.

[36] D. A. Dornfeld and M. F. DeVries. Neural Network Sensor Fusion for Tool Condition Monitoring. *CIRP Annals*, 39(1):101–105, Jan. 1990. ISSN 0007-8506. doi: 10.1016/S0007-8506(07)61012-9. URL https://www.sciencedirect.com/science/article/pii/S0007850607610129.

[37] J. Earle and S. Kuiry. Characterization of Lubricants for Research and Development, Quality Control and Application Engineering, 2012. URL https://mbns.bruker.com/acton/attachment/9063/f-04ec/1/-/-/-/-/AN1000-RevB0-Characterization_of_Lubricants_for_R%26D_QC_and_Application_Engineering-AppNote.pdf.

[38] M. Ebrahimi and R. Whalley. Analysis, modeling and simulation of stiffness in machine tool drives. *Computers & Industrial Engineering*, 38(1):93–105, Jan. 2000. ISSN 0360-8352. doi: 10.1016/S0360-8352(00)00031-0. URL https://www.sciencedirect.com/science/article/pii/S0360835200000310.

[39] G.-H. Feng and Y.-L. Pan. Establishing a cost-effective sensing system and signal processing method to diagnose preload levels of ball screws. *Mechanical*

Systems and Signal Processing, 28:78–88, Apr. 2012. doi: 10.1016/j.ymssp.2011.10.004. Publisher: Elsevier BV tex.readstatus: read.

[40] G.-H. Feng and Y.-L. Pan. Investigation of ball screw preload variation based on dynamic modeling of a preload adjustable feed-drive system and spectrum analysis of ball-nuts sensed vibration signals. *International Journal of Machine Tools and Manufacture*, 52(1):85–96, Jan. 2012. doi: 10.1016/j.ijmachtools.2011.09.008. Publisher: Elsevier BV tex.readstatus: read.

[41] G.-H. Feng and C.-C. Wang. Examining the misalignment of a linear guideway pair on a feed drive system under different ball screw preload levels with a cost-effective MEMS vibration sensing system. *Precision Engineering*, 50:467–481, Oct. 2017. doi: 10.1016/j.precisioneng.2017.07.001. Publisher: Elsevier BV tex.readstatus: skimmed.

[42] S. Frey, M. Walther, and A. Verl. Periodic variation of preloading in ball screws. *Production Engineering*, 4(2-3):261–267, 2010. Publisher: Springer.

[43] S. Frey, A. Dadalau, and A. Verl. Expedient modeling of ball screw feed drives. *Production Engineering*, 6(2):205–211, Apr. 2012. ISSN 1863-7353. doi: 10.1007/s11740-012-0371-0. URL `https://doi.org/10.1007/s11740-012-0371-0`.

[44] S. Gadsden and S. Habibi. A new robust filtering strategy for linear systems. *Journal of Dynamic Systems, Measurement, and Control*, 135(1):014503, Oct. 2013. doi: 10.1115/1.4006628. Publisher: American Society of Mechanical Engineers.

[45] S. A. Gadsden and M. Al-Shabi. The sliding innovation filter. *IEEE access : practical innovations, open solutions*, 8:96129–96138, 2020. Publisher: IEEE.

[46] S. A. Gadsden, Y. Song, and S. R. Habibi. Novel model-based estimators for the purposes of fault detection and diagnosis. *IEEE/ASME Transactions on Mechatronics*, 18(4):1237–1249, Aug. 2013. doi: 10.1109/tmech.2013.2253616. Publisher: IEEE.

[47] A. Giuliano, W. Hilal, N. Alsadi, S. A. Gadsden, and J. Yawney. A Review of Cognitive Dynamic Systems and Cognitive IoT. In *2022 IEEE International IOT, Electronics and Mechatronics Conference (IEMTRONICS)*, pages 1–7, June 2022. doi: 10.1109/IEMTRONICS55184.2022.9795834. URL `https://ieeexplore.ieee.org/abstract/document/9795834`.

[48] E. Glaessgen and D. Stargel. The digital twin paradigm for future NASA and US Air Force vehicles. page 1818, 2012.

[49] M. Glatt, C. Sinnwell, L. Yi, S. Donohoe, B. Ravani, and J. C. Aurich. Modeling and implementation of a digital twin of material flows based on physics simulation. *Journal of Manufacturing Systems*, 58:231–245, Jan. 2021. ISSN 0278-6125. doi: 10.1016/j.jmsy.2020.04.015. URL `https://www.sciencedirect.com/science/article/pii/S0278612520300595`.

[50] M. Grieves. Digital Twin: Manufacturing Excellence through Virtual Factory Replication. Mar. 2015.

[51] M. Grieves and J. Vickers. Digital Twin: Mitigating Unpredictable, Undesirable Emergent Behavior in Complex Systems. In F.-J. Kahlen, S. Flumerfelt, and A. Alves, editors, *Transdisciplinary Perspectives on Complex Systems: New Findings and Approaches*, pages 85–113. Springer International Publishing, Cham, 2017. ISBN 978-3-319-38756-7. doi: 10.1007/978-3-319-38756-7_4. URL https://doi.org/10.1007/978-3-319-38756-7_4.

[52] M. Guo, X. Fang, Z. Hu, and Q. Li. Design and research of digital twin machine tool simulation and monitoring system. *The International Journal of Advanced Manufacturing Technology*, 124(11):4253–4268, Feb. 2023. ISSN 1433-3015. doi: 10.1007/s00170-022-09613-2. URL https://doi.org/10.1007/s00170-022-09613-2.

[53] S. Habibi. The smooth variable structure filter. *Proceedings of the IEEE*, 95 (5):1026–1059, May 2007. doi: 10.1109/jproc.2007.893255. Publisher: IEEE.

[54] B. Heinzl, M. Landsiedl, F. Dür, A.-A. Dimitriou, W. Kastner, and F. Breitenecker. A Case Study on Object-oriented Modelling and Simulation of Machine Tools.

[55] W. Hilal, S. A. Gadsden, and J. Yawney. Cognitive Dynamic Systems: A Review of Theory, Applications, and Recent Advances. *Proceedings of the IEEE*, 111(6):575–622, June 2023. ISSN 1558-2256. doi: 10.1109/JPROC.2023.3272577. URL https://ieeexplore.ieee.org/abstract/document/10125578#citations. Conference Name: Proceedings of the IEEE.

[56] G. S. Hong, M. Rahman, and Q. Zhou. Using neural network for tool condition monitoring based on wavelet decomposition. *International Journal of*

Machine Tools and Manufacture, 36(5):551–566, May 1996. ISSN 0890-6955. doi: 10.1016/0890-6955(95)00067-4. URL https://www.sciencedirect.com/science/article/pii/0890695595000674.

[57] Z. Hu, S. Lou, Y. Xing, X. Wang, D. Cao, and C. Lv. Review and Perspectives on Driver Digital Twin and Its Enabling Technologies for Intelligent Vehicles. *IEEE Transactions on Intelligent Vehicles*, 7(3):417–440, Sept. 2022. ISSN 2379-8904. doi: 10.1109/TIV.2022.3195635. URL https://ieeexplore.ieee.org/abstract/document/9847095. Conference Name: IEEE Transactions on Intelligent Vehicles.

[58] H.-W. Huang, M.-S. Tsai, and Y.-C. Huang. Modeling and elastic deformation compensation of flexural feed drive system. *International Journal of Machine Tools and Manufacture*, 132:96–112, Sept. 2018. ISSN 0890-6955. doi: 10.1016/j.ijmachtools.2018.05.002. URL https://www.sciencedirect.com/science/article/pii/S0890695518300889.

[59] N. E. Huang, Z. Shen, S. R. Long, M. C. Wu, H. H. Shih, Q. Zheng, N.-C. Yen, C. C. Tung, and H. H. Liu. The empirical mode decomposition and the Hilbert spectrum for nonlinear and non-stationary time series analysis. *Proceedings of the Royal Society of London. Series A: Mathematical, Physical and Engineering Sciences*, 454(1971):903–995, Mar. 1998. doi: 10.1098/rspa.1998.0193. URL https://royalsocietypublishing.org/doi/abs/10.1098/rspa.1998.0193. Publisher: Royal Society.

[60] S. Huang, K. K. Tan, and T. H. Lee. Fault diagnosis and fault-tolerant control in linear drives using the kalman filter. *IEEE Transactions on Industrial*

Electronics, 59(11):4285–4292, Nov. 2012. doi: 10.1109/tie.2012.2185011. Publisher: Institute of Electrical and Electronics Engineers (IEEE) tex.readstatus: skimmed.

[61] T. Huang, Y. Kang, S. Du, Q. Zhang, Z. Luo, Q. Tang, and K. Yang. A survey of modeling and control in ball screw feed-drive system. *The International Journal of Advanced Manufacturing Technology*, 121(5):2923–2946, July 2022. ISSN 1433-3015. doi: 10.1007/s00170-022-09506-4. URL `https://doi.org/10.1007/s00170-022-09506-4`.

[62] X. Huang, F. Zhao, Z. Sun, Z. Zhu, and X. Mei. A novel condition monitoring signal analysis method of numerical control machine tools in varying duty operation. *IEEE Access*, 8:72577–72584, 2020. doi: 10.1109/access.2020.2988028. Publisher: Institute of Electrical and Electronics Engineers (IEEE) tex.readstatus: skimmed.

[63] Y.-C. Huang and Y.-K. Hsieh. Applying a support vector machine for hollow ball screw condition-based classification using feature extraction. *Proceedings of the Institution of Mechanical Engineers, Part B: Journal of Engineering Manufacture*, 236(14):1839–1852, Dec. 2022. ISSN 0954-4054. doi: 10.1177/0954405420958842. URL `https://doi.org/10.1177/0954405420958842`. Publisher: IMECHE.

[64] Y.-C. Huang, S.-L. Sun, and K.-H. Peng. Ball nut preload diagnosis of the hollow ball screw through sensed current signals. *International Journal of Automation and Smart Technology*, 4(3):134–142, 2014. ISSN 2223-9766.

[65] Y. Hun Jeong, B.-K. Min, and D.-W. Cho. Estimation of machine tool feed

drive inclination from current measurements and a mathematical model. *International Journal of Machine Tools and Manufacture*, 46(12):1343–1349, Oct. 2006. ISSN 0890-6955. doi: 10.1016/j.ijmachtools.2005.10.015. URL https://www.sciencedirect.com/science/article/pii/S0890695505002907.

[66] ifm. Frequency domain, Nov. 2023. URL https://www.ifm.com/de/en/shared/technologies/real-time-maintenance/technology/frequency-domain.

[67] W. Jin, Y. Chen, and J. Lee. Methodology for Ball Screw Component Health Assessment and Failure Analysis. American Society of Mechanical Engineers Digital Collection, Nov. 2013. doi: 10.1115/MSEC2013-1252. URL https://dx-doi-org.libaccess.lib.mcmaster.ca/10.1115/MSEC2013-1252.

[68] D. Jones, C. Snider, A. Nassehi, J. Yon, and B. Hicks. Characterising the Digital Twin: A systematic literature review. *CIRP Journal of Manufacturing Science and Technology*, 29:36–52, May 2020. ISSN 1755-5817. doi: 10.1016/j.cirpj.2020.02.002. URL https://www.sciencedirect.com/science/article/pii/S1755581720300110.

[69] A. Jönsson, J. Wall, and G. Broman. A virtual machine concept for real-time simulation of machine tool dynamics. *International Journal of Machine Tools and Manufacture*, 45(7):795–801, June 2005. ISSN 0890-6955. doi: 10.1016/j.ijmachtools.2004.11.012. URL https://www.sciencedirect.com/science/article/pii/S0890695504002986.

[70] R. E. Kalman. A new approach to linear filtering and prediction problems. *Journal of Basic Engineering*, 80:35–40, 1960.

[71] S. H. Khajavi, N. H. Motlagh, A. Jaribion, L. C. Werner, and J. Holmström. Digital Twin: Vision, Benefits, Boundaries, and Creation for Buildings. *IEEE Access*, 7:147406–147419, 2019. ISSN 2169-3536. doi: 10.1109/ACCESS.2019.2946515. URL `https://ieeexplore.ieee.org/abstract/document/8863491`. Conference Name: IEEE Access.

[72] S. Kim, J. Choi, and Y. Kim. Fault detection and diagnosis of aircraft actuators using fuzzy-tuning IMM filter. *IEEE Transactions on Aerospace and Electronic Systems*, 44(3):940–952, July 2008. doi: 10.1109/taes.2008.4655354. Publisher: IEEE.

[73] T. Kirubarajan and Y. Bar-Shalom. Kalman filter versus IMM estimator: when do we need the latter? *IEEE Transactions on Aerospace and Electronic Systems*, 39(4):1452–1457, Oct. 2003. doi: 10.1109/taes.2003.1261143. Publisher: IEEE.

[74] T. Kirubarajan, Y. Bar-Shalom, K. R. Pattipati, and I. Kadar. Ground target tracking with variable structure IMM estimator. *IEEE Transactions on Aerospace and Electronic Systems*, 36(1):26–46, 2000. doi: 10.1109/7.826310. Publisher: IEEE.

[75] R. Kou, S.-w. Lian, N. Xie, B.-e. Lu, and X.-m. Liu. Image-based tool condition monitoring based on convolution neural network in turning process. *The International Journal of Advanced Manufacturing Technology*, 119(5):3279–3291, Mar. 2022. ISSN 1433-3015. doi: 10.1007/s00170-021-08282-x. URL `https://doi.org/10.1007/s00170-021-08282-x`.

[76] M. Kyrnin. Thinking of Using Your PC for Audio? Here Are

Some Things to Know, July 2020. URL `https://www.lifewire.com/computer-audio-basics-831415`. Section: Lifewire.

[77] A. S. Lee, S. A. Gadsden, and M. Al-Shabi. An adaptive formulation of the sliding innovation filter. *IEEE Signal Processing Letters*, 28:1295–1299, 2021. Publisher: IEEE.

[78] W.-C. Lee and H.-L. Choi. Interactive multiple neural adaptive observer based sensor and actuator fault detection and isolation for quadcopter. In *2019 international conference on unmanned aircraft systems (ICUAS)*. IEEE, June 2019. doi: 10.1109/icuas.2019.8797779.

[79] W. G. Lee, J. W. Lee, M. S. Hong, S.-H. Nam, Y. Jeon, and M. G. Lee. Failure diagnosis system for a ball-screw by using vibration signals. *Shock and Vibration*, 2015:1–9, 2015. doi: 10.1155/2015/435870. Publisher: Hindawi Limited tex.readstatus: skimmed.

[80] Z. Lei, H. Zhou, W. Hu, G.-P. Liu, S. Guan, and X. Feng. Toward a Web-Based Digital Twin Thermal Power Plant. *IEEE Transactions on Industrial Informatics*, 18(3):1716–1725, Mar. 2022. ISSN 1941-0050. doi: 10.1109/TII.2021.3086149. URL `https://ieeexplore.ieee.org/abstract/document/9446630`. Conference Name: IEEE Transactions on Industrial Informatics.

[81] C. Li, M. Xu, W. Song, and H. Zhang. A review of static and dynamic analysis of ball screw feed drives, recirculating linear guideway, and ball screw. *International Journal of Machine Tools and Manufacture*, 188:104021, May

2023. ISSN 0890-6955. doi: 10.1016/j.ijmachtools.2023.104021. URL https://www.sciencedirect.com/science/article/pii/S0890695523000299.

[82] K. Li, C. Qiu, C. Li, S. He, B. Li, B. Luo, and H. Liu. Vibration-based health monitoring of ball screw in changing operational conditions. *Journal of Manufacturing Processes*, 53:55–68, May 2020. ISSN 1526-6125. doi: 10.1016/j.jmapro.2020.02.008. URL https://www.sciencedirect.com/science/article/pii/S1526612520300906.

[83] P. Li, X. Jia, J. Feng, H. Davari, G. Qiao, Y. Hwang, and J. Lee. Prognosability study of ball screw degradation using systematic methodology. *Mechanical Systems and Signal Processing*, 109:45–57, Sept. 2018. doi: 10.1016/j.ymssp.2018.02.046. Publisher: Elsevier BV.

[84] Z. Liang, S. Wang, Y. Peng, X. Mao, X. Yuan, A. Yang, and L. Yin. The process correlation interaction construction of Digital Twin for dynamic characteristics of machine tool structures with multi-dimensional variables. *Journal of Manufacturing Systems*, 63:78–94, Apr. 2022. ISSN 0278-6125. doi: 10.1016/j.jmsy.2022.03.002. URL https://www.sciencedirect.com/science/article/pii/S0278612522000371.

[85] L. Liao and R. Pavel. Machine tool feed axis health monitoring using plug-and-prognose technology. Proc. proceedings of the 2012 conference of the society for machinery failure prevention technology, Dayton, Ohio, 2012.

[86] W. Lin and J. Fu. Modeling and Application of Virtual Machine Tool. In *16th International Conference on Artificial Reality and Telexistence–Workshops*

(ICAT'06), pages 16–19, Nov. 2006. doi: 10.1109/ICAT.2006.85. URL https://ieeexplore.ieee.org/abstract/document/4089203.

[87] J. Liu and Y. Ou. Dynamic axial contact stiffness analysis of position preloaded ball screw mechanism. *Advances in Mechanical Engineering*, 11(1):1687814018819289, Jan. 2019. ISSN 1687-8132. doi: 10.1177/1687814018819289. URL https://doi.org/10.1177/1687814018819289. Publisher: SAGE Publications.

[88] K. Liu, L. Song, W. Han, Y. Cui, and Y. Wang. Time-Varying Error Prediction and Compensation for Movement Axis of CNC Machine Tool Based on Digital Twin. *IEEE Transactions on Industrial Informatics*, 18(1):109–118, Jan. 2022. ISSN 1941-0050. doi: 10.1109/TII.2021.3073649. URL https://ieeexplore.ieee.org/abstract/document/9405443. Conference Name: IEEE Transactions on Industrial Informatics.

[89] W. Luo, T. Hu, C. Zhang, and Y. Wei. Digital twin for CNC machine tool: modeling and using strategy. *Journal of Ambient Intelligence and Humanized Computing*, 10(3):1129–1140, Mar. 2019. ISSN 1868-5145. doi: 10.1007/s12652-018-0946-5. URL https://doi.org/10.1007/s12652-018-0946-5.

[90] W. Luo, T. Hu, Y. Ye, C. Zhang, and Y. Wei. A hybrid predictive maintenance approach for CNC machine tool driven by Digital Twin. *Robotics and Computer-Integrated Manufacturing*, 65:101974, Oct. 2020. ISSN 0736-5845. doi: 10.1016/j.rcim.2020.101974. URL https://www.sciencedirect.com/science/article/pii/S0736584519306660.

[91] C. Ma, H. Gui, and J. Liu. Self learning-empowered thermal error control

method of precision machine tools based on digital twin. *Journal of Intelligent Manufacturing*, 34(2):695–717, Feb. 2023. ISSN 1572-8145. doi: 10.1007/s10845-021-01821-z. URL https://doi.org/10.1007/s10845-021-01821-z.

[92] D. Maier and U. Heisel. A comparision of model and signal based condition monitoring and mode separation for predictive maintenance of feed drives. *Journal of Machine Engineering*, (Vol. 11, No. 4):138–151, 2011. ISSN 1895-7595, 2391-8071. URL https://www.infona.pl//resource/bwmeta1.element.baztech-8ed7db64-506f-4d39-8e69-c6e58a2c2df7.

[93] B. Marripati. Linear drive assembly model by Bhargava Marripati - Cad Crowd, 2023. URL https://www.cadcrowd.com/3d-models/linear-drive-assembly.

[94] Marshward. Bellow Couplings | Comintec, 2023. URL http://marshward.com/catalog/product/bellow-coupling-gsf.

[95] Maverick. Maverick Industrial Sales, 2023. URL https://maverickindustrialsales.com/collections/vendors?q=rpm.

[96] X. Min and S. Jiang. A thermal model of a ball screw feed drive system for a machine tool. *Proceedings of the Institution of Mechanical Engineers, Part C: Journal of Mechanical Engineering Science*, 225(1):186–193, Jan. 2011. ISSN 0954-4062. doi: 10.1177/09544062JMES2148. URL https://doi.org/10.1177/09544062JMES2148. Publisher: IMECHE.

[97] R. Mitchell. Neural Networks: The Missing Link of AI? - News,

Feb. 2017. URL https://www.allaboutcircuits.com/news/neural-networks-the-missing-link-of-ai/.

[98] A. S. Mohan and A. Kishore. Interactive Multiple Model Approach to Actuator Fault Detection, Estimation and Reconfiguration of a Satellite Launch Vehicle. In *2021 5th International Conference on Electronics, Communication and Aerospace Technology (ICECA)*, pages 1099–1104, Dec. 2021. doi: 10.1109/ICECA52323.2021.9676096. URL https://ieeexplore.ieee.org/document/9676096.

[99] P. Muthuswamy and S. K. Artificial intelligence based tool condition monitoring for digital twins and industry 4.0 applications. *International Journal on Interactive Design and Manufacturing (IJIDeM)*, 17(3):1067–1087, June 2023. ISSN 1955-2505. doi: 10.1007/s12008-022-01050-5. URL https://doi.org/10.1007/s12008-022-01050-5.

[100] T. L. Nguyen, S.-K. Ro, and J.-K. Park. Study of ball screw system preload monitoring during operation based on the motor current and screw-nut vibration. *Mechanical Systems and Signal Processing*, 131:18–32, Sept. 2019. doi: 10.1016/j.ymssp.2019.05.036. Publisher: Elsevier BV tex.readstatus: read.

[101] NSK. Support Units for Light Load and Small Equipment, 2023. URL https://www.nskamericas.com/en/services/downloads/linear-components.html.

[102] C. Okwudire. *Finite element modeling of ballscrew feed drive systems for control purposes*. PhD thesis, University of British Columbia, 2005. URL https://open.library.ubc.ca/soa/cIRcle/collections/ubctheses/831/items/1.0080753.

[103] C. Okwudire and Y. Altintas. Minimum Tracking Error Control of Flexible Ball Screw Drives Using a Discrete-Time Sliding Mode Controller. *Journal of Dynamic Systems, Measurement, and Control*, 131(051006), Aug. 2009. ISSN 0022-0434. doi: 10.1115/1.3155005. URL `https://doi.org/10.1115/1.3155005`.

[104] C. E. Okwudire and Y. Altintas. Hybrid Modeling of Ball Screw Drives With Coupled Axial, Torsional, and Lateral Dynamics. *Journal of Mechanical Design*, 131(071002), May 2009. ISSN 1050-0472. doi: 10.1115/1.3125887. URL `https://doi.org/10.1115/1.3125887`.

[105] Z. Pandilov, A. Milecki, A. Nowak, F. Górski, D. Grajewski, D. Ciglar, M. Klaić, and T. Mulc. Virtual Modelling and Simulation of a CNC Machine Feed Drive System. *Transactions of FAMENA*, 39(4):37–54, 2015. ISSN 1333-1124, 1849-1391. URL `https://hrcak.srce.hr/clanak/223893`. Publisher: Fakultet strojarstva i brodogradnje.

[106] D. Papageorgiou, M. Blanke, H. H. Niemann, and J. H. Richter. Robust backlash estimation for industrial drive-train Systems—Theory and validation. *IEEE Transactions on Control Systems Technology*, 27(5):1847–1861, Sept. 2019. doi: 10.1109/tcst.2018.2837642. Publisher: Institute of Electrical and Electronics Engineers (IEEE) tex.readstatus: skimmed.

[107] D. Papageorgiou, M. Blanke, H. Henrik Niemann, and J. H. Richter. Online friction parameter estimation for machine tools. *Advanced Control for Applications: Engineering and Industrial Systems*, 2(1):e28, 2020. ISSN 2578-0727. Publisher: Wiley Online Library tex.readstatus: skimmed.

[108] K. Patra, A. K. Jha, T. Szalay, J. Ranjan, and L. Monostori. Artificial

neural network based tool condition monitoring in micro mechanical peck drilling using thrust force signals. *Precision Engineering*, 48:279–291, Apr. 2017. ISSN 0141-6359. doi: 10.1016/j.precisioneng.2016.12.011. URL https://www.sciencedirect.com/science/article/pii/S0141635916304470.

[109] K. Pichler, J. Klinglmayr, and M. Pichler-Scheder. Detecting Wear in a Ball Screw Using a Data-Driven Approach. In *2018 IEEE International Conference on Systems, Man, and Cybernetics (SMC)*, pages 3123–3128, Oct. 2018. doi: 10.1109/SMC.2018.00529. URL https://ieeexplore.ieee.org/document/8616526. ISSN: 2577-1655.

[110] C. Sadhukhan, S. K. Mitra, R. Biswas, and M. K. Naskar. Tool condition monitoring: unscented Kalman filter for tool flank wear estimation in turning of Inconel 718. *Machining Science and Technology*, 25(2):331–348, Mar. 2021. ISSN 1091-0344. doi: 10.1080/10910344.2020.1855650. URL https://doi.org/10.1080/10910344.2020.1855650. Publisher: Taylor & Francis _eprint: https://doi.org/10.1080/10910344.2020.1855650.

[111] H. Saglam and A. Unuvar. Tool condition monitoring in milling based on cutting forces by a neural network. *International Journal of Production Research*, 41 (7):1519–1532, Jan. 2003. ISSN 0020-7543. doi: 10.1080/0020754031000073017. URL https://doi.org/10.1080/0020754031000073017. Publisher: Taylor & Francis _eprint: https://doi.org/10.1080/0020754031000073017.

[112] A. Salimiasl and A. Özdemir. Analyzing the performance of artificial neural network (ANN)-, fuzzy logic (FL)-, and least square (LS)-based models for online

tool condition monitoring. *The International Journal of Advanced Manufacturing Technology*, 87(1):1145–1158, Oct. 2016. ISSN 1433-3015. doi: 10.1007/s00170-016-8548-x. URL https://doi.org/10.1007/s00170-016-8548-x.

[113] K. Samuel and J. Choi. Improved IMM filter for tracking a highly maneuvering target with mixed system noises. *International Journal of Control, Automation and Systems*, 16(6):2763–2771, Nov. 2018. doi: 10.1007/s12555-018-0301-9. Publisher: Springer.

[114] P. Shan, H. Lv, L. Yu, H. Ge, Y. Li, and L. Gu. A multisensor data fusion method for ball screw fault diagnosis based on convolutional neural network with selected channels. *IEEE Sensors Journal*, 20(14):7896–7905, July 2020. doi: 10.1109/jsen.2020.2980868. Publisher: Institute of Electrical and Electronics Engineers (IEEE).

[115] J.-W. Shen, H.-T. Feng, C.-G. Zhou, Z.-T. Chen, and Y. Ou. A new two-stage degradation model for the preload of ball screws considering geometric errors. *Wear : an international journal on the science and technology of friction lubrication and wear*, 500-501:204352, July 2022. doi: 10.1016/j.wear.2022.204352. Publisher: Elsevier BV.

[116] N. Shen, Y. Wu, J. Li, T. He, Y. Lu, and Y. Xu. Research on procedure optimisation for composite grinding based on Digital Twin technology. *International Journal of Production Research*, 61(6):1736–1754, Mar. 2023. ISSN 0020-7543. doi: 10.1080/00207543.2022.2045378. URL https://doi.org/10.1080/00207543.2022.2045378. Publisher: Taylor & Francis _eprint: https://doi.org/10.1080/00207543.2022.2045378.

[117] S. Shi, J. Lin, X. Wang, and X. Xu. Analysis of the transient backlash error in CNC machine tools with closed loops. *International Journal of Machine Tools and Manufacture*, 93:49–60, June 2015. ISSN 0890-6955. doi: 10.1016/j.ijmachtools.2015.03.009. URL https://www.sciencedirect.com/science/article/pii/S0890695515300237.

[118] B. Sicard, N. Alsadi, P. Spachos, Y. Ziada, and S. A. Gadsden. Predictive Maintenance and Condition Monitoring in Machine Tools: An IoT Approach. In *2022 IEEE International IOT, Electronics and Mechatronics Conference (IEMTRONICS)*, pages 1–9, June 2022. doi: 10.1109/IEMTRONICS55184.2022.9795726.

[119] B. Sicard, Q. Butler, P. Kosierb, Y. Wu, Y. Ziada, and S. A. Gadsden. Design Considerations for Building an IoT Enabled Digital Twin Machine Tool Sub-System. In *2023 IEEE International Conference on Artificial Intelligence, Blockchain, and Internet of Things (AIBThings)*, pages 1–5, Sept. 2023. doi: 10.1109/AIBThings58340.2023.10292492. URL https://ieeexplore.ieee.org/abstract/document/10292492.

[120] B. Sicard, Q. Butler, P. Kosierb, Y. Wu, Y. Ziada, and S. A. Gadsden. IIoDT: Industrial Internet of Digital Twins for Hierarchical Asset Management in Manufacturing. In *2023 IEEE International Conference on Artificial Intelligence, Blockchain, and Internet of Things (AIBThings)*, pages 1–5, Sept. 2023. doi: 10.1109/AIBThings58340.2023.10292454. URL https://ieeexplore.ieee.org/abstract/document/10292454.

[121] B. Sicard, Q. Butler, Y. Ziada, and S. A. Gadsden. Experimental Setups

for Linear Feed Drive Predictive Maintenance: A Review. In *2023 IEEE International Conference on Prognostics and Health Management (ICPHM)*, pages 357–367, June 2023. doi: 10.1109/ICPHM57936.2023.10194225. URL https://ieeexplore.ieee.org/document/10194225. ISSN: 2166-5656.

[122] B. S. Sicard, Q. Butler, Y. Ziada, and S. A. Gadsden. Cognitive dynamic digital twin: enhancements for digital twin platforms based on human cognition. In *Big Data V: Learning, Analytics, and Applications*, volume 12522, pages 48–63. SPIE, June 2023. doi: 10.1117/12.2664017. URL https://www.spiedigitallibrary.org/conference-proceedings-of-spie/12522/125220B/Cognitive-dynamic-digital-twin--enhancements-for-digital-twin-platforms/10.1117/12.2664017.full.

[123] B. S. Sicard, Q. Butler, Y. Ziada, E. Hughey, and S. A. Gadsden. Preload Loss Detection in a Ball Screw System Using Interacting Models. *IEEE Open Journal of Instrumentation and Measurement*, 2:1–12, 2023. ISSN 2768-7236. doi: 10.1109/OJIM.2023.3301905. Conference Name: IEEE Open Journal of Instrumentation and Measurement.

[124] Siemens. Robustness improvements for SINAMICS S120 Booksize external cooling in harsh environments.

[125] Siemens. Drive Optimization Guide, May 2019.

[126] S. Silva, B. Cardoso Filho, M. Murta G Cardoso, and M. Rocha Braga. Blower

drive system based on synchronous motor with solid salient-pole rotor: performance under starting and voltage sag conditions. *IEEE Transactions on Industry Applications*, 39(5):1429–1435, Sept. 2003. ISSN 1939-9367. doi: 10.1109/TIA.2003.816511. URL https://ieeexplore.ieee.org/document/1233604. Conference Name: IEEE Transactions on Industry Applications.

[127] J. Son, S. Zhou, C. Sankavaram, X. Du, and Y. Zhang. Remaining useful life prediction based on noisy condition monitoring signals using constrained Kalman filter. *Reliability Engineering & System Safety*, 152:38–50, Aug. 2016. ISSN 0951-8320. doi: 10.1016/j.ress.2016.02.006. URL https://www.sciencedirect.com/science/article/pii/S0951832016000478.

[128] M. Sparham, A. A. D. Sarhan, N. A. Mardi, and M. Hamdi. Designing and manufacturing an automated lubrication control system in CNC machine tool guideways for more precise machining and less oil consumption. *The International Journal of Advanced Manufacturing Technology*, 70(5):1081–1090, Feb. 2014. ISSN 1433-3015. doi: 10.1007/s00170-013-5325-y. URL https://doi.org/10.1007/s00170-013-5325-y.

[129] J. Sprovieri. Linear Guides Provide Smooth, Precise Positioning, Nov. 2019. URL https://www.assemblymag.com/articles/95252-linear-guides-provide-smooth-precise-positioning.

[130] L. Stan, A. F. Nicolescu, C. Pupăză, and G. Jiga. Digital Twin and web services for robotic deburring in intelligent manufacturing. *Journal of Intelligent Manufacturing*, 34(6):2765–2781, Aug. 2023. ISSN 1572-8145. doi: 10.1007/s10845-022-01928-x. URL https://doi.org/10.1007/s10845-022-01928-x.

[131] O. Surucu, S. A. Gadsden, and J. Yawney. Condition Monitoring using Machine Learning: A Review of Theory, Applications, and Recent Advances. *Expert Systems with Applications*, 221:119738, July 2023. ISSN 0957-4174. doi: 10.1016/j.eswa.2023.119738. URL https://www.sciencedirect.com/science/article/pii/S0957417423002397.

[132] F. Tao, H. Zhang, A. Liu, and A. Y. C. Nee. Digital Twin in Industry: State-of-the-Art. *IEEE Transactions on Industrial Informatics*, 15(4):2405–2415, Apr. 2019. ISSN 1941-0050. doi: 10.1109/TII.2018.2873186. Conference Name: IEEE Transactions on Industrial Informatics.

[133] THK. THK ball screw general catalogue. manual, THK, Tokyo, Japan, 2021.

[134] X. Tong, Q. Liu, S. Pi, and Y. Xiao. Real-time machining data application and service based on IMT digital twin. *Journal of Intelligent Manufacturing*, 31 (5):1113–1132, June 2020. ISSN 1572-8145. doi: 10.1007/s10845-019-01500-0. URL https://doi.org/10.1007/s10845-019-01500-0.

[135] P. Tsai, C. Cheng, and Y. Hwang. Ball screw preload loss detection using ball pass frequency. *Mechanical Systems and Signal Processing*, 48(1-2):77–91, Oct. 2014. doi: 10.1016/j.ymssp.2014.02.017. Publisher: Elsevier BV tex.readstatus: skimmed.

[136] A. Verl and S. Frey. Correlation between feed velocity and preloading in ball screw drives. *CIRP Annals*, 59(1):429–432, Jan. 2010. ISSN 0007-8506. doi: 10.1016/j.cirp.2010.03.136. URL https://www.sciencedirect.com/science/article/pii/S000785061000137X.

[137] A. Verl, U. Heisel, M. Walther, and D. Maier. Sensorless automated condition monitoring for the control of the predictive maintenance of machine tools. *CIRP Annals*, 58(1):375–378, 2009. doi: 10.1016/j.cirp.2009.03.039. Publisher: Elsevier BV tex.readstatus: skimmed.

[138] D. A. Vicente, R. L. Hecker, F. J. Villegas, and G. M. Flores. Modeling and vibration mode analysis of a ball screw drive. *The International Journal of Advanced Manufacturing Technology*, 58(1):257–265, Jan. 2012. ISSN 1433-3015. doi: 10.1007/s00170-011-3375-6. URL https://doi.org/10.1007/s00170-011-3375-6.

[139] G. W. Vogl and M. E. Sharp. Diagnostics of machine tool linear axes via separation of geometric error sources. In *Annual Conference of the PHM Society*, volume 9, 2017. doi: 10.36001/phmconf.2017.v9i1.2485. URL http://papers.phmsociety.org/index.php/phmconf/article/view/2485. Number: 1.

[140] C.-P. Wang, K. Erkorkmaz, J. McPhee, and S. Engin. In-process digital twin estimation for high-performance machine tools with coupled multibody dynamics. *CIRP Annals*, 69(1):321–324, Jan. 2020. ISSN 0007-8506. doi: 10.1016/j.cirp.2020.04.047. URL https://www.sciencedirect.com/science/article/pii/S000785062030069X.

[141] K.-J. Wang, Y.-H. Lee, and S. Angelica. Digital twin design for real-time monitoring – a case study of die cutting machine. *International Journal of Production Research*, 59(21):6471–6485, Nov. 2021. ISSN 0020-7543. doi: 10.1080/00207543.2020.1817999. URL https://doi.org/

10.1080/00207543.2020.1817999. Publisher: Taylor & Francis _eprint: https://doi.org/10.1080/00207543.2020.1817999.

[142] W. Wang, Y. Zhang, and C. Li. Dynamic reliability analysis of linear guides in positioning precision. *Mechanism and Machine Theory*, 116:451–464, Oct. 2017. ISSN 0094-114X. doi: 10.1016/j.mechmachtheory.2017.06.011. URL https://www.sciencedirect.com/science/article/pii/S0094114X17306675.

[143] B. Warfield. CNC Control Market Shares: What Are the Most Popular Controls?, Aug. 2012. URL https://www.cnccookbook.com/cnc-control-market-shares-what-are-the-most-popular-controls/.

[144] S. Weckx, B. Meyers, J. Jordens, S. Robyns, J. Baake, P. Lietaert, R. De Geest, and D. Maes. Development and deployment of a digital twin for monitoring of an adaptive clamping mechanism, used for high performance composite machining. *IET Collaborative Intelligent Manufacturing*, 4(2):112–122, 2022. ISSN 2516-8398. doi: 10.1049/cim2.12052. URL https://onlinelibrary.wiley.com/doi/abs/10.1049/cim2.12052. _eprint: https://onlinelibrary.wiley.com/doi/pdf/10.1049/cim2.12052.

[145] C. C. Wei, J. F. Lin, and J.-H. Horng. Analysis of a ball screw with a preload and lubrication. *Tribology International*, 42(11-12):1816–1831, 2009. Publisher: Elsevier.

[146] Y. Wei, T. Hu, T. Zhou, Y. Ye, and W. Luo. Consistency retention method for CNC machine tool digital twin model. *Journal of Manufacturing Systems*, 58:313–322, Jan. 2021. ISSN 0278-6125. doi: 10.1016/j.jmsy.

2020.06.002. URL https://www.sciencedirect.com/science/article/pii/S0278612520300923.

[147] J. Wen and H. Gao. Remaining useful life prediction of the ball screw system based on weighted Mahalanobis distance and an exponential model. *Journal of Vibroengineering*, 20(4):1691–1707, 2018. ISSN 1392-8716. doi: 10.21595/jve.2018.19099. URL https://www.extrica.com/article/19099. Number: 4 Publisher: JVE International Ltd.

[148] C.-H. Wu and Y.-T. Kung. Thermal analysis for the feed drive system of a CNC machine center. *International Journal of Machine Tools and Manufacture*, 43(15):1521–1528, Dec. 2003. ISSN 0890-6955. doi: 10.1016/j.ijmachtools.2003.08.008. URL https://www.sciencedirect.com/science/article/pii/S0890695503002207.

[149] T. Xi, S. Kehne, T. Fujita, A. Epple, and C. Brecher. Condition monitoring of ball-screw drives based on frequency shift. *IEEE/ASME Transactions on Mechatronics*, 25(3):1211–1219, June 2020. doi: 10.1109/tmech.2020.2969846. Publisher: Institute of Electrical and Electronics Engineers (IEEE) tex.readstatus: skimmed.

[150] Y. Xie, K. Lian, Q. Liu, C. Zhang, and H. Liu. Digital twin for cutting tool: Modeling, application and service strategy. *Journal of Manufacturing Systems*, 58:305–312, Jan. 2021. ISSN 0278-6125. doi: 10.1016/j.jmsy.2020.08.007. URL https://www.sciencedirect.com/science/article/pii/S0278612520301400.

[151] R. Xue, P. Zhang, Z. Huang, and J. Wang. Digital twin-driven fault diagnosis

for CNC machine tool. *The International Journal of Advanced Manufacturing Technology*, Aug. 2022. doi: 10.1007/s00170-022-09978-4.

[152] H. Yang, Z. Wang, T. Zhang, and F. Du. A review on vibration analysis and control of machine tool feed drive systems. *The International Journal of Advanced Manufacturing Technology*, 107(1):503–525, Mar. 2020. ISSN 1433-3015. doi: 10.1007/s00170-020-05041-2. URL https://doi.org/10.1007/s00170-020-05041-2.

[153] X. Yang, Y. Ran, G. Zhang, H. Wang, Z. Mu, and S. Zhi. A digital twin-driven hybrid approach for the prediction of performance degradation in transmission unit of CNC machine tool. *Robotics and Computer-Integrated Manufacturing*, 73:102230, Feb. 2022. ISSN 0736-5845. doi: 10.1016/j.rcim.2021.102230. URL https://www.sciencedirect.com/science/article/pii/S0736584521001125.

[154] C.-H. Yeung, Y. Altintas, and K. Erkorkmaz. Virtual CNC system. Part I. System architecture. *International Journal of Machine Tools and Manufacture*, 46(10):1107–1123, Aug. 2006. ISSN 0890-6955. doi: 10.1016/j.ijmachtools.2005.08.002. URL https://www.sciencedirect.com/science/article/pii/S089069550500218X.

[155] H. Yi-Cheng and Z. Jing-Hong. Ball nut preload diagnosis of the hollow ball screw through support vector machine. *Advances in Technology Innovation*, 3 (2):94, 2018. ISSN 2415-0436. Publisher: Taiwan Association of Engineering and Technology Innovation tex.readstatus: read.

[156] W. S. Yun, S. K. Kim, and D. W. Cho. Thermal error analysis for a

CNC lathe feed drive system. *International Journal of Machine Tools and Manufacture*, 39(7):1087–1101, July 1999. ISSN 0890-6955. doi: 10.1016/S0890-6955(98)00073-X. URL https://www.sciencedirect.com/science/article/pii/S089069559800073X.

[157] M. Zaeh and D. Siedl. A New Method for Simulation of Machining Performance by Integrating Finite Element and Multi-body Simulation for Machine Tools. *CIRP Annals*, 56(1):383–386, Jan. 2007. ISSN 0007-8506. doi: 10.1016/j.cirp.2007.05.089. URL https://www.sciencedirect.com/science/article/pii/S0007850607000935.

[158] M. F. Zaeh and T. Oertli. Finite Element Formulation of Pre-Stressed Ball Screw Drives. pages 289–296. American Society of Mechanical Engineers Digital Collection, Nov. 2008. doi: 10.1115/ESDA2004-58281. URL https://dx.doi.org/10.1115/ESDA2004-58281.

[159] M. F. Zaeh, T. Oertli, and J. Milberg. Finite Element Modelling of Ball Screw Feed Drive Systems. *CIRP Annals*, 53(1):289–292, Jan. 2004. ISSN 0007-8506. doi: 10.1016/S0007-8506(07)60700-8. URL https://www.sciencedirect.com/science/article/pii/S0007850607607008.

[160] C. Zhang, X. Yao, J. Zhang, and H. Jin. Tool Condition Monitoring and Remaining Useful Life Prognostic Based on a Wireless Sensor in Dry Milling Operations. *Sensors*, 16(6):795, June 2016. ISSN 1424-8220. doi: 10.3390/s16060795. URL https://www.mdpi.com/1424-8220/16/6/795. Number: 6 Publisher: Multidisciplinary Digital Publishing Institute.

[161] H. Zhang, Q. Gao, and F. Pan. An online fault diagnosis method for actuators

of quadrotor UAV with novel configuration based on IMM. In *2020 chinese automation congress (CAC)*. IEEE, Nov. 2020. doi: 10.1109/cac51589.2020.9326877.

[162] L. Zhang, H. Gao, D. Dong, G. Fu, and Q. Liu. Wear calculation-based degradation analysis and modeling for remaining useful life prediction of ball screw. *Mathematical Problems in Engineering*, 2018:1–18, Nov. 2018. doi: 10.1155/2018/2969854. Publisher: Hindawi Limited tex.readstatus: skimmed.

[163] W. Zhang, D. Zhu, Z. Huang, Y. Zhu, and J. Zhu. Dynamic parameters identification of rolling joints based on the digital twin dynamic model of an assembled ball screw feed system. *Advances in Mechanical Engineering*, 14(6):16878132221108491, June 2022. ISSN 1687-8132. doi: 10.1177/16878132221108491. URL `https://doi.org/10.1177/16878132221108491`. Publisher: SAGE Publications.

[164] Y. Zhang and J. Jiang. Integrated active fault-tolerant control using IMM approach. *IEEE Transactions on Aerospace and Electronic Systems*, 37(4): 1221–1235, Oct. 2001. ISSN 1557-9603. doi: 10.1109/7.976961. URL `https://ieeexplore.ieee.org/document/976961`. Conference Name: IEEE Transactions on Aerospace and Electronic Systems.

[165] J. Zhao, M. Lin, X. Song, and N. Wei. A modeling method for predicting the precision loss of the preload double-nut ball screw induced by raceway wear based on fractal theory. *Wear*, 486-487:204065, Dec. 2021. ISSN 0043-1648. doi: 10.1016/j.wear.2021.204065. URL `https://www.sciencedirect.com/science/article/pii/S0043164821004518`.

[166] C.-G. Zhou, H.-T. Feng, Z.-T. Chen, and Y. Ou. Correlation between preload and no-load drag torque of ball screws. *International Journal of Machine Tools and Manufacture*, 102:35–40, 2016. Publisher: Elsevier.

[167] H.-X. Zhou, C.-G. Zhou, H.-T. Feng, and Y. Ou. Theoretical and experimental analysis of the preload degradation of double-nut ball screws. *Precision Engineering*, 65:72–90, 2020. Publisher: Elsevier.

[168] Y. Zhou, Z. Ma, X. Shi, and K. Zhang. An adaptive clustering method detecting the surface defects on linear guide rails. *International Journal of Computer Integrated Manufacturing*, 32(8):798–808, July 2019. doi: 10.1080/0951192x.2019.1636409. Publisher: Informa UK Limited.

[169] C. Zhu, L. Zhu, and J. Shi. Research on dynamic performance of feed drive systems by integrating the virtual prototype and finite element method. *Journal of Vibroengineering*, 17(4):1660–1670, June 2015. ISSN 1392-8716, 2538-8460. URL `https://www.extrica.com/article/15144`. Number: 4 Publisher: JVE International Ltd.